UNIVERSITÀ DEGLI STUDI DI NAPOLI FEDERICO II

DIPARTIMENTO DI MATEMATICA E APPLICAZIONI
"RENATO CACCIOPPOLI"

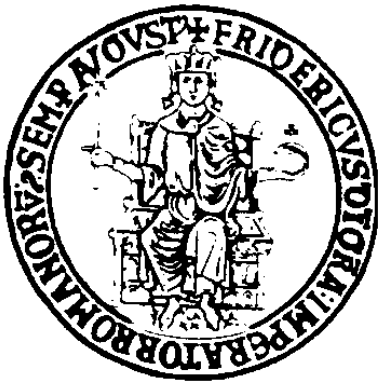

DOTTORATO DI RICERCA IN MATEMATICA E APPLICAZIONI

XXXIV CICLO

Ph.D. THESIS

"**A MODELLING AND NUMERICAL STUDY OF S-BASED DENITRIFICATION SYSTEMS**"

Grazia Guerriero

This PhD research was conducted as part of the Campania Region Operational Program, European Social Fund, 2014-2020 ASSE III - Specific objective 14 Action 10.5.2 - Public notice "Innovative Doctorates with Industrial Characterization".

PhD Promoter

Prof. L. Frunzo,

Associate Professor
Department of Mathematics and Applications "Renato Caccioppoli"
University of Naples "Federico II", Naples, Italy

Thesis Committee

Thesis Supervisors

Prof. L. Frunzo,
Associate Professor
Department of Mathematics and Applications "Renato Caccioppoli"
University of Naples "Federico II", Naples, Italy

Dr. M.R. Mattei,
Research fellow
Department of Mathematics and Applications "Renato Caccioppoli"
University of Naples "Federico II", Naples, Italy

Thesis Co-Supervisors

Dr. S. Papirio,
Research fellow
Department of Civil, Building and Environmental Engineering (DICEA)
University of Naples "Federico II", Naples, Italy

Dr. G. Esposito,
Full Professor
Department of Civil, Building and Environmental Engineering (DICEA)
University of Naples "Federico II", Naples, Italy

Instructors

Dr. C. Huiliñir,
Associate Professor
Departamento de Ingeniería Química,
Universidad de Santiago de Chile, Santiago, Chile

Dr. A.Trucchia,
Research fellow
CIMA Research Foundation, Savona, Italy

Abstract

English

This thesis work concerns the mathematical modeling of an innovative biological process for wastewater treatment and its global sensitivity analysis. The aim of the presented mathematical model is to evaluate the effect of production and consumption of soluble microbial products (SMP) and addition of an external carbon source during a sulfur-based autotrophic denitrification. Such compounds during elemental sulfur-based autotrophic denitrification promotes the natural growth of heterotrophic microbial families, which are mainly represented by denitrifiers and sulfate-reducing bacteria.

First, a state of art of the biological process from both experimental and modelling points of view is provided. An overview on autotrophic denitrification driven by elemental sulfur is given as well as a critical analysis on the existing experimental and mathematical studies on the process investigated.

Afterwards, the mathematical model proposed is accurately described in the second chapter, and all mathematical and biological assumptions are detailed. The process was supposed to occur in a sequencing batch reactor to investigate the effects of the COD injection and the time in which this injection occurs on all the processes considered. To model this reactor configuration, a system of nonlinear impulsive differential equations was defined to simulate a system undergoing to instantaneous changes after a continuous period. The equations were solved numerically. The model was tested under ideal conditions where the settling efficiency of the reactor is supposed to be perfect. The model was tested varying different parameters: cycle duration, day of the injection of external COD and quantity of COD added. Albeit the high amount of sludge produced, it appears that SMP are not able to significantly support sulfate reduction. However, when an adequate amount of external carbon source is provided, the system is able to remove high nitrate concentrations without having high sulfate concentrations in the effluent, due to the work of both heterotrophic families involved in the model.

In the following part, the perfect settling efficiency assumption was removed, and the volume of treated influent was increased in each cycle, testing the model under more real conditions. From the simulations performed, it was observed that an efficient settlement is needed to

improve the concentration of microorganisms and increase the removal of nitrate and sulfate. In both this case and the previous one, in all simulations performed, even when COD is added, autotrophic denitrifiers remain the predominant microbial family in the reactor.

Finally, a global sensitivity analysis was carried out to find out the parameters more affecting the process. All kinetic parameters involved in the model were first screened using the Morris method. From this initial analysis, it was evident that the removal of nitrogen compounds and the effluent sulfate concentration are mainly sensitive to parameters related to the hydrolysis of elemental sulfur into bioavailable sulfur and maximum growth rate of autotrophic denitrifiers. Then, a second analysis was carried out with machine learning systems, considering only the most sensitive kinetic parameters. The results confirmed those obtained with the previous method and showed that the decay constants of heterotrophic biomasses also turn out to be sensitive parameters. This last study will represent the major tool for the future experimental calibration and validation of the model.

Italiano

Il presente lavoro di tesi riguarda la modellazione matematica di un nuovo processo biologico per il trattamento delle acque reflue e la sua analisi globale di sensitività. Il modello matematico introdotto è stato costruito con l'obiettivo di studiare un nuovo processo biologico di trattamento di denitrificazione, esaminando gli aspetti matematici e biologici di tale processo.

Lo scopo del modello matematico presentato è quello di valutare sia l'effetto della produzione e consumo di prodotti solubili derivanti dall'attività microbica (SMP) sia dell'aggiunta di una fonte di carbonio esterna durante un processo di denitrificazione autotrofa a base di zolfo. Questi composti, durante la denitrificazione autotrofa a base di zolfo elementare, promuovono la crescita naturale delle biomasse eterotrofe, rappresentate principalmente da denitrificanti eterotrofi e solfato-riduttori.

In primo luogo, viene presentato uno stato dell'arte del processo biologico dal punto di vista sperimentale e modellistico. Infatti, viene fornita una panoramica sulla denitrificazione autotrofa guidata dallo zolfo elementare sugli studi sperimentali e i modelli matematici relativi a talu processi biologici. Successivamente, viene poi riportato il modello e vengono spiegati tutte le ipotesi matematiche e biologiche che ne sono alla base. Il processo si ipotizza avvenga in un reattore batch sequenziale per indagare gli effetti dell'aggiunta di COD e del tempo in cui questa avviene su tutti i processi considerati. Inoltre, questa configurazione del reattore è utile per incentivare la produzione e il consumo di SMP favorendo le condizioni di feast-famine. Per modellare questa configurazione del reattore, è stato definito un sistema di equazioni differenziali impulsive non lineari adatte a simulare un sistema che subisce cambiamenti istantanei dopo un periodo continuo; tali equazioni sono state risolte numericamente. Il modello è stato testato in condizioni ideali in cui si suppone che l'efficienza di sedimentazione del reattore sia ottimale. Tuttavia, nonostante l'elevata quantità di fanghi prodotti, sembra che gli SMP non siano in grado di sostenere in modo significativo la riduzione dei solfati. Comunque, quando viene fornita un'adeguata quantità di sostanza organica dall'esterno, il sistema è in grado di rimuovere elevate concentrazioni di nitrati dalle acque reflue senza per questo avere elevate concentrazioni di solfati nell'effluente, per effetto del lavoro di entrambe le famiglie eterotrofe coinvolte nel modello. Il modello è stato testato variando diversi parametri: durata del ciclo, giorno di iniezione del COD esterno e quantità di COD aggiunto.

Nella parte successiva è stata eliminata l'ipotesi di perfetta efficienza di sedimentazione ed è stata incrementata la quantità di refluo trattato in ogni ciclo, applicando al modello condizioni più realistiche. Dalle simulazioni di questo secondo studio è emersa la necessità di un buon sistema di sedimentazione per incrementare la concentrazione di biomasse necessarie per aumentare l'efficienza del processo. Per di più, come nel caso precedente, in tutte le simulazioni effettuate, anche nel caso di aggiunta di COD, i denitrificanti autotrofi rimangono la famiglia microbica prevalente nel reattore.

Infine, è stata condotta un'analisi di sensibilità globale per individuare i parametri che più possono influenzare il processo. I parametri cinetici coinvolti nel modello sono stati prima tutti vagliati utilizzando il metodo Morris. Da questa prima analisi è emerso che la rimozione dei composti azotati e la concentrazione di solfato nell'effluente sono sensibili soprattutto ai parametri relativi all'idrolisi dello zolfo elementare in zolfo biodisponibile e ai denitrificanti autotrofi. È stata poi condotta una seconda analisi, con sistemi di machine learning, considerando solo i parametri cinetici che erano risultati più sensibili dalla prima analisi. I risultati hanno confermato quelli ottenuti con il metodo precedente e hanno mostrato che anche le costanti di decadimento delle biomasse eterotrofe risultano essere parametri sensibili. Quest'ultimo studio rappresenterà lo strumento principale per la futura calibrazione e validazione sperimentale del modello.

Summary

Chapter 1

Chapter 2

Chapter 3

Chapter 4

Chapter 5

List of Figures

List of Tables

Chapter 1

GENERAL INTRODUCTION AND THESIS OUTLINE

1.1 BACKGROUND AND PROBLEM STATEMENT

Nowadays, water scarcity is one of the leading challenges for sustainable development. In this context, great interest is addressed to innovative technologies aimed to remove contaminants from water [1]. One of the most common pollutants in water is represented by nitrate, deriving from anthropogenic activities and natural contamination [2]. High concentrations of nitrate could lead to different health problems, such as methemoglobinemia, also known as the baby-blue syndrome and cancer [3]–[5]. Furthermore, high concentrations of nitrate can negatively affect water basins, leading to eutrophication and death of water ecosystem [6].

The nitrogen removal from wastewater is conventionally performed by using biological treatments, in particular the heterotrophic denitrification [7]. The main drawback of this process is the need of high concentrations of organic compounds to be supplied, that increases the operating costs [8]. Moreover, another disadvantage in using this technology is related to the production of large amount of sludge, that must be further treated. [8], [9]. In this contest, the application of autotrophic denitrification for nitrate removal, led by electron donor different from organic compounds, represents a valid alternative to the conventional heterotrophic treatment [8], [10]. Among all the electron donors that could be used for autotrophic denitrification, elemental sulfur represents the most cost effective compound, and the easiest to be handled [11]. Furthermore, autotrophic denitrification leads to a lower sludge production, due to the lower growth rate of the biomass [8], [12].

In recent years, a two-step denitrification process based on elemental sulfur has been developed, to contain the main disadvantage of the process, represented by the sulfate production [13]. In this context, experimental studies have been carried out to reduce the shortcomings of the process [14]. One of the best options to prevent the problem associated with sulfate production is represented by the addition of low amount of external carbon source to enhance the growth of heterotrophic consortium [14], [15]. Sulfur based autotrophic denitrification results also to be the most promising alternative in autotrophic denitrification field as it has been already tested on both pilot and laboratory scale, providing excellent efficiency results [16].

Mathematical modelling can represent a crucial tool to study and investigate the main biological and engineering aspects and the effectiveness of this technology. In this perspective, a

mathematical model on sulfur based autotrophic denitrification has been developed. The model takes into account the addition of small amounts of external carbon source, aiming at the mitigations of the sulfate production without affecting the denitrification performance.

1.2 RESEARCH AIM AND OBJECTIVES

The main aim of this work is to define a mathematical model of the sulfur based autotrophic denitrification process, and investigate the effect of the addition of an external carbon source to the system. Specifically, to provide a comprehensive description of the biological system, the mathematical model takes into account the simultaneous co-occurrence of autotrophic denitrification, heterotrophic denitrification, and sulfate reduction. Furthermore, other subprocesses related to the natural biological activities and the production and consumption of soluble microbial products have been considered to limit the shortcomings resulting from the biological processes considered. Due to the nonlinearity of the reaction terms, the model has been investigated numerically.

The present work consists of five main chapters where the presented topic is addressed by focusing on the following aspects:

Chapter 2 **State of the art**: An overlook on the existing studies on sulfur-based denitrification systems is provided, including the description of the biological process of sulfur based autotrophic denitrification and mixotrophic denitrification. In this chapter, the state of art of the mathematical models on these two biological processes is also provided. In addition, an overview on the soluble microbial products is presented.

Chapter 3 **Mathematical model definition**: Definition of the mathematical model, where all biological and mathematical assumptions are described. Different simulations are carried out by considering a high initial nitrate concentration.

Chapter 4 **Model application**: The model described in the previous chapter is applied to real conditions still considering high nitrate concentration in the influent. Different simulations are carried out, providing an overview on the different scenarios derived from the application of the model.

Chapter 5 **Global sensitivity analysis**: The model is stressed by using different methodologies to perform a global sensitivity analysis and compare the results through different algorithms. The global sensitivity analysis is carried out considering all the kinetic parameters involved in

the model. Furthermore, the results obtained from this analysis will represent a useful tool for the experimental model validation.

Chapter 6 **Conclusion and future perspective**: the future steps of the study are described and an overlook on the feasible experimental validations is provided.

1.3 REFERENCES

[1] C. FN and M. MF, "Factors Affecting Water Pollution: A Review," *J. Ecosyst. Ecography*, vol. 07, no. 01, pp. 5–8, 2017, doi: 10.4172/2157-7625.1000225.

[2] M. F. Carboni, A. P. Florentino, R. B. Costa, X. Zhan, and P. N. L. Lens, "Enrichment of Autotrophic Denitrifiers From Anaerobic Sludge Using Sulfurous Electron Donors," *Front. Microbiol.*, vol. 12, no. June, 2021, doi: 10.3389/fmicb.2021.678323.

[3] M. H. Ward *et al.*, "Workgroup report: Drinking-water nitrate and health - Recent findings and research needs," *Environ. Health Perspect.*, vol. 113, no. 11, pp. 1607–1614, 2005, doi: 10.1289/ehp.8043.

[4] V. Migeot *et al.*, "Drinking-water exposure to a mixture of nitrate and low-dose atrazine metabolites and small-for-gestational age (SGA) babies: A historic cohortstudy," *Environ. Res.*, vol. 122, pp. 58–64, 2013, doi: 10.1016/j.envres.2012.12.007.

[5] R. Picetti *et al.*, "Nitrate and nitrite contamination in drinking water and cancer risk: A systematic review with meta-analysis," *Environ. Res.*, vol. 210, no. February, p. 112988, 2022, doi: 10.1016/j.envres.2022.112988.

[6] M. Tedengren, "Eutrophication and the disrupted nitrogen cycle: This article belongs to Ambio's 50th Anniversary Collection. Theme: Eutrophication," *Ambio*, vol. 50, no. 4, pp. 733–738, 2021, doi: 10.1007/s13280-020-01466-x.

[7] L. Miao, G. Yang, T. Tao, and Y. Peng, "Recent advances in nitrogen removal from landfill leachate using biological treatments – A review," *J. Environ. Manage.*, vol. 235, no. November 2018, pp. 178–185, 2019, doi: 10.1016/j.jenvman.2019.01.057.

[8] S. Sen Wang *et al.*, "Sulfur autotrophic denitrification filter and heterotrophic denitrification filter: Comparison on denitrification performance, hydrodynamic characteristics and operating cost," *Environ. Res.*, vol. 197, no. February, p. 111029, 2021, doi: 10.1016/j.envres.2021.111029.

[9] Y. X. Cui, B. K. Biswal, M. C. M. van Loosdrecht, G. H. Chen, and D. Wu, "Long term performance and dynamics of microbial biofilm communities performing sulfur-oxidizing autotrophic denitrification in a moving-bed biofilm reactor," *Water Res.*, vol.

166, 2019, doi: 10.1016/j.watres.2019.115038.

[10] F. Di Capua, F. Pirozzi, P. N. L. Lens, and G. Esposito, “Electron donors for autotrophic denitrification,” *Chem. Eng. J.*, vol. 362, no. 3, pp. 922–937, 2019, doi: 10.1016/j.cej.2019.01.069.

[11] M. F. Shao, T. Zhang, and H. H. P. Fang, “Sulfur-driven autotrophic denitrification: Diversity, biochemistry, and engineering applications,” *Appl. Microbiol. Biotechnol.*, vol. 88, no. 5, pp. 1027–1042, 2010, doi: 10.1007/s00253-010-2847-1.

[12] Y. X. Cui *et al.*, “Biological nitrogen removal from wastewater using sulphur-driven autotrophic denitrification,” *Appl. Microbiol. Biotechnol.*, vol. 103, no. 15, pp. 6023–6039, 2019, doi: 10.1007/s00253-019-09935-4.

[13] G. Guo *et al.*, “Advances in elemental sulfur-driven bioprocesses for wastewater treatment: From metabolic study to application,” *Water Res.*, vol. 213, no. January, p. 118143, 2022, doi: 10.1016/j.watres.2022.118143.

[14] Y. Y. Qiu *et al.*, “Overlooked pathways of denitrification in a sulfur-based denitrification system with organic supplementation,” *Water Res.*, vol. 169, 2020, doi: 10.1016/j.watres.2019.115084.

[15] Y. Liu *et al.*, “Optimizing sulfur-driven mixotrophic denitrification process: System performance and nitrous oxide emission,” *Chem. Eng. Sci.*, vol. 172, no. 2017, pp. 414–422, 2017, doi: 10.1016/j.ces.2017.07.005.

[16] E. Sahinkaya, A. Kilic, and B. Duygulu, “Pilot and full scale applications of sulfur-based autotrophic denitrification process for nitrate removal from activated sludge process effluent,” *Water Res.*, vol. 60, pp. 210–217, 2014, doi: 10.1016/j.watres.2014.04.052.

Chapter 2

STATE OF THE ART

2.1 AUTOTROPHIC DENITRIFICATION

Nitrogen is naturally present in various biological activities due to its important role as a nutrient, but it could also result from the contamination by industrial wastewater. In particular, nitrogen based compounds could derive from industrial processes or could be present in groundwater due to the extent presence of nitrogen in fertilizers, landfills and animal waste [1], [2]. Increased use of nitrogen in anthropogenic activities related to detergents and industrial wastewater causes an alteration of the nitrogen cycle, leading to an excess of nitrogen compounds in water bodies, that could result in water eutrophication problems. [3]–[5]. The eutrophication phenomena leads to high degradation of the marine and freshwater environment, reducing dissolved oxygen and consequently the possibility of wildlife in water [6]. High nitrogen concentrations in drinking water also bring serious disease such as childhood diabetes, methemoglobinemia known as blue baby syndrome, and cancer [7].

Nowadays, N-based compounds removal from water is performed using various treatments, which could be biological, chemical, or physical. Nevertheless, the most common are represented by biological processes. Among the latter, the most widespread is heterotrophic denitrification, which is considered the "traditional" method for nitrogen removal [8]. This treatment presents many disadvantages such as high sludge production and high cost of maintenance if the addition of an external carbon source is required [9]. A promising alternative to the classical heterotrophic denitrification is sulfur-based autotrophic denitrification, which have become increasingly popular in the field of sustainable, economic, and energy-efficient wastewater treatment in particular for organic deficient wastewater [4], [10]. Indeed, sulfur based autotrophic denitrification leads also to lower sludge production and the cost necessary to the removal of the same quantity of nitrogen compounds are lower with respect to the heterotrophic denitrification [11]. To perform sulfur based autotrophic denitrification different sources of sulfur can be used such mainly represented by: sulfide, thiosulfate, and elemental sulfur [12], [13]. Such different sulfur forms could be used separately or simultaneously in the same bioreactor [14], [15].

Biological denitrification is a reduction process where nitrate is the electron acceptor, and through a series of sequential reductive reactions the various transformations, here reported, occur:

NO_3^- (Nitrate**)→ NO_2^- (**Nitrite**)→ NO (**Nitric oxide**)→N_2O (**Nitrous oxide**)→ N_2 (**Nitrogen gas**)**

The transformations from nitrite into nitric oxide and from nitric oxide to nitrous oxide are usually neglected since the transformation from nitrate into nitrite is considered the limiting step. Thus, the process is usually synthesized as follows:

$$NO_3^- \rightarrow NO_2^- \rightarrow N_2$$

Although we generally consider only these two phases, it is worth noting that nitrous oxide is also a highly contaminating gas that has a strong impact in terms of the greenhouse effect, even in small traces. The importance of defining a proper biological and mathematical model of the process could also help to control the possible emission of N_2O, which is an intermediate of the denitrification process. The emission of N_2O in the denitrification leaded by sulfur compounds is lower than the classical heterotrophic denitrification process. In particular, among the several sulfur sources, elemental sulfur results in even lower emissions of nitrous oxide [4], [16].

2.2 ELEMENTAL SULFUR DRIVEN AUTOTROPHIC DENITRIFICATION

Among the different sulfur sources, elemental sulfur can be considered the most cost-effective electron donor and easily to handle [4], [17]. Usually, it is provided in solid form of lentils, and it could be used not only as electron donor but also as support for the biomass to growth [18]. However, it should be noted that the use of elemental sulfur has the advantage of being able to reuse the sulfur produced as waste from other processes such as gas desulfurization and biogas digester, from which sulfur is usually obtained in solid form [19]–[22]. Instead, the main disadvantages of the elemental sulfur with respect to the other sulfur form are the necessary solubilization prior to be taken up by the microorganisms and the production of sulfate [4], [23].

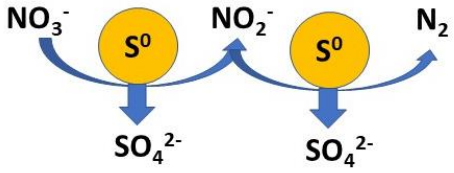

Fig. 2. 1 Two-step denitrification process leaded by elemental sulfur.

The two-step denitrification process driven by elemental sulfur is usually schematized as shown in Fig 2.1, whereby elemental sulfur is required for each transformation and sulfate is produced. The high concentration of sulfate in the effluent represents the main shortcoming of the process because, in high concentrations, it is itself a pollutant.

Another possible disadvantage of using elemental sulfur observed experimentally is related to the possible accumulation of nitrite that could slow or inhibit the process [18]. The nitrite accumulation could occur since nitrate is favored as electron donor with respect to nitrite and consequently could inhibit the process efficiency due to the simultaneous presence of both compounds [24]. Indeed, Sierra-Alvarez et al., 2007 [25], reports high maximum growth rate regarding the autotrophic denitrifiers referred to the transformation of nitrate into nitrite. Because of the necessary solubilization of elemental sulfur, which may not be in sufficient concentrations when required, some studies involve the simultaneous use of different forms of sulfur. Indeed, sometimes sulfide, thiosulfate or both can be supplied in addition to elemental sulfur to reduce nitrite accumulation in the effluent. [14], [26].

However, among all electron donors available for autotrophic denitrification, elemental sulfur also leads to lower accumulation of nitrite with respect to the other sources [27]. It must be also mentioned that elemental sulfur appears as intermediate in the reaction of autotrophic denitrification led by sulfide [28].

Nitrate removal using elemental sulfur can be applied in the case of both low concentrations typical of groundwater and high concentrations from industrial wastewater [25], [29]. The ability to apply the process to systems subject to large variations in nitrate loading makes this system very flexible and useful [30].

The elemental sulfur used in the sulfur driven autotrophic denitrification could be furnished in two different forms which are biogenic sulfur and chemical elemental sulfur [10], [18], [31]. Between organic sulfur and chemical sulfur, the former is a better option in terms of nitrate removal efficiency due to its greater willingness to be absorbed by microorganisms but, as reported by Ucar et al., 2021 [32] ,at the same time it will result in higher by-product production that could lead to higher operational costs if further treatments are required.

Regarding elemental chemical sulfur, the main limiting step is the high time required for its solubilization, which was first evaluated by Anastasiia Kostrytsia et al., 2018 [18], who also identified the presence of a hydrolytic biomass responsible for the solubilization of chemical sulfur into bioavailable sulfur.

The hydrolyzation step represents the limiting stage of the process, which is strongly influenced by the size of the particles used in the reactor [28]. Indeed, sensitivity analysis conducted on

mathematical biological models considering this phase, shows that the hydrolysis constant and particle size are the most sensitive parameters [33], [34].

2.2.1 CHEMICAL, PHYSICAL, AND BIOLOGICAL OVERVIEW OF THE PROCESS

Autotrophic denitrification is strongly dependent on pH and temperature. The pH range in which the best performance of the process has been reached is 7.5-8, while the optimal growth temperature is around 30°C [35]. Maintaining the system in optimal operating condition can avoid the risk of nitrous acid accumulation, which decreases its rate of reduction for lower temperatures [36], [37]. Such results have been widely confirmed experimentally since the investigated conditions represent the most common natural environment for the prolification of the autotrophic denitrifiers, in particular the *Thiobacillus Denitrificans* and *Sulfurimonas*[19], [38], [39].

During sulfur-based autotrophic denitrification, biological analysis shows that when no COD is added, traces of sulfate reducing bacteria (SRB) are found [19], [40], [41]. The presence of these species is also evidenced by a lower effluent sulfate concentration than expected stoichiometrically if a small quantity of COD is added or not [42], [43]. In particular, the presence of SRB is mainly accentuated for reactors which have been in operation for longer periods of time [43]. On the other hand, when COD is provided in higher amount, the biological evidence shows that the preponderant biomass after the autotrophic one is the denitrifying heterotrophic one [44]. This abundance derives from the support given by heterotrophs in terms of removal of Nitrogen compounds. Actually, denitrifying heterotrophs working faster than autotrophs reduce the time required for the N-based compounds.

Sulfur particle size plays a key role relative to sulfur hydrolysis, as reported by A. Kostrytsia et al., 2018's sensitivity analysis [33]. Indeed, to achieve high solubility, it is necessary to have a high specific surface area, which is achieved by reducing the particle size, which usually takes values between 0.5 and 0.6 mm. At the same time, the particles should not be too small to avoid problems of reduced porosity and process efficiency [23], [45].

2.2.2 REACTOR CONFIGURATION

Autotrophic denitrification by elemental sulfur can be carried out in different reactor configurations: packed bed reactors [46], [47], membrane reactors [10] and moving bed biofilm reactor [14]. Among these, the most widely used configuration is the packed-bed reactor, due to its solid form of the sulfur, which allows a high concentration of biomass growing attached to a support usually represented by the sulfur lentils themselves. In addition, this reactor configuration results in a lower concentration of secondary pollutants, consequently reducing the possibility of affecting subsequent processes, if present. Also, pilot full scale application of sulfur based autotrophic denitrification in packed bed reactor has been carried out by Sahinkaya et al., 2014 [48], where domestic wastewater have been used as influent and COD was also present in the influent. In this case the small quantity of COD have reported to be a valid support both for denitrification both to maintain acceptable values of acidity which could be a serious problem in pure sulfur-based autotrophic denitrification [49].

In addition, among the already mentioned advantages of sulfur-based autotrophic denitrification, it should be noted that studies have been conducted using different substrates in the tributary, such as wastewater obtained from graphite production [38]. Another advantage is the fast recovery time of the system following forced long-term interruptions showed during laboratory experiments, which can be a positive factor in case of influent arrival interruptions [46]. Furthermore also the longer solid retention time helps to reduce the shortcomings related to the process [50].

Mathematical modelling represents the most useful tool to support the development of higher scale treatment plant for accessibility to elemental sulfur for the microbial families [28].

2.3 ELEMENTAL SULFUR WITH COD

Given the necessary solubilization of elemental sulfur to be utilized by biomass, the system can lead to a slowdown in denitrification by autotrophic pathways, particularly for high nitrate concentrations. A solution to speed up the process and prevent nitrite accumulation could be encouraging the growth of heterotrophic denitrifiers [9], [51]. Indeed, by the addition of COD to sulfur-based autotrophic denitrification system, lower concentration of sulfate are present in the effluent than pure autotrophic denitrification, which enhances a stable growth of biofilm [52].

When elemental sulfur is used as electron donor in autotrophic denitrification and the process is coupled with heterotrophic denitrification supported by external carbon source addition, it results easier to achieve a balance of the alkalinity in the system without the addition of limestone, which could affect the water quality and further increase the cost of the process [4], [50], [53].

To promote the growth of heterotrophic species via external carbon source addition, an appropriate quantity of COD to stimulate the growth of heterotrophic denitrifiers must be provided. It is important to note that this solution should be carefully carried out, to avoid several shortcomings, such as high concentrations of COD in the effluent or the prevalence of denitrifying heterotrophs over autotrophs. Indeed, as the heterotrophic biomass has a higher growth rate, it could prevail bringing to the failure of the system. In addition, if the amount of COD relative to C/N remains less than 0.5, it maintains a good trade-off between autotrophic and heterotrophic denitrification [44].

Different organic substrates have been experimentally tested to favor the growth of the heterotrophic denitrifiers, in particular Oh et al., 2003 [51], reported that acetate and ethanol are the ones with the lowest inhibition towards autotrophic biomass in elemental sulfur-based autotrophic system. In contrast, when methanol is furnished, despite being the most widely used compound in heterotrophic denitrification, it turns out to have the slowest response when added to the system [54].

The external carbon source could be provided not only in liquid form, but also in solid form, for example by using wood, as reported by Yamashita et al., 2011 [55], where sulfate reduction and heterotrophic denitrification also take place. Indeed, heterotrophic denitrification and sulfate reduction can occur simultaneously to autotrophic denitrification due to the presence of organic carbon and sulphate. In addition, providing an external carbon source could help reduce the problem associated with N_2O production and nitrite accumulation [13].

In addition, the simultaneous growth of heterotrophic denitrifiers could be useful if there is an unexpected increase in the concentration of N compounds in the influent, since it is possible to maintain the same performances feeding the reactor with an higher amount of organic matter,

To reduce the negative aspects of the autotrophic denitrification mainly caused by the production of sulfate, some model and experimental works have been carried out coupling with heterotrophic denitrification to optimize the process [44], [50], [56].

2.4 SIMULTANEOUS REMOVAL OF C, N, S

Mixotrophic denitrification is defined as the simultaneous occurrence of autotrophic and heterotrophic denitrification. From the biological evidence reported in previous experimental studies, different heterotrophic species have been encountered during sulfur based autotrophic denitrification such as heterotrophic denitrifiers and sulfate reducing bacteria. An overlook on the process involving such species is provided in this work of thesis.

Wastewater could derive from different sources which means that different concentration of various pollutants can be present. The most common contaminants are represented by organic matter, nitrogen compounds and sulfur compounds. Indeed, many industrial wastewaters could have higher concentrations of Sulfur or Nitrogen and organic compounds simultaneously. Several studies have proved that it is possible to have the co-presence of different microbial families such as heterotrophic denitrifiers, sulfate reducing bacteria and autotrophic denitrifiers, working together without inhibiting each other. Those works have been mainly carried out to analyze the simultaneous removal of sulfide nitrate and organic carbon [53], [57], [58]. Furthermore, other studies have been carried out to evaluate just the process improvement of the autotrophic denitrification with the addition of external carbon source [13], [45].

However, in previous works elemental sulfur is usually considered as end-product, since it represents the results of the sulfide oxidation [57]. Furthermore, it results that the systems where different microbial families are involved are more robust, implying that variations of influent concentrations can be better withstood compared to the systems working with a single process [59].

2.5 MATHEMATICAL MODELLING

2.5.1 ELEMENTAL SULFUR-BASED MODEL

The first model regarding the autotrophic denitrification based on elemental sulfur is the kinetic model developed by Batchelor and Lawrence, 1978 [60], where a biofilm growing on the sulfur particle is described. In the field of Sulfur based autotrophic denitrification, this model represents the oldest model reported in literature. Its model assumptions, based on scientific evidence, have been considered in all the subsequent models. In this model, during the biological process two main steps are identified: Sulfur has to be hydrolyzed and transported

into the biofilm to be used by the microbial families; simultaneously nitrate needs to diffuse from the bulk liquid to the biofilm. Indeed, other models have demonstrated that the low solubility of the elemental sulfur is related to the particle size where the biofilm is supposed to growth on, which consequently affects the reaction velocity of the process [61], [62].

The model presented by Anastasiia Kostrytsia et al., 2018 [18], is the first model which takes into account the hydrolysis step considering the presence of an hydrolytic biomass necessary growing on the sulfur lentil responsible for the transformation of chemical elemental sulfur into bioavailable sulfur. This step is related to physical properties and hydrolytic biomass. Such parameters resulted in the bottleneck parameters of the whole process by the local sensitivity analysis A. Kostrytsia et al., 2018 [33]. This model was validated by Huiliñir et al., 2020 [34], which also performed a local sensitivity analysis and confirmed the results previously obtained. The results given by these confirm what has been experimentally observed: a sulfur lentil with higher specific surface area can speed up the process. Other modelling works related to the use of pure elemental sulfur performed a sensitivity analysis mainly on the parameters related to the biofilm growth [63]. Furthermore, other experimental studies confirmed that no inhibition term needs to be considered if the autotrophic biomass considered is previously acclimatized [64].

Table 2. 1 Resume of the models performing sulfur based autotrophic denitrification leaded by elemental sulfur.

Type of reactor	**Type of equations**	**Order of the kinetic S^0**	**Order of the kinetic NO_3^-**	**Order of the kinetic NO_2^-**	**Inhibition term**	**Hydrolysis**	**Sensitivity analysis**	**N_2O step**	**Ref.**
Batch	PDE	First-order	Zero-order	Not present	NO	Considered but not evaluated	NO	NO	[60]
Packed bed reactor	PDE	Not reported	Half-order	Not present	NO	Considered but not evaluated	NO	NO	[61]
Packed bad reactor	PDE	Not reported	Half-order	Not present	NO	Considered but not evaluated	NO	NO	[62]
Packed bad reactor	PDE	Not reported	Half-order	Not present	NO	Considered but not evaluated	NO	NO	[47]
Batch reactor	PDE	Not reported	Half order	Not present	NO	Considered but not evaluated	NO	NO	[65]
Batch reactor	ODE	First order	2 order	2 order	YES	Evaluated	YES[33]	NO	[18]
Batch reactor	ODE and PDE	Not reported	2 order	2 order	NO	Considered but not evaluated	YES	SI	[63]
Batch reactor	ODE	First order	2 order	2 order	NO	Evaluated	YES	NO	[34]
Fixed bed columns	Polynomial equation	Not reported	Not reported	Not reported	NO	Considered but not evaluated	NO	NO	[66]

All models reported in Table 2.1 consider the growth of species on the sulfur lentils and have been experimentally calibrated manly using packed bed reactor. In these cases, nitrate diffusion within the biofilm, whose thickness is fixed, is modeled. The parameters are calibrated using different biofilm dimensions. Some biofilm models have been developed considering the uptake of three different sulfur forms such as sulfide, elemental sulfur, and thiosulfate [14]. Some of them identify as a rate limiting factor the mass transport and diffusion within the biofilm [14]. As for the case of the model of by Decru et al., 2021 [14] which is modelled using biofilm assumption. Also, this model has been subjected to a local sensitivity analysis where the parameters related to the affinity between elemental sulfur and biomass have been investigated.

Models describing sulfur-based autotrophic denitrification can be based on different kinetic orders, starting with zero-order kinetics, moving through 1/2-order kinetics, first-order kinetics, and second-order kinetics. The choice of the kinetic order depends on the experimental results obtained and the calibrated kinetic parameters. In the case of pure elemental sulfur, the kinetics

are related to biofilm models that grow on sulfur lentils and present mostly half-order reaction kinetics.

The last model reported in Table 2.1 is a mathematical model experimentally calibrated but whose equations are defined on a response surface model which results useful only to give a preview on the system dimension and removal efficiency [66]. The model has been developed using a first order polynomial equation calibrated with new experimental data. The output surface is defined by three parameters: nitrate in the inlet, nitrate in the outlet, and hydraulic retention time, giving to this model a useful tool in the practical specific application.

2.5.2 ELEMENTAL SULFUR-BASED MODEL WITH COD ADDITION

Since the necessity to improve the process of sulfur based autotrophic denitrification based on elemental sulfur and to prevent nitrite accumulation reducing the concentration of sulfate in the effluent, mathematical models accounting the addition of COD have been developed and experimentally calibrated.

The COD addition can reduce the sulfate concentration in the effluent and promote the growth of heterotrophic biomass, which denitrifies some of the nitrite and nitrate leading to a reduction of sulfates concentration in the effluent [44], [50], [59], [67]. Moreover, some model considers the nitrous oxide production, limiting its formation by adding COD to the autotrophic denitrification system, so in mixotrophic conditions [50].

Mathematical models have been developed considering the simultaneous presence of both autotrophic and heterotrophic species to mitigate the disadvantage of both processes, due to the necessity to treat water with high concentrations of nitrate and low concentrations of COD [44], [68]. Those models consider the elemental sulfur based autotrophic denitrification as the main process and evaluate interactions with heterotrophic denitrifiers following the addition of external COD [69], [70]. Furthermore, all models reported in the literature are derived by mass balances considerations and consist of ordinary differential equations (ODEs). Particular mention should be given to the model developed by Liu et al., 2017 [50], in which the addition of COD is carried out to optimize the process not only focusing on nitrate removal and sulfate production in mixotrophic denitrification, but also considering the N_2O emission.

2.5.3 MIXOTROPHIC MODEL

Other models have been developed considering both autotrophic and heterotrophic families for the simultaneous removal of sulfide, nitrate, and acetate [57]. Indeed, mixotrophic models have been widely developed usually to consider the simultaneous presence of nitrogen, carbon and sulfur compounds [71]. In those models, the presence of the elemental sulfur is represented as intermediate of reaction for the sulfide removal.

With respect to the models using elemental sulfur as main electron, the models which consider sulfide as main source can provide a realistic ratio between sulfur and carbon source utilized. This is because elemental sulfur is supplied in solid form and time for solubilization is required, and, for these reasons, it is added in excess within the system. This causes the ratio between carbon and sulfur to become an influential parameter for nitrogen compound removal in these models [57], [58]. Such model are all developed assuming that those processes occur in a reactor that could be modelled using ODEs [57], [58].

2.6 SHORT OVERVIEW ON SMP

From the theory developed by Laspidou and Rittmann, 2002 [72] and proved by experimental validation the SMP are naturally produced from different and various types of biomass during the biological processes. Their formation and utilization have been studied in various biological processes, although an analysis of them has not been carried out in every study because of their difficult experimental identification.

Indeed, the evaluation of the SMP in terms of production and consumption have been carried out not only for the pure heterotrophic denitrifiers, but also for the sulfate reducing bacteria for different values of pH and temperature [73].

Since the soluble microbial products and the cell lysis are inevitable in a biological reactor, heterotrophic families are commonly found in reactors, leading to a faster development of the process [36], [44], [45] .

The production and the consumption of those substances have been studied in different systems and result that is mainly associated with the growth of heterotrophic families [74]. Furthermore, the production and consumption of the SMP is enhanced when the system undergoes to fast-famine conditions where their accumulation and then utilization are strong [72], [75]–[77].

Nowadays, there is an increasing interest in analyzing how those substances support and favor the growth of heterotrophic families [78].

The presence of SMP in effluent can cause serious problems if the system is subjected to further treatment, such as fouling problems in membrane reactors or production of other by-products as a result of disinfection treatments [46], [79], [80]. Since those considerations, the relations between the sulfur based autotrophic denitrification and SMP production has been investigated in the study by Ucar et al., 2021 [32] which analyzed the production of SMP using chemical elemental sulfur and biological elemental sulfur. However, none of the previous studies have calibrated the specific parameters related to the SMP production of the autotrophic denitrifiers during sulfur based autotrophic denitrification.

2.7 REFERENCES

[1] H. Chen *et al.*, "Full-scale evaluation of aerobic/extended-idle regime inducing biological phosphorus removal and its integration with intermittent sand filter to treat domestic sewage discharged from highway rest area," *Biochem. Eng. J.*, vol. 113, pp. 114–122, 2016, doi: 10.1016/j.bej.2016.06.002.

[2] W. Li, Q. liang Zhao, and H. Liu, "Sulfide removal by simultaneous autotrophic and heterotrophic desulfurization-denitrification process," *J. Hazard. Mater.*, vol. 162, no. 2–3, pp. 848–853, 2009, doi: 10.1016/j.jhazmat.2008.05.108.

[3] M. O. Rivett, S. R. Buss, P. Morgan, J. W. N. Smith, and C. D. Bemment, "Nitrate attenuation in groundwater: A review of biogeochemical controlling processes," *Water Res.*, vol. 42, no. 16, pp. 4215–4232, 2008, doi: 10.1016/j.watres.2008.07.020.

[4] Y. X. Cui *et al.*, "Biological nitrogen removal from wastewater using sulphur-driven autotrophic denitrification," *Appl. Microbiol. Biotechnol.*, vol. 103, no. 15, pp. 6023–6039, 2019, doi: 10.1007/s00253-019-09935-4.

[5] F. T. Wakida and D. N. Lerner, "Non-agricultural sources of groundwater nitrate: A review and case study," *Water Res.*, vol. 39, no. 1, pp. 3–16, 2005, doi: 10.1016/j.watres.2004.07.026.

[6] J. W. Roy and G. Bickerton, "Proactive screening approach for detecting groundwater contaminants along urban streams at the reach-scale," *Environ. Sci. Technol.*, vol. 44, no. 16, pp. 6088–6094, 2010, doi: 10.1021/es101492x.

[7] L. Knobeloch, B. Salna, A. Hogan, J. Postle, and H. Anderson, "Blue babies and nitrate-contaminated well water," *Environ. Health Perspect.*, vol. 108, no. 7, pp. 675–678, 2000, doi: 10.1289/ehp.00108675.

[8] L. L. Zhuang, T. Yang, J. Zhang, and X. Li, "The configuration, purification effect and mechanism of intensified constructed wetland for wastewater treatment from the aspect of nitrogen removal: A review," *Bioresour. Technol.*, vol. 293, no. July, 2019, doi: 10.1016/j.biortech.2019.122086.

[9] L. Christianson, C. Lepine, S. Tsukuda, K. Saito, and S. Summerfelt, "Nitrate removal effectiveness of fluidized sulfur-based autotrophic denitrification biofilters for

recirculating aquaculture systems," *Aquac. Eng.*, vol. 68, pp. 10–18, 2015, doi: 10.1016/j.aquaeng.2015.07.002.

[10] D. Ucar, T. Yilmaz, F. Di Capua, G. Esposito, and E. Sahinkaya, "Comparison of biogenic and chemical sulfur as electron donors for autotrophic denitrification in sulfur-fed membrane bioreactor (SMBR)," *Bioresour. Technol.*, vol. 299, no. October 2019, p. 122574, 2020, doi: 10.1016/j.biortech.2019.122574.

[11] J. Yang *et al.*, "Effects of different electron donors on nitrogen removal performance and microbial community of denitrification system," *J. Environ. Chem. Eng.*, vol. 10, no. 3, p. 107915, 2022, doi: 10.1016/j.jece.2022.107915.

[12] F. Di Capua, F. Pirozzi, P. N. L. Lens, and G. Esposito, "Electron donors for autotrophic denitrification," *Chem. Eng. J.*, vol. 362, no. 3, pp. 922–937, 2019, doi: 10.1016/j.cej.2019.01.069.

[13] R. B. Cardoso, R. Sierra-Alvarez, P. Rowlette, E. R. Flores, J. Gómez, and J. A. Field, "Sulfide oxidation under chemolithoautotrophic denitrifying conditions," *Biotechnol. Bioeng.*, vol. 95, no. 6, pp. 1148–1157, 2006, doi: 10.1002/bit.21084.

[14] S. O. Decru, J. E. Baeten, Y.-X. Cui, D. Wu, G.-H. Chen, and E. I. P. Volcke, "Model-based analysis of sulfur-based denitrification in a moving bed biofilm reactor," *Environ. Technol.*, vol. 0, no. 0, pp. 1–8, 2021, doi: 10.1080/09593330.2021.1910349.

[15] S. Feng *et al.*, "Simultaneous denitrification and desulfurization-S0 recovery of wastewater in trickling filters by bioaugmentation intervention based on avoiding collapse critical points," *J. Environ. Manage.*, vol. 292, no. March, p. 112834, 2021, doi: 10.1016/j.jenvman.2021.112834.

[16] W. Yang, Q. Zhao, H. Lu, Z. Ding, L. Meng, and G. H. Chen, "Sulfide-driven autotrophic denitrification significantly reduces N2O emissions," *Water Res.*, vol. 90, pp. 176–184, 2016, doi: 10.1016/j.watres.2015.12.032.

[17] L. Wu *et al.*, "Denitrifying biofilm processes for wastewater treatment: Developments and perspectives," *Environ. Sci. Water Res. Technol.*, vol. 7, no. 1, pp. 40–67, 2021, doi: 10.1039/d0ew00576b.

[18] A. Kostrytsia *et al.*, "Elemental sulfur-based autotrophic denitrification and

denitritation: microbially catalyzed sulfur hydrolysis and nitrogen conversions," *J. Environ. Manage.*, vol. 211, pp. 313–322, Apr. 2018, doi: 10.1016/j.jenvman.2018.01.064.

[19] Y. Wang, C. Bott, and R. Nerenberg, "Sulfur-based denitrification: Effect of biofilm development on denitrification fluxes," *Water Res.*, vol. 100, pp. 184–193, Sep. 2016, doi: 10.1016/j.watres.2016.05.020.

[20] A. Giordano, F. Di Capua, G. Esposito, and F. Pirozzi, "Long-term biogas desulfurization under different microaerobic conditions in full-scale thermophilic digesters co-digesting high-solid sewage sludge," *Int. Biodeterior. Biodegrad.*, vol. 142, no. May, pp. 131–136, 2019, doi: 10.1016/j.ibiod.2019.05.017.

[21] Z. Yuan *et al.*, "Efficient nitrite accumulation and elemental sulfur recovery in partial sulfide autotrophic denitrification system: Insights of seeding sludge, S/N ratio and flocculation strategy," *Chemosphere*, vol. 288, no. September, p. 132388, 2022, doi: 10.1016/j.chemosphere.2021.132388.

[22] F. Chen *et al.*, "Recirculation ratio regulates denitrifying sulfide removal and elemental sulfur recovery by altering sludge characteristics and microbial community composition in an EGSB reactor," *Environ. Res.*, vol. 181, no. November 2019, p. 108905, 2020, doi: 10.1016/j.envres.2019.108905.

[23] G. Guo *et al.*, "Advances in elemental sulfur-driven bioprocesses for wastewater treatment: From metabolic study to application," *Water Res.*, vol. 213, no. January, p. 118143, 2022, doi: 10.1016/j.watres.2022.118143.

[24] C. Glass and J. Silverstein, "Denitrification kinetics of high nitrate concentration water: pH effect on inhibition and nitrite accumulation," *Water Res.*, vol. 32, no. 3, pp. 831–839, 1998, doi: 10.1016/S0043-1354(97)00260-1.

[25] R. Sierra-Alvarez, R. Beristain-Cardoso, M. Salazar, J. Gómez, E. Razo-Flores, and J. A. Field, "Chemolithotrophic denitrification with elemental sulfur for groundwater treatment," *Water Res.*, vol. 41, no. 6, pp. 1253–1262, 2007, doi: 10.1016/j.watres.2006.12.039.

[26] H. X. Bao *et al.*, "Mitigating nitrite accumulation during S0-based autotrophic denitrification: Balancing nitrate-nitrite reduction rate with thiosulfate as external

electron donor," *Environ. Res.*, vol. 204, no. September 2021, 2022, doi: 10.1016/j.envres.2021.112016.

[27] M. F. Carboni, A. P. Florentino, R. B. Costa, X. Zhan, and P. N. L. Lens, "Enrichment of Autotrophic Denitrifiers From Anaerobic Sludge Using Sulfurous Electron Donors," *Front. Microbiol.*, vol. 12, no. June, 2021, doi: 10.3389/fmicb.2021.678323.

[28] L. Zhang, Y. Y. Qiu, Y. Zhou, G. H. Chen, M. C. M. van Loosdrecht, and F. Jiang, "Elemental sulfur as electron donor and/or acceptor: Mechanisms, applications and perspectives for biological water and wastewater treatment," *Water Res.*, vol. 202, no. June, p. 117373, 2021, doi: 10.1016/j.watres.2021.117373.

[29] C. Zeng *et al.*, "Elemental sulfur-driven autotrophic denitrification for advanced nitrogen removal from mature landfill leachate after PN/A pretreatment," *Chem. Eng. J.*, vol. 410, no. September 2020, pp. 1–10, 2021, doi: 10.1016/j.cej.2020.128256.

[30] W. Zhou *et al.*, "Sulfur-based autotrophic denitrification from the micro-polluted water," *J. Environ. Sci. (China)*, vol. 44, pp. 180–188, 2016, doi: 10.1016/j.jes.2016.01.002.

[31] F. Di Capua *et al.*, "Elemental sulfur-based autotrophic denitrification and denitritation: microbially catalyzed sulfur hydrolysis and nitrogen conversions," *Bioresour. Technol.*, vol. 211, no. August, pp. 359–367, Nov. 2018, doi: 10.1016/j.jenvman.2018.01.064.

[32] D. Ucar, F. Di Capua, A. Yücel, T. Nacar, and E. Sahinkaya, "Effect of nitrogen loading on denitrification, denitritation and filtration performances of membrane bioreactors fed with biogenic and chemical elemental sulfur," *Chem. Eng. J.*, vol. 419, no. February, 2021, doi: 10.1016/j.cej.2021.129514.

[33] A. Kostrytsia, S. Papirio, M. R. Mattei, L. Frunzo, P. N. L. Lens, and G. Esposito, "Sensitivity analysis for an elemental sulfur-based two-step denitrification model," *Water Sci. Technol.*, vol. 78, no. 6, pp. 1296–1303, Nov. 2018, doi: 10.2166/wst.2018.398.

[34] C. Huiliñir *et al.*, "Elemental sulfur-based autotrophic denitrification in stoichiometric S0/N ratio: Calibration and validation of a kinetic model," *Bioresour. Technol.*, vol. 307, Jul. 2020, doi: 10.1016/j.biortech.2020.123229.

[35] C. Fajardo, M. Mora, I. Fernández, A. Mosquera-Corral, J. L. Campos, and R. Méndez, "Cross effect of temperature, pH and free ammonia on autotrophic denitrification process with sulphide as electron donor," *Chemosphere*, vol. 97, pp. 10–15, 2014, doi: 10.1016/j.chemosphere.2013.10.028.

[36] J. J. Wang, B. C. Huang, J. Li, and R. C. Jin, "Advances and challenges of sulfur-driven autotrophic denitrification (SDAD) for nitrogen removal," *Chinese Chem. Lett.*, vol. 31, no. 10, pp. 2567–2574, 2020, doi: 10.1016/j.cclet.2020.07.036.

[37] Y. Liu *et al.*, "Evaluation of nitrous oxide emission from sulfide- and sulfur-based autotrophic denitrification processes," *Environ. Sci. Technol.*, vol. 50, no. 17, pp. 9407–9415, 2016, doi: 10.1021/acs.est.6b02202.

[38] X. Xu, R. Zhang, H. Jiang, and F. Yang, "Sulphur-based autotrophic denitrification of wastewater obtained following graphite production: Long-term performance, microbial communities involved, and functional gene analysis," *Bioresour. Technol.*, vol. 306, no. January, p. 123117, 2020, doi: 10.1016/j.biortech.2020.123117.

[39] F. Di Capua, S. H. Ahoranta, S. Papirio, P. N. L. Lens, and G. Esposito, "Impacts of sulfur source and temperature on sulfur-driven denitrification by pure and mixed cultures of Thiobacillus," *Process Biochem.*, vol. 51, no. 10, pp. 1576–1584, Oct. 2016, doi: 10.1016/j.procbio.2016.06.010.

[40] W. Li *et al.*, "Metagenomics and metatranscriptomics uncover the microbial community associated with high S0 production in a denitrifying desulfurization granular sludge reactor," *Water Res.*, vol. 203, no. August, p. 117505, 2021, doi: 10.1016/j.watres.2021.117505.

[41] R. Khanongnuch, F. Di Capua, A. M. Lakaniemi, E. R. Rene, and P. N. L. Lens, "Long-term performance evaluation of an anoxic sulfur oxidizing moving bed biofilm reactor under nitrate limited conditions," *Environ. Sci. Water Res. Technol.*, vol. 5, no. 6, pp. 1072–1081, 2019, doi: 10.1039/c9ew00220k.

[42] G. Xu, C. Feng, F. Fang, S. Chen, Y. Xu, and X. Wang, "The heterotrophic-combined-with-autotrophic denitrification process: Performance and interaction mechanisms," *Water Sci. Technol.*, vol. 71, no. 8, pp. 1212–1218, 2015, doi: 10.2166/wst.2015.097.

[43] Y. X. Cui, B. K. Biswal, M. C. M. van Loosdrecht, G. H. Chen, and D. Wu, "Long

term performance and dynamics of microbial biofilm communities performing sulfur-oxidizing autotrophic denitrification in a moving-bed biofilm reactor," *Water Res.*, vol. 166, 2019, doi: 10.1016/j.watres.2019.115038.

[44] Y. Y. Qiu *et al.*, "Overlooked pathways of denitrification in a sulfur-based denitrification system with organic supplementation," *Water Res.*, vol. 169, 2020, doi: 10.1016/j.watres.2019.115084.

[45] E. Sahinkaya and N. Dursun, "Sulfur-oxidizing autotrophic and mixotrophic denitrification processes for drinking water treatment: Elimination of excess sulfate production and alkalinity requirement," *Chemosphere*, vol. 89, no. 2, pp. 144–149, 2012, doi: 10.1016/j.chemosphere.2012.05.029.

[46] G. Asik, T. Yilmaz, F. Di Capua, D. Ucar, G. Esposito, and E. Sahinkaya, "Sequential sulfur-based denitrification/denitritation and nanofiltration processes for drinking water treatment," *J. Environ. Manage.*, vol. 295, no. June, p. 113083, 2021, doi: 10.1016/j.jenvman.2021.113083.

[47] H. S. Moon, K. H. Ahn, S. Lee, K. Nam, and J. Y. Kim, "Use of autotrophic sulfur-oxidizers to remove nitrate from bank filtrate in a permeable reactive barrier system," *Environ. Pollut.*, vol. 129, no. 3, pp. 499–507, Jun. 2004, doi: 10.1016/j.envpol.2003.11.004.

[48] E. Sahinkaya, A. Kilic, and B. Duygulu, "Pilot and full scale applications of sulfur-based autotrophic denitrification process for nitrate removal from activated sludge process effluent," *Water Res.*, vol. 60, pp. 210–217, 2014, doi: 10.1016/j.watres.2014.04.052.

[49] G. Xu *et al.*, "Evaluation of simultaneous autotrophic and heterotrophic denitrification processes and bacterial community structure analysis," *Appl. Microbiol. Biotechnol.*, vol. 99, no. 15, pp. 6527–6536, Aug. 2015, doi: 10.1007/s00253-015-6532-2.

[50] Y. Liu *et al.*, "Optimizing sulfur-driven mixotrophic denitrification process: System performance and nitrous oxide emission," *Chem. Eng. Sci.*, vol. 172, no. 2017, pp. 414–422, 2017, doi: 10.1016/j.ces.2017.07.005.

[51] S. E. Oh, M. S. Bum, Y. B. Yoo, A. Zubair, and I. S. Kim, "Nitrate removal by simultaneous sulfur utilizing autotrophic and heterotrophic denitrification under

different organics and alkalinity conditions: Batch experiments," *Water Sci. Technol.*, vol. 47, no. 1, pp. 237–244, 2003, doi: 10.2166/wst.2003.0061.

[52] L. Tang, J. Li, Y. Li, X. Zhang, and X. Shi, "Mixotrophic denitrification processes based on composite filler for low carbon/nitrogen wastewater treatment," *Chemosphere*, vol. 286, no. August 2021, p. 131781, 2021, doi: 10.1016/j.chemosphere.2021.131781.

[53] K. Y. Show, D. J. Lee, and X. Pan, "Simultaneous biological removal of nitrogen-sulfur-carbon: Recent advances and challenges," *Biotechnol. Adv.*, vol. 31, no. 4, pp. 409–420, 2013, doi: 10.1016/j.biotechadv.2012.12.006.

[54] L. Zhang, C. Zhang, C. Hu, H. Liu, Y. Bai, and J. Qu, "Sulfur-based mixotrophic denitrification corresponding to different electron donors and microbial profiling in anoxic fluidized-bed membrane bioreactors," *Water Res.*, vol. 85, pp. 422–431, 2015, doi: 10.1016/j.watres.2015.08.055.

[55] T. Yamashita, R. Yamamoto-Ikemoto, and J. Zhu, "Sulfate-reducing bacteria in a denitrification reactor packed with wood as a carbon source," *Bioresour. Technol.*, vol. 102, no. 3, pp. 2235–2241, 2011, doi: 10.1016/j.biortech.2010.10.015.

[56] E. Sahinkaya, N. Dursun, A. Kilic, S. Demirel, S. Uyanik, and O. Cinar, "Simultaneous heterotrophic and sulfur-oxidizing autotrophic denitrification process for drinking water treatment: Control of sulfate production," *Water Res.*, vol. 45, no. 20, pp. 6661–6667, 2011, doi: 10.1016/j.watres.2011.09.056.

[57] X. Xu *et al.*, "Simultaneous removal of sulfide, nitrate and acetate under denitrifying sulfide removal condition: Modeling and experimental validation," *J. Hazard. Mater.*, vol. 264, pp. 16–24, Jan. 2014, doi: 10.1016/j.jhazmat.2013.10.056.

[58] X. J. Xu *et al.*, "Mathematical modeling of simultaneous carbon-nitrogen-sulfur removal from industrial wastewater," *J. Hazard. Mater.*, vol. 321, pp. 371–381, 2017, doi: 10.1016/j.jhazmat.2016.08.074.

[59] E. Sahinkaya and A. Kilic, "Heterotrophic and elemental-sulfur-based autotrophic denitrification processes for simultaneous nitrate and Cr(VI) reduction," *Water Res.*, vol. 50, no. Reaction 1, pp. 278–286, 2014, doi: 10.1016/j.watres.2013.12.005.

[60] B. Batchelor and A. W. Lawrence, “Autotrophic Denitrification Using Elemental Sulfur,” 1978.

[61] A. Koenig and L. H. Liu, “Kinetic model of autotrophic denitrification in sulphur packed-bed reactors,” *Water Res.*, vol. 35, no. 8, pp. 1969–1978, 2001, doi: 10.1016/S0043-1354(00)00483-8.

[62] A. Darbi and T. Viraraghavan, “A kinetic model for autotrophic denitrification using sulphur: Limestone reactors,” *Water Qual. Res. J. Canada*, vol. 38, no. 1, pp. 183–192, 2003, doi: 10.2166/wqrj.2003.012.

[63] Y. Wang, F. Sabba, C. Bott, and R. Nerenberg, “Using kinetics and modeling to predict denitrification fluxes in elemental-sulfur-based biofilms,” *Biotechnol. Bioeng.*, vol. 116, no. 10, pp. 2698–2709, Oct. 2019, doi: 10.1002/bit.27094.

[64] J. L. Campos, S. Carvalho, R. Portela, A. Mosquera-Corral, and R. Méndez, “Kinetics of denitrification using sulphur compounds: Effects of S/N ratio, endogenous and exogenous compounds,” *Bioresour. Technol.*, vol. 99, no. 5, pp. 1293–1299, 2008, doi: 10.1016/j.biortech.2007.02.007.

[65] N. A. Qambrani, Y. S. Jung, J. E. Yang, Y. S. Ok, and S. E. Oh, “Application of half-order kinetics to sulfur-utilizing autotrophic denitrification for groundwater remediation,” *Environ. Earth Sci.*, vol. 73, no. 7, pp. 3445–3450, 2015, doi: 10.1007/s12665-014-3641-7.

[66] T. C. Zhang and H. Zeng, “Development of a Response Surface for Prediction of Nitrate Removal in Sulfur–Limestone Autotrophic Denitrification Fixed-Bed Reactors,” *J. Environ. Eng.*, vol. 132, no. 9, pp. 1068–1072, 2006, doi: 10.1061/(asce)0733-9372(2006)132:9(1068).

[67] D. Yánez, L. Guerrero, R. Borja, and C. Huiliñir, “Sulfur-based mixotrophic denitrification with the stoichiometric S0/N ratio and methanol supplementation: effect of the C/N ratio on the process,” *J. Environ. Sci. Heal. Part A*, vol. 56, no. 13, pp. 1420–1427, Nov. 2021, doi: 10.1080/10934529.2021.2004839.

[68] S. E. Oh, Y. B. Yoo, J. C. Young, and I. S. Kim, “Effect of organics on sulfur-utilizing autotrophic denitrification under mixotrophic conditions,” *J. Biotechnol.*, vol. 92, no. 1, pp. 1–8, 2001, doi: 10.1016/S0168-1656(01)00344-3.

[69] G. Guerriero, M. R. Mattei, S. Papirio, G. Esposito, and L. Frunzo, “Modelling the effect of SMP production and external carbon addition on S-driven autotrophic denitrification,” *Sci. Rep.*, vol. 12, no. 1, Dec. 2022, doi: 10.1038/S41598-022-10944-Z.

[70] Y. Yuan *et al.*, “Continuous sulfur biotransformation in an anaerobic-anoxic sequential batch reactor involving sulfate reduction and denitrifying sulfide oxidization,” *Chemosphere*, vol. 234, pp. 568–578, 2019, doi: 10.1016/j.chemosphere.2019.06.109.

[71] L. Guerrero *et al.*, “Autotrophic and heterotrophic denitrification for simultaneous removal of nitrogen, sulfur and organic matter,” *J. Environ. Sci. Heal. - Part A Toxic/Hazardous Subst. Environ. Eng.*, vol. 51, no. 8, pp. 650–655, 2016, doi: 10.1080/10934529.2016.1159875.

[72] C. S. Laspidou and B. E. Rittmann, “Non-steady state modeling of extracellular polymeric substances, soluble microbial products, and active and inert biomass,” *Water Res.*, vol. 36, no. 8, pp. 1983–1992, 2002, doi: 10.1016/S0043-1354(01)00414-6.

[73] J. Qian, J. Zhou, X. Pei, M. Zhang, and Y. Liu, “Bioactivities and formation/utilization of soluble microbial products (SMP) in the biological sulfate reduction under different conditions,” *Chemosphere*, vol. 221, pp. 37–44, 2019, doi: 10.1016/j.chemosphere.2018.12.208.

[74] J. Yang, X. Zhang, Y. Sun, A. Li, and F. Ma, “Formation of soluble microbial products and their contribution as electron donors for denitrification,” *Chem. Eng. J.*, vol. 326, pp. 1159–1165, 2017, doi: 10.1016/j.cej.2017.06.063.

[75] B. J. Ni, B. E. Rittmann, F. Fang, J. Xu, and H. Q. Yu, “Long-term formation of microbial products in a sequencing batch reactor,” *Water Res.*, vol. 44, no. 13, pp. 3787–3796, 2010, doi: 10.1016/j.watres.2010.04.035.

[76] B. V. Merkey, B. E. Rittmann, and D. L. Chopp, “Modeling how soluble microbial products (SMP) support heterotrophic bacteria in autotroph-based biofilms,” *J. Theor. Biol.*, vol. 259, no. 4, pp. 670–683, 2009, doi: 10.1016/j.jtbi.2009.05.010.

[77] B. J. Ni, F. Fang, B. E. Rittmann, and H. Q. Yu, “Modeling microbial products in activated sludge under feast#famine conditions,” *Environ. Sci. Technol.*, vol. 43, no. 7, pp. 2489–2497, 2009, doi: 10.1021/es8026693.

[78] B. J. Ni *et al.*, “Evaluation on factors influencing the heterotrophic growth on the soluble microbial products of autotrophs,” *Biotechnol. Bioeng.*, vol. 108, no. 4, pp. 804–812, 2011, doi: 10.1002/bit.23012.

[79] D. J. Barker and D. C. Stuckey, “A review of soluble microbial products (SMP) in wastewater treatment systems,” *Water Res.*, vol. 33, no. 14, pp. 3063–3082, 1999, doi: 10.1016/S0043-1354(99)00022-6.

[80] Y. yuan Wei *et al.*, “Influence of soluble microbial products (SMP) on wastewater disinfection byproducts: Trihalomethanes and haloacetic acid species from the chlorination of SMP,” *Environ. Sci. Pollut. Res.*, vol. 18, no. 1, pp. 46–50, 2011, doi: 10.1007/s11356-010-0356-5.

Chapter 3

MODELLING THE EFFECT OF SMP PRODUCTION AND EXTERNAL CARBON ADDITION ON S-DRIVEN AUTOTROPHIC DENITRIFICATION

This article has been published as:

Guerriero G, Mattei MR, Papirio S, Esposito G, Frunzo L.: "*Modelling the effect of SMP production and external carbon addition on S-driven autotrophic denitrification."* Scientific Reports. 2022 Apr;12(1):7008. https://doi.org/10.1038/s41598-022-10944-z

3.1 INTRODUCTION

During the last few years, nitrate removal through sulfur-driven autotrophic denitrification (SdAD) has been thoroughly investigated. Compared to conventional heterotrophic denitrification, SdAD allows lower sludge production and N_2O emissions [1] but results in the production of high sulfate concentrations as main shortcoming [2]. Among the various forms of S-based electron donors already studied, elemental sulfur is of economic interest despite the need to solubilize it prior to being effectively taken up by the microorganisms [1].

The growth of autotrophic microbial families using elemental sulfur as an electron donor often comes with the natural growth of heterotrophic families, which might be already present in the influent or proliferate in association with the activities of autotrophs [3], [4]. From a kinetic point of view, none of the previous studies on SdAD considered the natural production of organic matter deriving from the denitrifying sulfur-oxidizing autotrophic biomass. Indeed, as reported by Laspidou and Rittmann (2002)[5] and Ni et al. (2011) [6], soluble microbial products (SMP) are the result of the autotrophic and heterotrophic activity and can effectively become bioavailable for concomitant heterotrophic denitrifiers (HD) [7]. The SMP produced during SdAD are made up of organic byproducts associated with biomass metabolism and decay [6], [8], [9]. In particular, part of SMP comprises a readily available carbon source, i.e. biomass associated products (BAP) and utilization-associated products (UAP), while another part is made up of extracellular polymeric substances (EPS) and stocked biodegradable substances (STOB), which need a preliminary hydrolysis step to become more bioavailable [10].

During the SdAD maintained by a mixed microbial consortium, the most relevant heterotrophic microorganisms are denitrifying bacteria (HD) and sulfate reducing bacteria (SRB) [3], [4], [11]. The presence of denitrifying heterotrophs was evident in full scale SdAD studies in the presence of chemical oxygen demand (COD) removal [12] and in experimental studies conducted under feast-famine conditions [13]. Also, Qiu et al. (2020)[14] highlighted the possibility to add various organic compounds to a denitrifying autotrophic microbial consortium aiming to improve the process efficiency and to reduce the sulfate output without modifying the optimal working parameters. The favorable effects of organic supplementation on the performance of SdAD has not

been attributed to the role of SRB but rather to the activity of HD, which considerably reduce the nitrate loading on autotrophic denitrifiers [15], [16].

Mathematical modelling is a useful tool to elucidate the competition among different microbial families and the performances of the SdAD process. Previous mathematical models focusing on the co-occurrence of SdAD, heterotrophic denitrification and sulfate reduction involved the use of sulfide as sulfurous electron donor and did not take into account the SMP production [17]. Other models focused on the use of elemental sulfur to fuel SdAD, but only aimed at evaluating the kinetics of the process in terms of nitrate removal and nitrite accumulation [4] or the emission of N_2O [18]. Also, other mathematical models simulated the reduction of the effluent sulfate concentrations by adding organic matter in the presence of sulfide as main inorganic electron source [19]. None of the existing models has provided a thorough picture on the competition among different bacterial families and the growth of those on SMP during SdAD.

In this context, this work proposes a mathematical model to study the concomitance of SdAD, as the main process, heterotrophic denitrification and sulfate reduction on UAP and BAP in the presence or absence of an external carbon source. The processes were simulated in a sequencing batch reactor (SBR), which was chosen as bioreactor configuration to enhance the formation and the uptake of SMP by the heterotrophic families. Indeed, a SBR allows to operate under feast-famine conditions that are needed to let the active bacteria use the SMP as main organic source while promoting the accumulation of biomass [10]. When an external source of organics was considered, the timing of supplementation of such carbon source was investigated, being this of crucial importance due to the presence of two heterotrophic families. This is another aspect that makes the model here proposed novel compared to the existing ones.

3.2 BIOLOGICAL MODEL

The three main processes considered in the mathematical model are SdAD with elemental sulfur, heterotrophic denitrification and sulfate reduction, as shown in Fig. 3.1. HD and SRB were assumed to grow on UAP, BAP and external COD (Fig. 3.1).

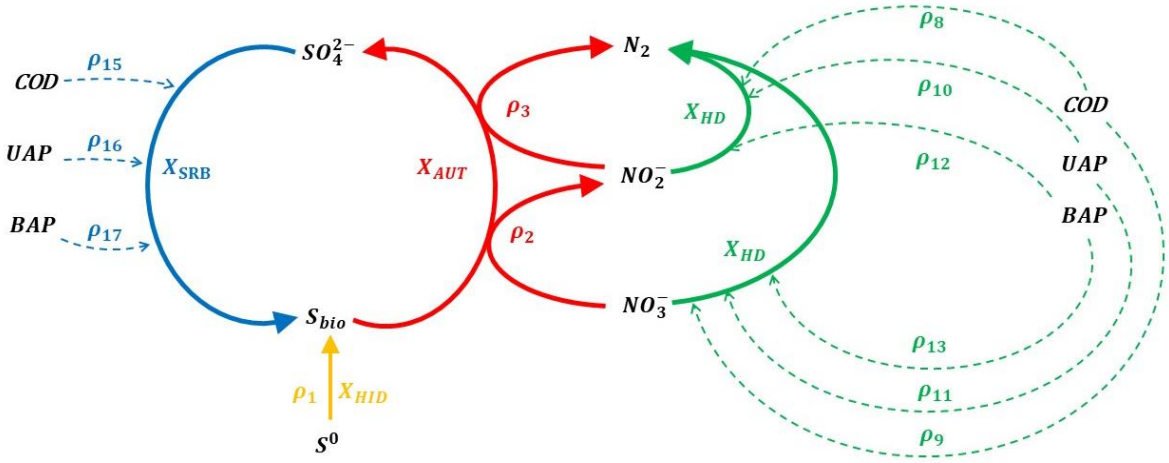

Fig. 3. 1 Schematic representation of the biological processes considered in the proposed model: sulfate reduction maintained on external COD, BAP and UAP (blue), sulfur-based autotrophic denitrification (red), heterotrophic denitrification maintained on external COD, BAP and UAP (green), elemental sulfur hydrolysis (yellow). Each ρ_i represent a term of i^{th}-reaction.

Elemental sulfur (S^0) was assumed to be supplemented in the form of "lentils". Hence, a preliminary microbially-catalyzed hydrolysis step for the conversion of S^0 into a more bioavailable form (S_{bio}) by a hydrolytic biomass (HYD) was also considered [4] and indicated in yellow in Fig.3.1 (ρ_1). S^0 lentils were supposed to constantly remain in the reactor after each SBR cycle (see section "Numerical simulations"), representing a support for the growth of the different microbial families involved and a continuous source of S_{bio} over time [10]. The S_{bio} generated by S^0 hydrolysis was assumed to remain within the solid S^0 lentils [3], [20], [21] and, thus, not escaping the reactor in contrast with the soluble substrates (i.e. NO_3^-, NO_2^-, SO_4^{2-}).

When S_{bio} is consumed, SdAD was assumed to proceed as a two-step process consisting of a first transformation from NO_3^- to NO_2^- (ρ_2,) and a second from NO_2^- to N_2 (ρ_3). The intermediate steps allowing the production of NO and N_2O were not considered, assuming the occurrence of optimal conditions in the system that allow those steps not to be limiting [22]. Sulfate reduction is carried out by SRB, which transform the sulfate produced by the denitrifying autotrophs into sulfide (S^{2-}),

using all the carbon sources available (i.e. UAP, BAP and external COD). The sulfide produced was assumed to be used again by autotrophic denitrifying bacteria as S_{bio}. The assimilation between S^{2-} and S_{bio} was possible being the typical sulfide-driven autotrophic denitrification kinetics faster than those obtained with S_{bio} [1], and thus not limiting for the SdAD process here considered. Heterotrophic denitrification was assumed to occur on all bioavailable organic compounds (BAP, UAP, COD) and convert NO_3^- (ρ_9 , ρ_{11} , ρ_{13}) and NO_2^- (ρ_8, ρ_{10}, ρ_{12}) into N_2.

To take into account the natural production of organics from the growth and decay of biomass, it was considered that all the microbial families involved lead to the production of SMP (Fig. 3.2). In particular, BAP, inert material and STOB are released during the decay of the microbial families. With regard to the microbial growth, denitrifying autotrophs and heterotrophs as well as SRB result in the production of UAP and EPS, which are further solubilized into BAP prior to being bioavailable for the heterotrophs. The hydrolytic biomass was excluded from the production of SMP during the growth phase due to a lack of information regarding the process in which it is involved.

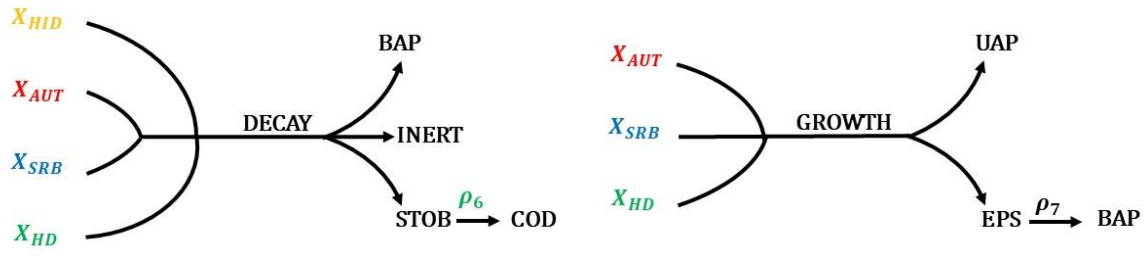

Fig. 3. 2 Endogenous processes of microbial families and production of SMP deriving from microbial activities. The biomass decay (left-hand side) associated with the hydrolytic (X_{HID}), autotrophic denitrifying (X_{AUT}), heterotrophic denitrifying (X_{HD}) and sulfate reducing (X_{SRB}) families releases BAP, INERT and STOB, with the latter being hydrolyzed into bioavailable COD by reaction ρ_6. During the growth of the microbial families (right-hand side), denitrifying autotrophs (X_{AUT}), denitrifying heterotrophs (X_{HD}) and SRB (X_{SRB}) produce UAP and BAP, with the latter deriving from the hydrolysis of EPS as regulated by reaction ρ_7.

3.3 MATHEMATICAL MODEL

A differential model describing the dynamics of autotrophic, denitrifying heterotrophs and sulfate reducing bacteria has been formulated based on mass balance considerations. The model considers seven different biomasses $X_i, i = [HYD, AUT, STO, EPS, HD, SRB, I]$and nine different compounds $S_j, j = [S_0, S_b, NO_3^-, NO_2^-, N_2, SO_4^{2-}, UAP, BAP, COD]$. The four active biomasses are represented by: X_{HYD} which is the hydrolyzing biomass responsible of the transformation of elemental sulfur into bioavailable sulfur, X_{AUT} autotrophic denitrifying biomass that uses sulfur as electron donor, X_{HD} heterotrophic biomass that uses different types of organic matter as substrate, X_{SRB} sulfate reducing bacteria which also use all the organic matter as substrate to reduce sulfate. The inactive biomasses are: X_{EPS} , X_{STO} and inert material X_I derived from the biomass decay. The substrates involved in the model are: S_{S^0}, S_{S_b}, $S_{NO_3^-}$, $S_{NO_2^-}$, S_{N_2}, $S_{SO_4^{2-}}$, S_{UAP}, S_{BAP}, S_{COD}. The biomasses X_i and substrates S_j interact according to the biological processes described in the previous Section.

The mathematical model developed in the present work is made up by a system of first order impulsive ordinary differential equations (IDEs), which are used to model the biological processes described in the previous section occurring in a SBR configuration. Indeed, such equations are well-suited to model processes that are continuous under most conditions but undergo instantaneous changes. An impulsive differential equation is described by three components: a continuous-time differential equation, which governs the state of the system between impulses; an impulse equation, which models an impulsive jump defined by a jump function at the instant an impulse occurs; and a jump criterion, which defines a set of jump events in which the impulse equation is active [23]. The main features of the SBR configuration which are repeated for each cycle after the first initial filling have been considered as follows:

1. First Reaction period (continuous)
2. Injection of COD (instantaneous)
3. Secondo Reaction period (continuous)
4. Settling (instantaneous)
5. Emptying (instantaneous)
6. Filling (instantaneous)

In the present study, the settling, emptying and refilling processes were approximated by an instantaneous change of state of the system, which occurred at a prescribed time dictated by the duration of the combined cyclical reaction phases. The duration of each cycle is denoted as τ and the time of injection of COD is denoted as $\tau_d \leq \tau$. The model is described by the following impulsive differential equations for both substrates and microbial species:

$$\dot{S}_j(t) = r_{S,j}(t, \boldsymbol{S}, \boldsymbol{X}), t \in J = [0, T], t \neq t_k, S_j(0) = S_{j0}, (3.1)$$

$$\dot{X}_i(t) = r_{X,i}(t, \boldsymbol{S}, \boldsymbol{X}), t \in J = [0, T], t \neq t_k, X_i(0) = X_{i0}, (3.2)$$

$$\Delta S_j(t_k) = -\alpha_j S_j(t_{k^-}) + \alpha_j S_{in,j} \quad k=1,....,m, \quad (3.3)$$

$$\Delta X_i(t_k) = -\gamma_i X_i(t_k^-), k = 1, \ldots., m, (3.4)$$

Where:

$S_j(t), X_i(t)$ are the j[th] substrate and the i[th] biomass concentrations at time t respectively;

$r_{S,j}$ and $r_{X,i}$ are the reaction terms for the j[th] substrate and the i[th] biomass.

S_{j0} and X_{i0} are the initial concentration within the reactor for the j[th] substrate and the i[th] biomass;

$S_{in,j}$ is the concentration of the j[th] substrate in the fresh influent;

$0=t_0 < t_1 < \cdots < t_m < t_{m+1} = T$, $t_{k+1} - t_k = \tau$, where τ denotes the duration of each cycle , $\Delta S_j(t_k) = S_j(t_k^+) - S_j(t_k^-)$, $\Delta X_i(t_k) = X_i(t_k^+) + X_i(t_k^-)$, with $S_j(t_k^+)$, $X_i(t_k^+)$, $S_j(t_k^-)$, $X_i(t_k^-)$, being the right and left limits of $S_j(t)$ and $X_i(t)$ at time $t = t_k$; α_j represents the emptying/refilling ratio and γ_i takes into account the fraction of biomass removed from the system during the emptying phase.

The $r_{S,j}$ and $r_{X,i}$ are expressed as a combination of the kinetic terms and stoichiometric parameters reported in the Table 3.S.1 3.S.2 and 3.S.4 of the supplementary information. (section S.3)

For all the biomasses the coefficient γ_i has been considered equal to zero simulating a settling process with 100% efficiency. The dilution was only applied to the substrates which were considered in dissolved form: $S_{SO_4^{2-}}$,S_{UAP}, S_{BAP}, S_{COD}, $S_{NO_3^-}$, $S_{NO_2^-}$. All the other compounds included in the model are supposed to undergo a complete sedimentation. According to Sierra-Alvarez et al., 2007 [24], and Liu et al., 2016b [25], in the present model is assumed that the

bioavailable sulfur cannot be washed out during the emptying phase since it is supposed to be retained within the microbial sludge. The value of α_j has been set equal for all the dissolved substrates.

The first and second reaction periods are discriminated by the time of soluble COD injection in the system. Such operation is considered to occur instantaneously and does not affect the concentration of the other compounds.

$$\begin{cases} (k-1)\cdot\tau < t \leq (k-1)\tau + \tau_d \quad k = 1,\dots,n, \quad FIRST\ REACTION\ PERIOD \\ (k-1)\cdot\tau + \tau_d < t \leq k\cdot\tau \quad k = 1,\dots,n, \quad SECOND\ REACTION\ PERIOD \end{cases} \quad (3.5)$$

The equation that defines the jump function for COD between the two reaction periods is:

$$\Delta S_{\mathrm{COD}}\big((k-1)\tau + \tau_d\big) = S_{in,COD},\ k = 1,\dots,n \quad (3.6)$$

where τ represents the duration of each cycle, τ_d represents the duration of the first reaction period until the COD injection occurs, n is the number of cycles which varies with respect to different retention times, $S_{in,COD}$ is the concentration of COD that must be reached in the reactor at that time.

3.3.1 PROCESS RATES

The reaction terms in equations (3.1) and (3.2) have been formulated as Monod kinetics and their expressions are reported in table 3.S.4 in the supplementary material. According to Kostrytsia et al. (2018) [4], elemental sulfur is not directly oxidized, but an hydrolysis step is taken into account to model its conversion to bioavailable sulfur. This conversion is modelled through a nonlinear reaction term, which depends on the concentration of the hydrolyzing biomass, the amount of available elemental sulfur and its mass specific area. Autotrophic denitrification takes place in two sequential steps: a first step from nitrate to nitrite and then from nitrite to molecular nitrogen. As the same biomass carries out both denitrification steps, a fractional term was introduced. According to Huiliñir et al. (2020) [26], the inhibition term regarding nitrite accumulation has not been considered. To take into account that the same biomass cannot work simultaneously on different substrates, fractional terms were added with respect to a classic Monod kinetics for the heterotrophic species growing on different carbon sources and nitrogen compounds. Due to the lack of experimental measurements of the specific EPS production from the different microbial family involved in the model, the same hydrolysis constant for the EPS produced was used [8].

Since no specific values are available regarding the use of BAP and UAP as organic substrates by SRB, the same reducing growth factor of HD on BAP and UAP was considered.

3.4 NUMERICAL SIMULATIONS

The initial amount of sulfur was set to 21 g/L (Table 3.2) for each simulation. Consequently, for all the conditions investigated the final simulation time was set to 300 days, which is the evaluated time needed to achieve the complete solubilization of the initial elemental sulfur.

The simulations were carried out for three different scenarios depending on the duration of each SBR cycle and on the time of COD injection. Scenario I simulated the occurrence of the three main processes in the SBR in the absence of external COD and was used as reference. Scenario II was characterized by the injection of an amount of COD (380 mg/l) corresponding to the stoichiometric value needed to achieve a complete sulfate reduction [27]. In Scenario III, the COD was supplied in excess (i.e. 500 mg/l) to the stoichiometric value. For all scenarios, three different SBR cycle durations τ of 10, 15 and 20 days were investigated. The time of COD injection τ_d after the start of each cycle was varied depending on the duration of the cycle. The summary of all simulation parameters is shown in Tables 3.1 and 3.2.

Table 3. 1 Resume of the simulations performed. The duration of each cycle and the time of COD injection are reported. The simulations in the presence of added COD were performed with both a stoichiometric COD amount and an excess of COD with respect to the complete sulfate reduction requirements.

Scenario	***COD***	***Durations of the cycles τ (days)***	***Period after the injection of COD occurs***
Scenario I	Absent	10-15-20	Not present
Scenario II	Stoichiometric and in excess with respect to the complete sulfate reduction	10-15-20	5-8-10-15

The initial data for each simulation are reported below:

Table 3. 2 Initial data for all the simulations performed.

X_{HYD} (mg/l)	X_{AUT} (mg/l)	X_{STOB} (mg/l)	X_{EPS} (mg/l)	X_{HD} (mg/l)	X_{SRB} (mg/l)	X_I (mg/l)
500	1100	0	0	0.1	0.1	0

S_{S_0} (mg/l)	S_{S_b} (mg/l)	$S_{NO_3^-}$ (mg/l)	$S_{NO_2^-}$ (mg/l)	S_{N_2} (mg/l)	$S_{SO_4^{2-}}$ (mg/l)	S_{UAP} (mg/l)	S_{BAP} (mg/l)	S_{COD} (mg/l)
21’000	0	210	0	0	0	0	0	0

The initial concentration of both $\boldsymbol{X_{SRB}}$ and $\boldsymbol{X_{HD}}$ was assumed to be considerably lower than that of autotrophic biomass, in order to better study their natural growth in an original autotrophic-dominated consortium.

3.5 RESULTS AND DISCUSSION

3.5.1 SCENARIO I - NO COD INJECTION

The numerical studies in Scenario I without any external COD supplementation were conducted to elucidate the effect of SMP production on the competition among the different microbial families and to serve as a reference to better highlight the effect of COD addition studied in the other two scenarios. Fig. 3.3 shows the evolution of nitrate, nitrite and sulfate concentrations during SdAD with three different values of SBR cycle duration τ.

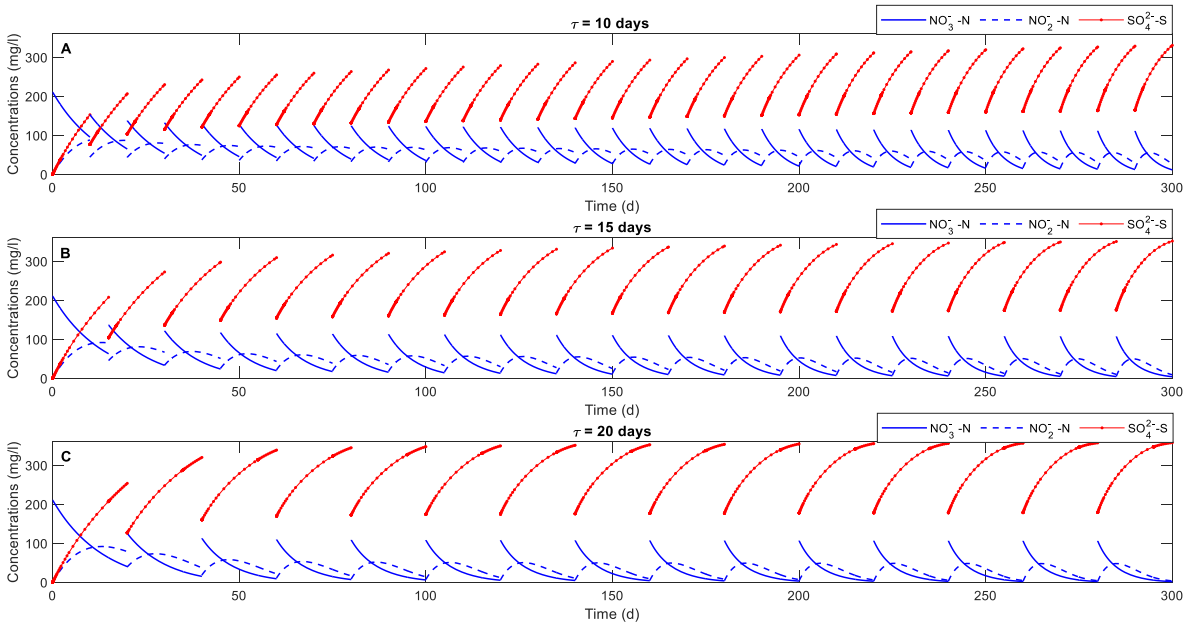

Fig. 3. 3 Autotrophic denitrification performances in terms of nitrate removal (solid blue), nitrite evolution (dashed blue) and sulfate production (solid red) with three different SBR cycle durations, τ =10 (A), 15 (B) and 20 (C) days, in the absence of external COD addition.

It is possible to observe that an increase of τ leads to an increase of the nitrate removal efficiency, which results in a higher sulfate production. When τ is set at 15 days, the nitrate removal efficiency is close to 100% in the latest cycles (n>14) and nitrite concentration approaches to zero after being

accumulated up to approximately 50 mg/l. Conversely, the nitrate removal efficiency approaches to 100% only after 4 cycles when a duration of the cycle τ of 20 days was used. According to Kostrytsia et al. (2018) [4], shorter retention times lead to a not complete process. Indeed, a higher NO_2^- concentration is evident when the duration of the cycle is 10 days, which results in an incomplete denitrification process.

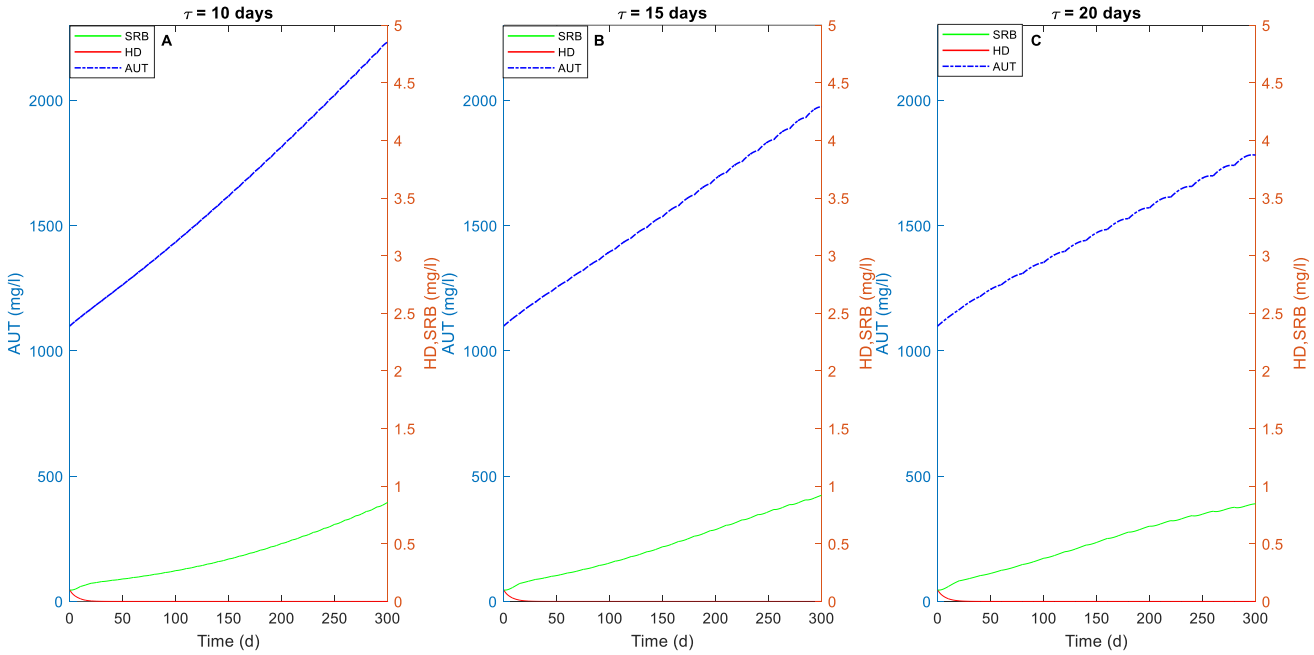

Fig. 3. 4 Evolution of the concentration (in mg COD/l) of autotrophs (blue line), heterotrophic denitrifiers (red line) and sulfate reducing bacteria (green line) overtime for three different durations of the SBR cycle (τ=10, 15 and 20 days) in the absence of external COD.

The autotrophic biomass concentration increases in the reactor overtime for all the SBR cycle durations. In particular, the highest concentration of autotrophic biomass up to approximately 2200 mg COD/L is obtained when τ is 10 days (Fig. 3. 4A). The higher biomass concentration at τ=10 d is an indicator of the higher biomass activity, which was likely stimulated by the more frequent replacement of the influent solution. Moreover, comparing Fig. 3.3A and Fig. 3.4A it can be noticed that the increase of the concentration of autotrophic denitrifiers over time leads to a higher N-based compounds removal, which however requires longer reaction times to be completed. Regarding the two heterotrophic families, the results suggest that HD are less resistant than SRB for the whole cycle duration, with the latter being more capable to survive in the absence of external

carbon source (Fig. 3.4) as high sulfate concentrations are present. In the absence of SRB (data not shown), HD are able to growth on the organic carbon deriving from the microbial activities, as experimentally demonstrated by Wang et al. (2016) [3]

The increase of the biomass activities over time reported in Fig. 3.4 results in an increased SMP production, as shown in Fig. 3.5. The highest EPS concentration is obtained at the shortest cycle duration and reaches approximately 3.65 mg/l (Fig. 3.5A) at the end of the simulation period. However, comparing the simulations carried out with the three different τ values, it is possible to observe that the production of both BAP and UAP is higher at longer τ. The increase of the BAP production over time is due to both EPS hydrolyzation and the decay of the microbial families, with the latter being higher for longer cycle durations. Furthermore, the consumption of BAP and UAP is higher in the case of longer cycles as well.

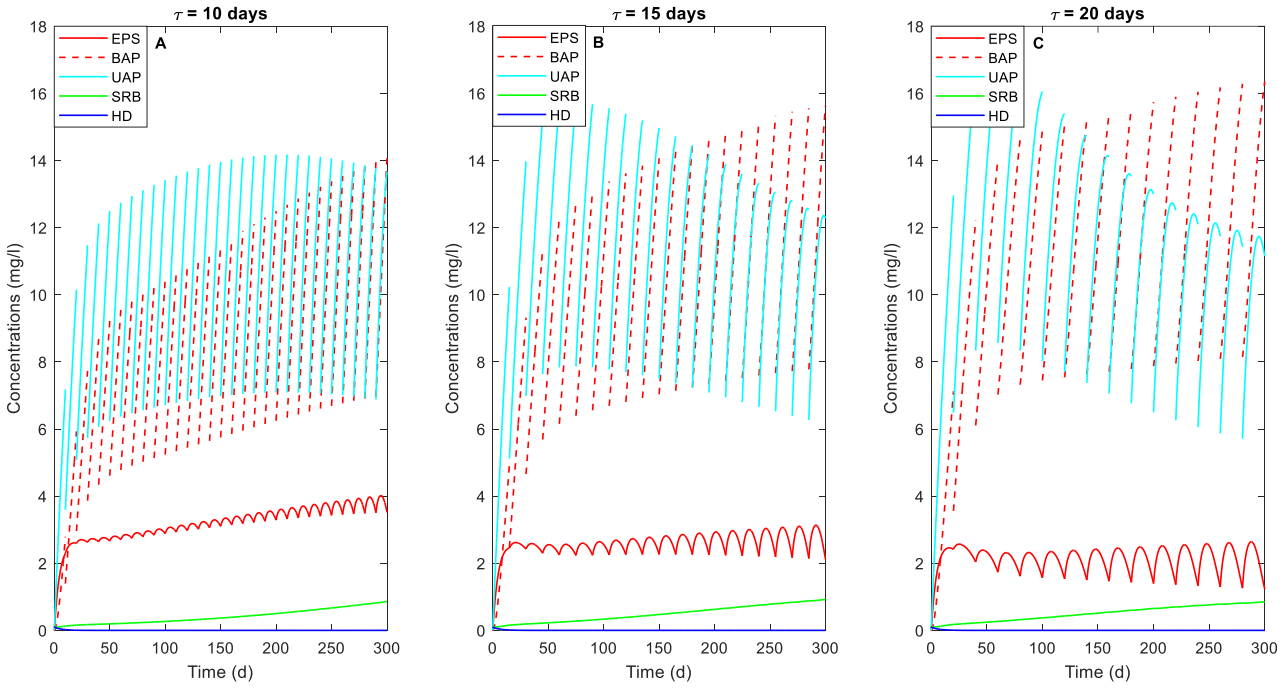

Fig. 3. 5 SMP production and concentration of heterotrophic families (i.e. HD and SRB) overtime with no external source of COD for three different values of τ =10 days (A), 15 days (B), 20 days (C). The solid dark blue line represents the heterotrophic denitrifiers (HD), while the solid green line indicates the sulfate-reducing bacteria (SRB). The solid red line indicates the EPS, which leads to the production of BAP (red dashed line) after hydrolysis. The solid light blue line represents the UAP.

Fig. 3.5 also shows that the denitrifying heterotrophic biomass is not able to grow on BAP and UAP and is outcompeted by both AUT and SRB, with the latter growing on the sulfate produced

during SdAD. SRB are likely able to grow on UAP and responsible for their degradation, confirming what was previously observed in experimental studies when SMP were used as electron donor for sulfate reduction under famine conditions [7], [13].

3.5.2 SCENARIO II - COD INJECTION

3.5.2.1 Evolution of nitrate, nitrite and sulfate at different COD amounts and injection times

Fig. 3.6 shows the effect of adding an external COD source on the three processes investigated at different τ and τ_d values. In each case, the system reaches a pseudo steady state after approximately 4-5 cycles and the effects of the injection, whether in excess or stoichiometric, are positive for nitrate and sulfate removal.

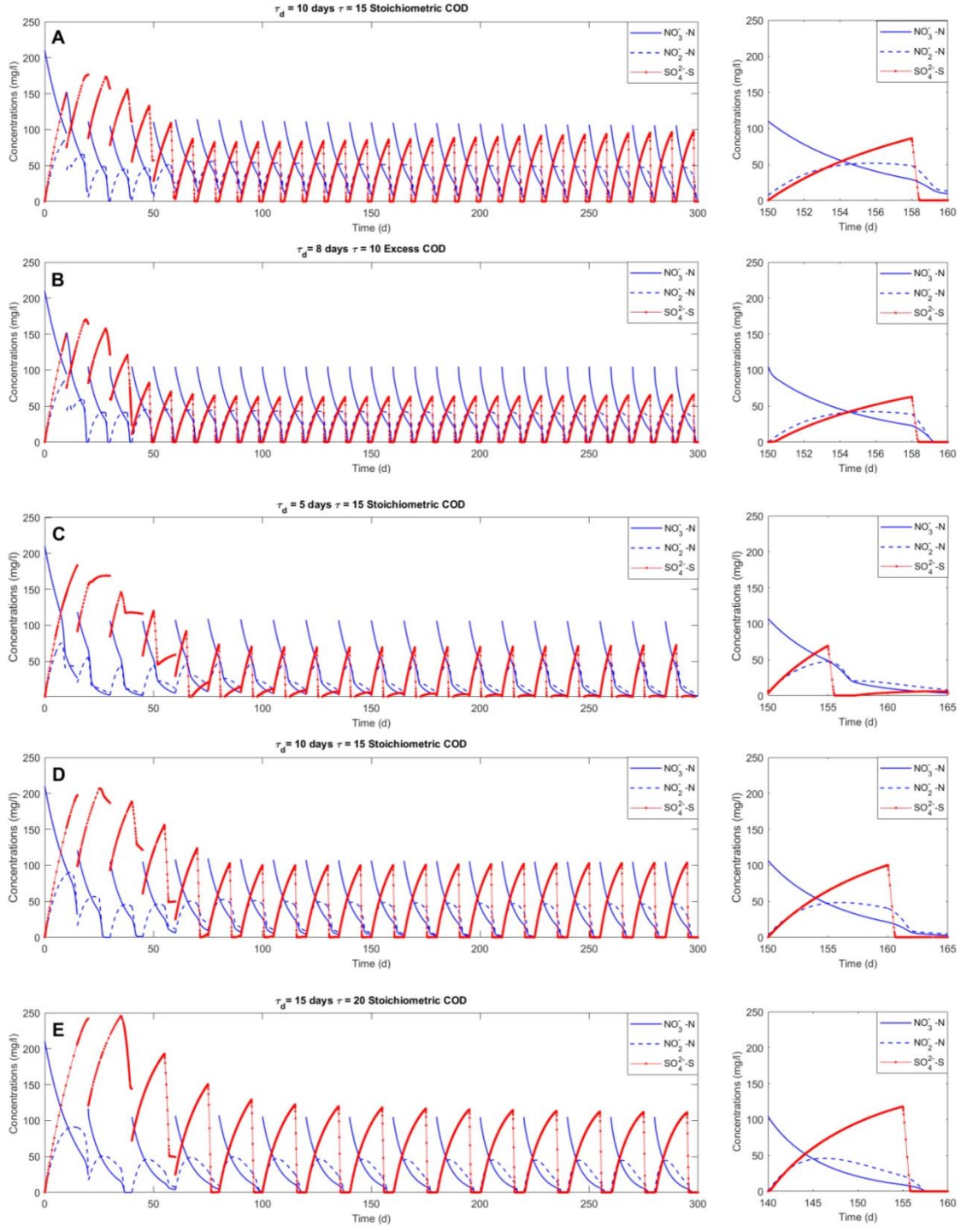

Fig. 3. 6 Nitrate removal (solid blue), nitrite evolution (dashed blue), sulfate production and consumption (solid red) in four different cases: A (τ = 10 days an injection of stoichiometric COD at τ_d = 8 days), B (τ = 10 days an injection in excess of COD at τ_d = 8 days), C (τ =15 days an injection of stoichiometric COD at τ_d = 5 days), D (τ =15 days an injection of stoichiometric COD at τ_d = 10 days) , E(τ = 20 days an injection of stoichiometric COD at τ_d = 15 days).

Fig. 3.6C and 3.6D highlight that the time of COD injection mainly affects the production and consumption of sulfate. Indeed, when COD is added prior to the complete nitrate removal by autotrophs, the growth of HD is favored due to their higher growth rate. From Fig. 3.6C it can be noticed that nitrate and nitrite (previously produced by SdAD) are quickly removed by heterotrophs when the addition of COD occurs on day 5, as shown by the change of the slope in nitrate evolution. A lower τ_d leads to a lower sulfate production since nitrate reduction is mainly performed by HD in the presence of external COD. A direct consequence of the consumption of the COD by the HD is the uncomplete sulfate reduction. It can be observed (Fig. 3.6C) that lower values of τ_d lead to a temporary increase of the sulfate concentrations when a stoichiometric amount of COD is added, since SRB are outcompeted by HD for the COD consumption. In both cases (Fig. 3.6C and 3.6D) the sulfate concentration attains very low values at the end of the SBR cycle after the attainment of the pseudo steady state. For longer τ (Fig 3.6E), a higher percentage of nitrate is removed through autotrophic denitrification favoring sulfate production (3.6A and 3.6C).

For shorter SBR cycles (τ = 10 days), the addition of a higher amount of COD, with respect to the stoichiometric quantities (Fig. 3.6A), is required (Fig. 3.6B) to obtain a similar performance efficiency in terms of nitrate removal and sulfate reduction. The excess of COD added is mainly used by HD, leading to a reduction of the time needed to obtain a complete denitrification and a lower sulfate production, as reported experimentally by Sahinkaya et al. (2014). Furthermore, the addition of an external carbon source was observed to enhance heterotrophic denitrification resulting in a lower nitrite accumulation. Nitrite has been reported to negatively affect autotrophic denitrifiers [14], [28], [29]. The marginal presence of nitrite in the SBR here investigated justifies the choice of not considering any inhibition term on autotrophic denitrifiers due to nitrite in this model [30].

It must be also reported that the simultaneous activity of autotrophic and heterotrophic denitrifying families was experimentally observed to decrease N_2O accumulation and emission [31], which was, however, not evaluated in the present model. Previous studies also demonstrated that the addition of organic substances have a good influence on pH that makes the typical addition of limestone during SdAD unnecessary [15].

With respect to the previous works, the time of COD injection was here investigated for the first time, as the addition of external carbon has only been considered at the beginning of the process in other studies [31], [32]. The variation of τ_d has a strong influence on the whole process (Fig. 3.6). For $\tau_d > \tau/2$, autotrophic denitrification prevails over heterotrophic denitrification resulting in lower treatment costs and sludge production. Conversely, for $\tau_d < \tau/2$, in particular for the shortest duration cycle (τ =15d) the removal efficiency of nitrate and sulfate decreases if is not injected an excess quantity of COD. In addition, the choice of a proper time of COD addition can result in positive economic consequences as, for instance, a lower amount of COD can be supplemented to obtain optimal effluent nitrate, nitrite and sulfate concentrations. Furthermore, sulfate reduction enhanced by COD addition leads not only to the absence of sulfate in the effluent, but also to the possibility to reuse and consequently reduce the total sulfur used in the process. Indeed, based on the model assumption, the reduced sulfate is converted in sulfide that can be used by the autotrophic species [17], [30].

3.5.2.2 Competition between microbial families

The results obtained in terms of removal efficiency of nitrogenous compounds and sulfate are reflected in the growth trend of the microbial families involved in the process. The results in terms of HD, AUT and SRB concentrations are reported in Fig. 3.7 for different τ_d values and a stoichiometric COD addition.

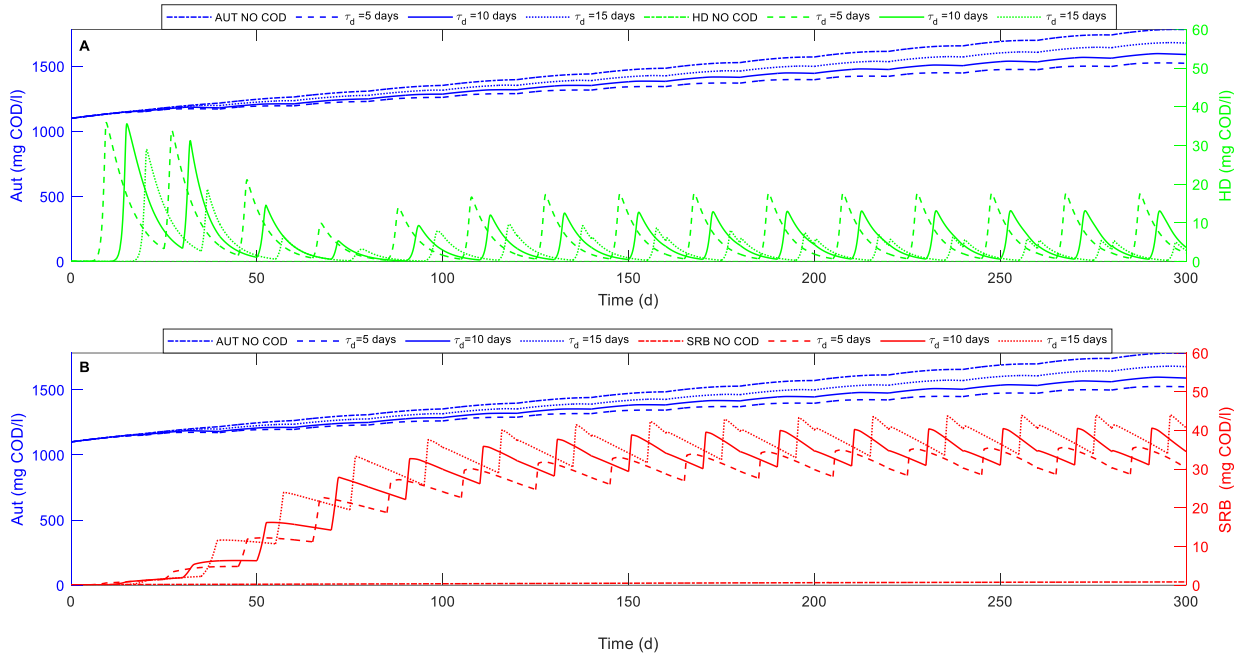

Fig. 3. 7 Time evolution of heterotrophic species (SRB and HD) concentrations and autotrophic biomass concentration for an SBR cycle duration of 20 days with no COD (. -) and stoichiometric COD injection at three different τ_d of 5(---), 10(-) and 15(…) days.

Despite an initial increase of HD observed for all τ_d values (Fig. 3.7A) during the first SBR cycles, the lowest value of τ_d led to the highest concentration of HD, which remained lower than the SRB concentration. The growth of autotrophic denitrifiers is mainly observed after the first three SBR cycles leading to a higher sulfate production coupled to a higher SRB growth. Thus, the value of τ_d has a strong influence on the evolution of the concentration of the three microbial families (Fig. 3.7). An increase of τ_d results in a longer first reaction period where the main process is SdAD, while a lower τ_d leads to an increase of the HD growth. This is enhanced by the higher nitrate and nitrite concentrations available (Fig. 3.6C). At the same time, a longer τ_d leads to a higher sulfate accumulation (Fig. 3.6E and 3.6D), which stimulates the growth of SRB. Moreover, the growth of the heterotrophic biomasses (both HD and SRB) is higher when a higher COD amount is provided at lower τ_d values, as it is possible to observe by the fast consumption of sulfate and nitrate in Fig. 3.6C and Fig. 3.6B. The τ_d variation affects the two different reaction phases and has an impact on the competition between the different microbial families involved except for HYD (data not shown), whose growth only depends on the initial concentration of both biomass and elemental sulfur.

The results obtained with this model in terms of microbial families profiles are consistent with those achieved experimentally, which show that the heterotrophic denitrifying bacteria never prevail over autotrophic denitrifiers when a proper acclimatation of autotrophs on elemental sulfur is performed [4]. Indeed, the prevalent microbial family is represented by the autotrophic denitrifiers in each simulated scenario (Fig. 3.7). As discussed before, heterotrophic denitrification is faster than SdAD, but the two processes do not significantly affect each other [15], [32].

3.5.2.3 SMP evolution

The simultaneous presence of different active microbial families leads to an increased SMP production compared to that obtained when only autotrophic denitrifiers are the main bacteria involved (Fig. 3.5). In particular, the higher concentration of heterotrophic families, both HD and SRB, in the presence of external COD implies higher EPS, BAP and UAP concentrations (Fig. 3.8).

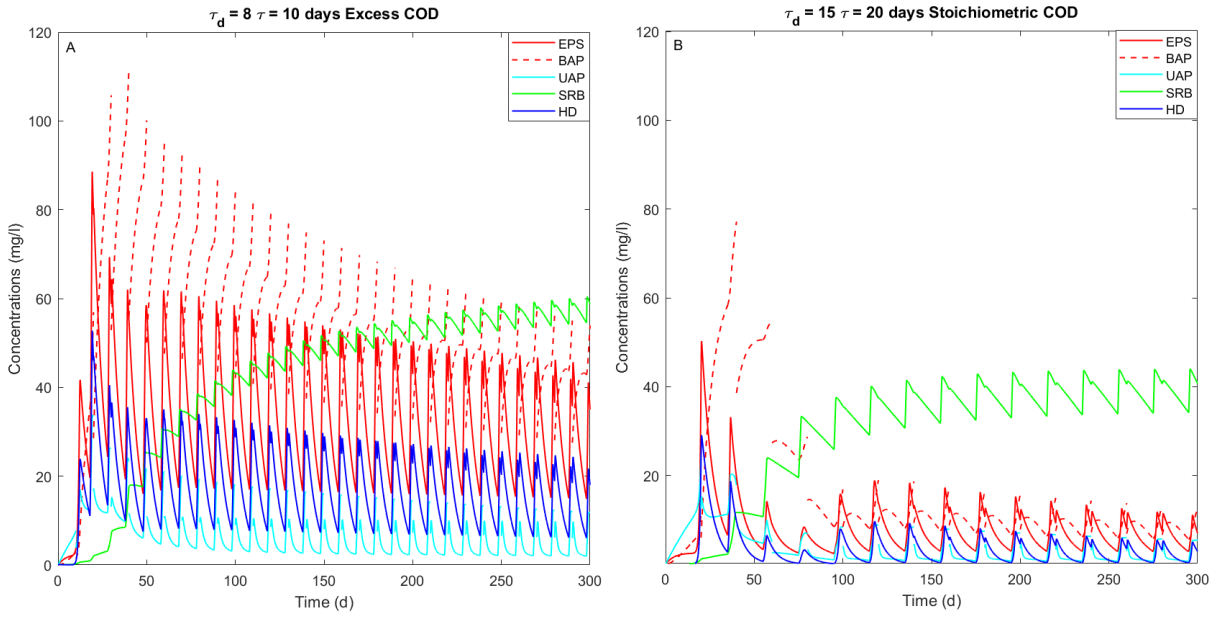

Fig. 3.8 SMP production and concentration of heterotrophic families (i.e. HD and SRB) overtime in two different cases: A) excess COD at τ_d = 8 days and τ = 10 days; B) stoichiometric COD at τ_d = 15 days and τ = 20 days. The solid dark blue line represents the heterotrophic denitrifiers (HD), while the solid green line indicates the sulfate-reducing bacteria (SRB). The solid red line indicates the EPS, which allows the production of BAP (red dashed line) after hydrolysis. The solid light blue line represents the UAP.

The highest SMP concentrations are obtained in the presence of a COD injection in excess to the theoretical value required for complete sulfate reduction (Fig. 3.8A). Moreover, as it possible to observe from Fig. 3.6B (excess COD at τ_d= 8 days, τ = 10 days,) and 3.6E (stoichiometric COD at τ_d= 15 days, τ = 20 days), the nitrate and sulfate removal efficiencies follow a similar trend in both simulations, but the different SMP amounts produced (Fig. 3.8) is the result of the different families involved in the two cases. When the denitrification is mostly conducted by autotrophs (Fig 3.6E), as indicated by the higher sulfate production and the lower HD concentration, lower SMP amounts are produced (Fig. 3.8B). This is because the activity of heterotrophs result in a higher SMP production rate.

The evaluation of the SMP associated with the growth of the microbial families could be also used to control and prevent the undesirable COD production, which is normally considered as a secondary pollution in the effluent [14]. With respect to the case without COD addition (Fig. 3.5), the injection of a stoichiometric COD amount promotes the growth of both heterotrophic families (i.e. SRB and HD) and consequently the production of UAP and EPS (Fig. 3.9). About the formation and use of SMP, UAP and BAP, this is higher in the cases of short cycle durations and low τ_d, since the growth of HD is enhanced by the excess COD concentration (Fig 3.8A). This observation is in line with experimental evidences from Tian et al. (2011) [33], who evaluated the concentration of SMP produced during the simultaneous growth of heterotrophs and autotrophs where a higher heterotrophic growth was associated with a higher SMP production.

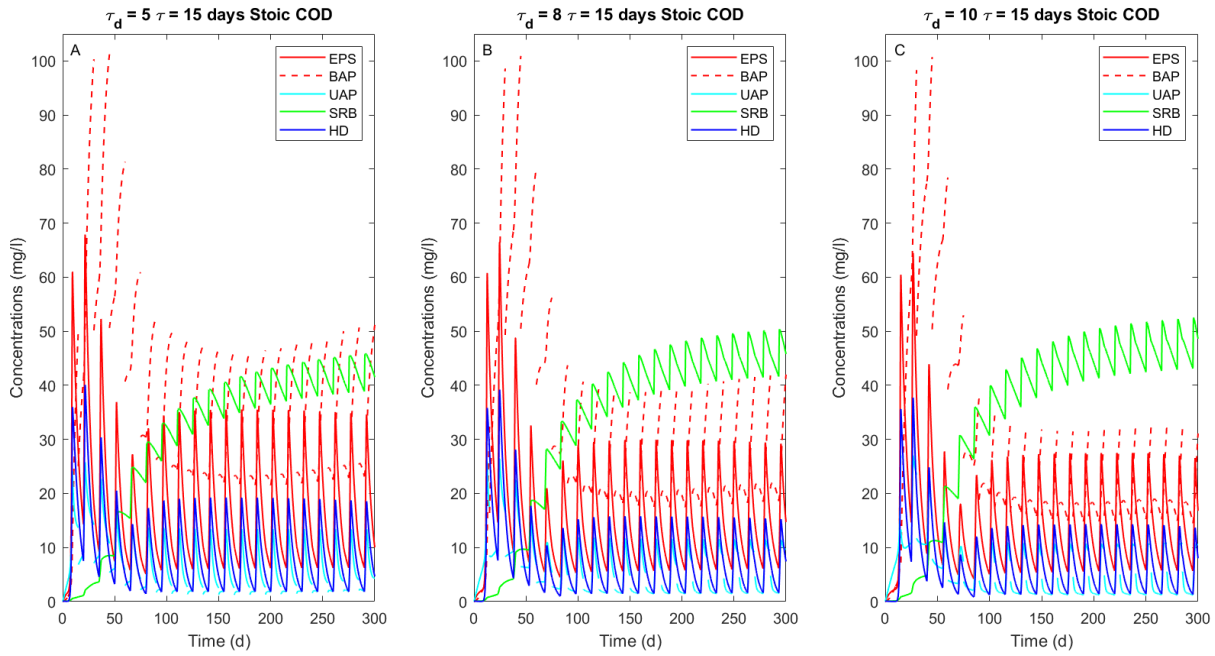

Fig. 3. 9 SMP production and concentration of heterotrophic families (i.e. HD and SRB) overtime increasing τ_d from 5 (A) to 8 (B) and 10 days (C) with an injection of stoichiometric COD. The solid dark blue line represents the heterotrophic denitrifiers (HD), while the solid green line indicates the sulfate-reducing bacteria (SRB). The solid red line indicates the EPS, which allows the production of BAP (red dashed line) after hydrolysis. The solid light blue line represents the UAP.

3.6 CONCLUSION

In this work, we presented a model investigating the dynamics of SdAD as the main process occurring in the presence of elemental sulfur as inorganic electron donor. The model also takes into account the growth of two heterotrophic families, i.e. HD and SRB, naturally growing in sulfur-governed autotrophic systems. Numerical simulations investigated to which extent the heterotrophic denitrification and sulfate reduction, promoted by COD addition and SMP production, affect autotrophic denitrification performance. We observed that the growth of the two heterotrophic families these two microbial families is favored by SMP production and mainly COD when an external carbon source is provided. The results obtained are in line with the intended objectives: (I) the concentration of sulfate in the effluent is lower in the scenarios where the COD injection occurs, even for low values of τ_d; (II) the simultaneous activity of both heterotrophic

biomasses leads to a better performance of the process; (III) SRB can also grow also in the absence of an external carbon addition.

The model reproduces with a good approximation the experimental observations in terms of microbial families and process performance, representing a tool capable of responding to different needs that are mainly represented by:

- nitrate, nitrite and sulfate effluent concentrations;
- the simultaneous growth of three different microbial families;
- the competition between the two heterotrophic families involved;
- the effects of SMP on the heterotrophic growth;
- the influence of the reaction period;
- the influence of COD addition on the efficiency of SdAD, heterotrophic denitrification and sulfate reduction.

Future work will be necessary to calibrate and validate the model experimentally.

3.7 REFERENCES

[1] Y. X. Cui *et al.*, "Biological nitrogen removal from wastewater using sulphur-driven autotrophic denitrification," *Appl. Microbiol. Biotechnol.*, vol. 103, no. 15, pp. 6023–6039, 2019, doi: 10.1007/s00253-019-09935-4.

[2] A. Kostrytsia *et al.*, "Biofilm carrier type affects biogenic sulfur-driven denitrification performance and microbial community dynamics in moving-bed biofilm reactors," *Chemosphere*, vol. 287, no. P1, p. 131975, 2021, doi: 10.1016/j.chemosphere.2021.131975.

[3] Y. Wang, C. Bott, and R. Nerenberg, "Sulfur-based denitrification: Effect of biofilm development on denitrification fluxes," *Water Res.*, vol. 100, pp. 184–193, Sep. 2016, doi: 10.1016/j.watres.2016.05.020.

[4] A. Kostrytsia *et al.*, "Elemental sulfur-based autotrophic denitrification and denitritation: microbially catalyzed sulfur hydrolysis and nitrogen conversions," *J. Environ. Manage.*, vol. 211, pp. 313–322, Apr. 2018, doi: 10.1016/j.jenvman.2018.01.064.

[5] C. S. Laspidou and B. E. Rittmann, "Non-steady state modeling of extracellular polymeric substances, soluble microbial products, and active and inert biomass," *Water Res.*, vol. 36, no. 8, pp. 1983–1992, 2002, doi: 10.1016/S0043-1354(01)00414-6.

[6] B. J. Ni *et al.*, "Evaluation on factors influencing the heterotrophic growth on the soluble microbial products of autotrophs," *Biotechnol. Bioeng.*, vol. 108, no. 4, pp. 804–812, 2011, doi: 10.1002/bit.23012.

[7] J. Qian, J. Zhou, X. Pei, M. Zhang, and Y. Liu, "Bioactivities and formation/utilization of soluble microbial products (SMP) in the biological sulfate reduction under different conditions," *Chemosphere*, vol. 221, pp. 37–44, 2019, doi: 10.1016/j.chemosphere.2018.12.208.

[8] W. M. Xie, B. J. Ni, T. Seviour, G. P. Sheng, and H. Q. Yu, "Characterization of autotrophic and heterotrophic soluble microbial product (SMP) fractions from activated sludge," *Water Res.*, vol. 46, no. 19, pp. 6210–6217, Dec. 2012, doi: 10.1016/j.watres.2012.02.046.

[9] D. Ucar, F. Di Capua, A. Yücel, T. Nacar, and E. Sahinkaya, "Effect of nitrogen loading on denitrification, denitritation and filtration performances of membrane bioreactors fed with biogenic and chemical elemental sulfur," *Chem. Eng. J.*, vol. 419, no. February, 2021, doi: 10.1016/j.cej.2021.129514.

[10] B. J. Ni, B. E. Rittmann, F. Fang, J. Xu, and H. Q. Yu, "Long-term formation of microbial products in a sequencing batch reactor," *Water Res.*, vol. 44, no. 13, pp. 3787–3796, 2010, doi: 10.1016/j.watres.2010.04.035.

[11] H. Lu, D. Wu, D. T. W. Tang, G. H. Chen, M. C. M. Van Loosdrecht, and G. Ekama, "Pilot scale evaluation of SANI® process for sludge minimization and greenhouse gas reduction in saline sewage treatment," *Water Sci. Technol.*, vol. 63, no. 10, pp. 2149–2154, 2011, doi: 10.2166/wst.2011.342.

[12] E. Sahinkaya, A. Kilic, and B. Duygulu, “Pilot and full scale applications of sulfur-based autotrophic denitrification process for nitrate removal from activated sludge process effluent,” *Water Res.*, vol. 60, pp. 210–217, 2014, doi: 10.1016/j.watres.2014.04.052.

[13] J. Yang, X. Zhang, Y. Sun, A. Li, and F. Ma, “Formation of soluble microbial products and their contribution as electron donors for denitrification,” *Chem. Eng. J.*, vol. 326, pp. 1159–1165, 2017, doi: 10.1016/j.cej.2017.06.063.

[14] Y. Y. Qiu *et al.*, “Overlooked pathways of denitrification in a sulfur-based denitrification system with organic supplementation,” *Water Res.*, vol. 169, 2020, doi: 10.1016/j.watres.2019.115084.

[15] S. E. Oh, M. S. Bum, Y. B. Yoo, A. Zubair, and I. S. Kim, “Nitrate removal by simultaneous sulfur utilizing autotrophic and heterotrophic denitrification under different organics and alkalinity conditions: Batch experiments,” *Water Sci. Technol.*, vol. 47, no. 1, pp. 237–244, 2003, doi: 10.2166/wst.2003.0061.

[16] C. Zeng *et al.*, “Elemental sulfur-driven autotrophic denitrification for advanced nitrogen removal from mature landfill leachate after PN/A pretreatment,” *Chem. Eng. J.*, vol. 410, no. September 2020, pp. 1–10, 2021, doi: 10.1016/j.cej.2020.128256.

[17] X. J. Xu *et al.*, “Mathematical modeling of simultaneous carbon-nitrogen-sulfur removal from industrial wastewater,” *J. Hazard. Mater.*, vol. 321, pp. 371–381, 2017, doi: 10.1016/j.jhazmat.2016.08.074.

[18] Y. Wang, F. Sabba, C. Bott, and R. Nerenberg, “Using kinetics and modeling to predict denitrification fluxes in elemental-sulfur-based biofilms,” *Biotechnol. Bioeng.*, vol. 116, no. 10, pp. 2698–2709, Oct. 2019, doi: 10.1002/bit.27094.

[19] Y. Liu *et al.*, “Evaluation of nitrous oxide emission from sulfide- and sulfur-based autotrophic denitrification processes,” *Environ. Sci. Technol.*, vol. 50, no. 17, pp. 9407–9415, 2016, doi: 10.1021/acs.est.6b02202.

[20] A. Koenig and L. H. Liu, “Kinetic model of autotrophic denitrification in sulphur packed-bed reactors,” *Water Res.*, vol. 35, no. 8, pp. 1969–1978, 2001, doi: 10.1016/S0043-1354(00)00483-8.

[21] B. Batchelor and A. W. Lawrence, “Autotrophic Denitrification Using Elemental Sulfur,” 1978.

[22] G. Sin *et al.*, “Modelling nitrite in wastewater treatment systems: A discussion of different modelling concepts,” *Water Sci. Technol.*, vol. 58, no. 6, pp. 1155–1171, 2008, doi: 10.2166/wst.2008.485.

[23] A. S. Abdel-Rady, A. M. A. El-Sayed, S. Z. Rida, and I. Ameen, “On some impulsive differential equations,” *Math. Sci. Lett.*, vol. 1, no. 2, pp. 105–113, 2012, doi: 10.12785/msl/010203.

[24] R. Sierra-Alvarez, R. Beristain-Cardoso, M. Salazar, J. Gómez, E. Razo-Flores, and J. A. Field, “Chemolithotrophic denitrification with elemental sulfur for groundwater treatment,” *Water Res.*, vol. 41, no. 6, pp. 1253–1262, 2007, doi: 10.1016/j.watres.2006.12.039.

[25] Y. Liu, J. Sun, L. Peng, D. Wang, X. Dai, and B. J. Ni, “Assessment of heterotrophic growth supported by soluble microbial products in anammox biofilm using multidimensional modeling,” *Sci. Rep.*, vol. 6, no. June, pp. 1–11, 2016, doi: 10.1038/srep27576.

[26] C. Huiliñir *et al.*, “Elemental sulfur-based autotrophic denitrification in stoichiometric S0/N ratio: Calibration and validation of a kinetic model,” *Bioresour. Technol.*, vol. 307, Jul. 2020, doi: 10.1016/j.biortech.2020.123229.

[27] S. V. Kalyuzhnyi and V. V. Fedorovich, “Mathematical modelling of competition between sulphate reduction and methanogenesis in anaerobic reactors,” *Bioresour. Technol.*, vol. 65, no. 3, pp. 227–242, 1998, doi: 10.1016/S0960-8524(98)00019-4.

[28] K. Y. Show, D. J. Lee, and X. Pan, “Simultaneous biological removal of nitrogen-sulfur-carbon: Recent advances and challenges,” *Biotechnol. Adv.*, vol. 31, no. 4, pp. 409–420, 2013, doi: 10.1016/j.biotechadv.2012.12.006.

[29] A. Kostrytsia, S. Papirio, M. R. Mattei, L. Frunzo, P. N. L. Lens, and G. Esposito, “Sensitivity analysis for an elemental sulfur-based two-step denitrification model,” *Water Sci. Technol.*, vol. 78, no. 6, pp. 1296–1303, Nov. 2018, doi: 10.2166/wst.2018.398.

[30] G. Xu *et al.*, “Evaluation of simultaneous autotrophic and heterotrophic denitrification processes and bacterial community structure analysis,” *Appl. Microbiol. Biotechnol.*, vol. 99, no. 15, pp. 6527–6536, Aug. 2015, doi: 10.1007/s00253-015-6532-2.

[31] Y. Liu *et al.*, “Optimizing sulfur-driven mixotrophic denitrification process: System performance and nitrous oxide emission,” *Chem. Eng. Sci.*, vol. 172, no. 2017, pp. 414–422, 2017, doi: 10.1016/j.ces.2017.07.005.

[32] Y. Sun and M. Nemati, “Evaluation of sulfur-based autotrophic denitrification and denitritation for biological removal of nitrate and nitrite from contaminated waters,” *Bioresour. Technol.*, vol. 114, pp. 207–216, 2012, doi: 10.1016/j.biortech.2012.03.061.

[33] Y. Tian, L. Chen, and T. Jiang, “Characterization and modeling of the soluble microbial products in membrane bioreactor,” *Sep. Purif. Technol.*, vol. 76, no. 3, pp. 316–324, 2011, doi: 10.1016/j.seppur.2010.10.022.

Chapter 3.S Supplementary information

MODELLING THE EFFECT OF SMP PRODUCTION AND EXTERNAL CARBON ADDITION ON S-DRIVEN AUTOTROPHIC DENITRIFICATION

3.S.1 KINETIC AND STOICHIOMETRIC REALTION

Table 3.S. 1 Matrix for the stoichiometric values referred to biomasses.

REACTION TYPE	X_{HID}	X_{AUT}	X_{STOB}	X_{EPS}	X_{HD}	X_{SRB}	X_I
1. Hydrolysis of S_0							
2. Autotrophic denitrification $NO_3^- \rightarrow NO_2^-$		$1 - f_{EPS,AUT} - f_{UAP,AUT}$		$f_{EPS,AUT}$			
3. Autotrophic denitrification $NO_2^- \rightarrow N_2$		$1 - f_{EPS,AUT} - f_{UAP,AUT}$		$f_{EPS,AUT}$			
4. Decay X_{HID}	-1		$1 - f_I$				f_I
5. Decay X_{AUT}		-1	$1 - f_I - f_{BAP}$				f_I
6. Hydrolysis of X_{STOB}			-1				
7. Release of X_{EPS}				-1			
8. Growth of X_{HD} on S_{COD} and S_{NO2}				$\frac{k_{EPS}}{y_{H,COD}}$	$1 - \frac{k_{UAP}}{y_{H,COD}} - \frac{k_{EPS}}{y_{H,COD}}$		
9. Growth of X_{HD} on S_{COD} and S_{NO3}				$\frac{k_{EPS}}{y_{H,COD}}$	$1 - \frac{k_{UAP}}{y_{H,COD}} - \frac{k_{EPS}}{y_{H,COD}}$		
10. Growth of X_{HD} on S_{UAP} and S_{NO2}					1		
11. Growth of X_{HD} on S_{UAP} and S_{NO3}					1		
12. Growth of X_{HD} on S_{BAP} and S_{NO2}					1		
13. Growth of X_{HD} on S_{BAP} and S_{NO3}					1		
14. Decay of X_{HD}			$1 - f_I - f_{BAP}$		-1		f_I
15. Growth of X_{SRB} on S_{COD}				$f_{EPS,SRB}$		$1 - f_{EPS,SRB} - f_{UAP,SRB}$	
16. Decay of X_{SRB}			$1 - f_I - f_{BAP}$			-1	f_I
17. Growth of X_{SRB} on S_{UAP}						1	
18. Growth of X_{SRB} on S_{BAP}						1	

Table 3.S. 2 Matrix for the stoichiometric values referred to Substrates.

REACTION TYPE	S_{S_0}	S_{S_b}	$S_{NO_3^-}$	$S_{NO_2^-}$	S_{N_2}	$S_{SO_4^{2-}}$	S_{UAP}	S_{BAP}	S_{COD}
1. Hydrolysis of S_0	-1	1							
2. Autotrophic denitrification $NO_3^- \rightarrow NO_2^-$		$-\frac{b_1}{y_{AUT,NO_3^-}}$	$-\frac{1}{y_{AUT,NO_3^-}}$	$\frac{1}{y_{AUT,NO_3^-}}$		$\frac{b_1}{y_{AUT,NO_3^-}}$	$f_{UAP,AUT}$		
3. Autotrophic denitrification $NO_2^- \rightarrow N_2$		$-\frac{b_2}{y_{AUT,NO_2^-}}$		$-\frac{1}{y_{AUT,NO_2^-}}$	$\frac{1}{y_{AUT,NO_2^-}}$	$\frac{b_2}{y_{AUT,NO_2^-}}$	$f_{UAP,AUT}$		
4. Decay X_{HID}								f_{BAP}	
5. Decay X_{AUT}								f_{BAP}	
6. Hydrolysis of X_{STOB}									1
7. Release of X_{EPS}								1	
8. Growth of X_{HD} on S_{COD} and S_{NO2}				$-\frac{(1-y_{H,COD})(1-k_{UAP}-k_{EPS})}{1{,}71y_{H,COD}}$	$\frac{(1-y_{H,COD})(1-k_{UAP}-k_{EPS})}{1{,}71y_{H,COD}}$		$\frac{k_{UAP}}{y_{H,COD}}$		$-\frac{1}{y_{H,COD}}$
9. Growth of X_{HD} on S_{COD} and S_{NO3}			$-\frac{(1-y_{H,COD})(1-k_{UAP}-k_{EPS})}{2{,}86y_{H,COD}}$		$\frac{(1-y_{H,COD})(1-k_{UAP}-k_{EPS})}{2{,}86y_{H,COD}}$		$\frac{k_{UAP}}{y_{H,COD}}$		$-\frac{1}{y_{H,COD}}$
10. Growth of X_{HD} on S_{UAP} and S_{NO2}				$-\frac{(1-y_{H,UAP})}{1{,}71y_{H,UAP}}$	$\frac{(1-y_{H,UAP})}{1{,}71y_{H,UAP}}$		$-\frac{1}{y_{H,UAP}}$		
11. Growth of X_{HD} on S_{UAP} and S_{NO3}			$-\frac{(1-y_{H,UAP})}{2{,}86y_{H,UAP}}$		$\frac{(1-y_{H,UAP})}{2{,}86y_{H,UAP}}$		$-\frac{1}{y_{H,UAP}}$		
12. Growth of X_{HD} on S_{BAP} and S_{NO2}				$-\frac{(1-y_{H,BAP})}{1{,}71y_{H,BAP}}$	$\frac{(1-y_{H,BAP})}{1{,}71y_{H,BAP}}$			$-\frac{1}{y_{H-BAP}}$	
13. Growth of X_{HD} on S_{BAP} and S_{NO3}			$-\frac{(1-y_{H,BAP})}{2{,}86y_{H,BAP}}$		$\frac{(1-y_{H,BAP})}{2{,}86y_{H,BAP}}$			$-\frac{1}{y_{H-BAP}}$	
14. Decay of X_{HD}								f_{BAP}	
15. Growth of X_{SRB} on S_{COD}		$\frac{1}{2}\left(\frac{1-y_{SRB}}{y_{SRB}}\right)$				$-\frac{1}{2}\left(\frac{1-y_{SRB}}{y_{SRB}}\right)$	$f_{UAP,SRB}$		$-\frac{1}{y_{SRB}}$
16. Decay of X_{SRB}								f_{BAP}	
17. Growth of X_{SRB} on S_{UAP}		$\frac{1}{2}\left(\frac{1-y_{SRB}}{y_{SRB}}\right)$				$-\frac{1}{2}\left(\frac{1-y_{SRB}}{y_{SRB}}\right)$	$-\frac{1}{y_{SRB}}$		
18. Growth of X_{SRB} on S_{BAP}		$\frac{1}{2}\left(\frac{1-y_{SRB}}{y_{SRB}}\right)$				$-\frac{1}{2}\left(\frac{1-y_{SRB}}{y_{SRB}}\right)$		$-y_{SRB}$	

Table 3.S. 3 Stoichiometric constant values.

	Description	Value	Unit	Source
$f_{EPS,AUT}$	Fraction of X_{EPS} for X_{AUT} biomass growth	0.09	mg COD/mg N	[1]
$f_{UAP,AUT}$	Fraction of S_{UAP} for X_{AUT} biomass growth	0.14	mg COD/mg N	[1]
f_{BAP}	Fraction of S_{BAP} for biomass growth	0.0215	mg COD/mg COD	[2]
f_I	Fraction of X_I in biomass decay	0.08	mg COD/mg COD	[3]
k_{EPS}	Yield coefficient for X_{EPS} for X_{HD}	0.14	mg COD/mg COD	[4]
k_{UAP}	Yield coefficient for S_{UAP} for X_{HD}	0.09	mg COD/mg COD	[4]
b_1	S_{S_b} to $S_{NO_3^-}$ stoichiometric ratio	1.2	mg S/ mg N	[5]
b_2	S_{S_b} to $S_{NO_2^-}$ stoichiometric ratio	0.55	mg S/ mg N	[5]
y_{AUT,NO_3^-}	Yield coefficient for X_{AUT} on $S_{NO_3^-}$	0.37	mg COD/mg N	[6]
y_{AUT,NO_2^-}	Yield coefficient for X_{AUT} on $S_{NO_2^-}$	0.414	mg COD/mg N	[6]
$f_{EPS,SRB}$	Fraction of X_{EPS} for X_{SRB} biomass growth	0.9	mg COD/mg COD	assumed
$f_{UAP,SRB}$	Fraction of S_{UAP} for X_{SRB} biomass growth	0.14	mg COD/mg COD	assumed
$y_{H,COD}$	Yield coefficient for X_{HD} on S_{COD}	0.34	mg COD/mg COD	[4]
$y_{H,UAP}$	Yield coefficient for X_{HD} on S_{UAP}	0.45	mg COD/mg COD	[4]
$y_{H,BAP}$	Yield coefficient for X_{HD} on S_{BAP}	0.45	mg COD/mg COD	[4]
y_{SRB}	Yield coefficient for X_{SRB}	0.0568	mg COD/mg COD	[7]

Table 3.S. 4 Reaction terms.

j- process		*Process rate (ρ_j)*
1	Hydrolysis of elemental sulfur $S_0 \rightarrow S_{bio}$	$K_0 \cdot k_1 \frac{S_{S^0}}{\frac{K_1}{a^*} + S_{S^0}} X_{HID}$
2	Autotrophic denitrification $NO_3^- \rightarrow NO_2^-$	$\mu_{S_b,NO_3^-}^{max} \frac{S_{S_b}}{k_{AUT,S_b} + S_{NO_2^-}} \cdot \frac{S_{NO_3^-}}{k_{AUT,NO_3^-} + S_{NO_3^-}} \cdot \frac{S_{NO_3^-}}{S_{NO_3^-} + S_{NO_2^-}} \cdot X_{AUT}$
3	Autotrophic denitrification $NO_2^- \rightarrow N_2$	$\mu_{S_b,NO_2^-}^{max} \frac{S_{S_b}}{k_{AUT,S_b} + S_{S_b}} \cdot \frac{S_{NO_2^-}}{k_{AUT,NO_2^-} + S_{NO_2^-}} \cdot \frac{S_{NO_2^-}}{S_{NO_3^-} + S_{NO_2^-}} \cdot X_{AUT}$
4	Decay of HYD	$k_{d,HID} \cdot X_{HID}$
5	Decay of AUT	$k_{d,AUT} \cdot X_{AUT}$
6	Hydrolysis of organic carbon $X_{STO} \rightarrow S_{COD}$	$k_{HID,STOB} \cdot \frac{X_{STO} / X_{HD}}{k_{STOB,COD} + X_{STO} / X_{HD}} X_{HD}$
7	Release of EPS $X_{EPS} \rightarrow S_{BAP}$	$K_{HID,EPS} \cdot X_{EPS}$
8	Growth of X_{HD} on S_S and S_{NO2}	$\mu_{HD,COD} \cdot \eta_{ox} \cdot \frac{S_{COD}}{k_{COD,HD} + S_{COD}} \cdot \frac{S_{NO_2^-}}{k_{NO_2}^{HD} + S_{NO_2^-}} \cdot \frac{S_{NO_2^-}}{S_{NO_2^-} + S_{NO_3^-}} \cdot \frac{S_{COD}}{S_{UAP} + S_{BAP} + S_{COD}} \cdot X_{HD}$
9	Growth of X_{HD} on S_S and S_{NO3}	$\mu_{HD,COD} \cdot \eta_{ox} \cdot \frac{S_{COD}}{k_{COD,HD} + S_{COD}} \cdot \frac{S_{NO_3^-}}{k_{NO_3}^{HD} + S_{NO_3^-}} \cdot \frac{S_{NO_3^-}}{S_{NO_2^-} + S_{NO_3^-}} \cdot \frac{S_{COD}}{S_{UAP} + S_{BAP} + S_{COD}} \cdot X_{HD}$
10	Growth of X_{HD} on S_{UAP} and S_{NO2}	$\mu_{HD,UAP} \cdot \eta_{OX} \cdot \frac{S_{UAP}}{k_{UAP} + S_{UAP}} \cdot \frac{S_{NO_2^-}}{k_{NO_2}^{HD} + S_{NO_2^-}} \cdot \frac{S_{NO_2^-}}{S_{NO_2^-} + S_{NO_3^-}} \cdot \frac{S_{UAP}}{S_{UAP} + S_{BAP} + S_{COD}} \cdot X_{HD}$
11	Growth of X_{HD} on S_{UAP} and S_{NO3}	$\mu_{HD,UAP} \cdot \eta_{OX} \cdot \frac{S_{UAP}}{k_{UAP} + S_{UAP}} \cdot \frac{S_{NO_3^-}}{k_{NO_3}^{HD} + S_{NO_3^-}} \cdot \frac{S_{NO_3^-}}{S_{NO_2^-} + S_{NO_3^-}} \cdot \frac{S_{UAP}}{S_{UAP} + S_{BAP} + S_{COD}} \cdot X_{HD}$
12	Growth of X_{HD} on S_{BAP} and S_{NO2}	$\mu_{HD,BAP} \cdot \eta_{OX} \cdot \frac{S_{BAP}}{k_{BAP} + S_{BAP}} \cdot \frac{S_{NO_2^-}}{k_{NO_2}^{HD} + S_{NO_2^-}} \cdot \frac{S_{NO_2^-}}{S_{NO_2^-} + S_{NO_3^-}} \cdot \frac{S_{BAP}}{S_{UAP} + S_{BAP} + S_{COD}} \cdot X_{HD}$
13	Growth of X_{HD} on S_{BAP} and S_{NO3}	$\mu_{HD,BAP} \cdot \eta_{OX} \cdot \frac{S_{BAP}}{k_{BAP} + S_{BAP}} \cdot \frac{S_{NO_3^-}}{k_{NO_3}^{HD} + S_{NO_3^-}} \cdot \frac{S_{NO_3^-}}{S_{NO_2^-} + S_{NO_3^-}} \cdot \frac{S_{BAP}}{S_{UAP} + S_{BAP} + S_{COD}} \cdot X_{HD}$
14	Decay of X_{HD}	$k_{d,HD} \cdot X_{HD}$
15	Growth of X_{SRB} on S_S	$\mu_{SRB} \cdot \frac{S_{COD}}{k_{COD,SRB} + S_{COD}} \cdot \frac{S_{SO_4^{2-}}}{k_{SRB,SO_4} + S_{SO_4^{2-}}} \cdot \frac{S_{COD}}{S_{UAP} + S_{BAP} + S_{COD}} \cdot X_{SRB}$
16	Growth of X_{SRB} on UAP	$\mu_{SRB} \cdot \frac{\mu_{HD,UAP}}{\mu_{HD,COD}} \cdot \frac{S_{UAP}}{k_{COD,SRB} + S_{UAP}} \cdot \frac{S_{SO_4^{2-}}}{k_{SRB,SO_4} + S_{SO_4^{2-}}} \cdot \frac{S_{UAP}}{S_{UAP} + S_{BAP} + S_{COD}} \cdot X_{SRB}$
17	Growth of X_{SRB} on BAP	$\mu_{SRB} \cdot \frac{\mu_{HD,BAP}}{\mu_{HD,COD}} \cdot \frac{S_{BAP}}{k_{COD,SRB} + S_{BAP}} \cdot \frac{S_{SO_4^{2-}}}{k_{SRB,SO_4} + S_{SO_4^{2-}}} \cdot \frac{S_{BAP}}{S_{UAP} + S_{BAP} + S_{COD}} \cdot X_{SRB}$
18	Decay of X_{SRB}	$k_{d,SRB} \cdot X_{SRB}$

Table 3.S. 5 Kinetic constant values.

	Description	Value	Unit	Ref.
K_0	Efficiency growth coefficient for X_{HID}	0.1	mg COD/ mg S	[8]
$\mu_{S_b,NO_3^-}^{max}$	Maximum growth rate for X_{AUT} on $S_{NO_3^-}$	0.0067	d^{-1}	[8]
$\mu_{S_b,NO_2^-}^{max}$	Maximum growth rate for X_{AUT} on $S_{NO_2^-}$	0.0058	d^{-1}	[8]
k_{AUT,S_b}	Half-saturation constant for S_{S_b}	0.215	mg S/l	[9]
k_{AUT,NO_3^-}	Half-saturation constant for $S_{NO_3^-}$	36	mg N/l	[8]
k_{AUT,NO_2^-}	Half-saturation constant for $S_{NO_3^-}$	40	mg N/l	[6]
k_1	Hydrolysis kinetic constant	0.081	mg S/ mg COD ·d	[8]
κ_1	Volume specific half-saturation constant for S_{S^0}	5.1	1/dm	[8]
a^*	Mass specific area	0.0008164	dm^2/mg	[8]
$k_{d,HID}$	Decay rate coefficient for X_{HYD}	0.0006	d^{-1}	[10]
$k_{d,AUT}$	Decay rate coefficient for X_{AUT}	0.0006	d^{-1}	[10]
$k_{HID,STOB}$	Hydrolysis rate constant	3	d^{-1}	[11]
$k_{STOB,COD}$	Hydrolysis saturation constant	1	mg COD / mg COD	[11]
$K_{HID,EPS}$	EPS hydrolysis rate coefficient	0.1704	d^{-1}	[4]
η_{OX}	Anoxic reduction factor	0.6		[11]
$\mu_{HD,COD}$	Maximum growth rate of HD on COD	5.76	d^{-1}	[12]
$\mu_{HD,UAP}$	Maximum growth rate of HD on UAP	1.272	d^{-1}	[4]
$\mu_{HD,BAP}$	Maximum growth rate of HD on BAP	0.0696	d^{-1}	[4]
$k_{d,HD}$	Death rate coefficient of HD	0.1992	d^{-1}	[3]
$k_{NO_2}^{HD}$	$S_{NO_2^-}$ affinity constant for HD	0.5	mg/l	[3]
$k_{NO_3}^{HD}$	$S_{NO_3^-}$ affinity constant for HD	0.5	mg/l	[3]
$k_{COD,HD}$	biomass affinity constant for COD	2	mg/l	[3]
k_{UAP}	biomass affinity constant for UAP	100	mg/l	[4]
k_{BAP}	biomass affinity constant for BAP	85	mg/l	[4]
μ_{SRB}	Maximum growth rate of SRB	0.55	d^{-1}	[7]
$k_{COD,SRB}$	Half saturation value of SRB for COD	6	mg/l	[7]
k_{SRB,SO_4}	Half saturation value of SRB for $S_{SO_4^{2-}}$	3.2	mg/l	[13]
$k_{d,SRB}$	Death rate coefficient of SRB	0.02	d^{-1}	[14]

3.S.2 REFERENCES

[1] B. J. Ni, M. Ruscalleda, and B. F. Smets, "Evaluation on the microbial interactions of anaerobic ammonium oxidizers and heterotrophs in Anammox biofilm," *Water Res.*, vol. 46, no. 15, pp. 4645–4652, Oct. 2012, doi: 10.1016/j.watres.2012.06.016.

[2] T. Jiang *et al.*, "Modelling the production and degradation of soluble microbial products (SMP) in membrane bioreactors (MBR)," *Water Res.*, vol. 42, no. 20, pp. 4955–4964, 2008, doi: 10.1016/j.watres.2008.09.037.

[3] M. Henze, W. Gujer, T. Mino, and M. van Loosedrecht, "Activated Sludge Models ASM1, ASM2, ASM2d and ASM3." IWA Publishing, Oct. 01, 2006. doi: 10.2166/9781780402369.

[4] C. S. Laspidou and B. E. Rittmann, "Non-steady state modeling of extracellular polymeric substances, soluble microbial products, and active and inert biomass," *Water Res.*, vol. 36, no. 8, pp. 1983–1992, 2002, doi: 10.1016/S0043-1354(01)00414-6.

[5] R. Sierra-Alvarez, R. Beristain-Cardoso, M. Salazar, J. Gómez, E. Razo-Flores, and J. A. Field, "Chemolithotrophic denitrification with elemental sulfur for groundwater treatment," *Water Res.*, vol. 41, no. 6, pp. 1253–1262, 2007, doi: 10.1016/j.watres.2006.12.039.

[6] G. Xu, F. Yin, S. Chen, Y. Xu, and H. Q. Yu, "Mathematical modeling of autotrophic denitrification (AD) process with sulphide as electron donor," *Water Res.*, vol. 91, pp. 225–234, 2016, doi: 10.1016/j.watres.2016.01.011.

[7] S. V. Kalyuzhnyi and V. V. Fedorovich, "Mathematical modelling of competition between sulphate reduction and methanogenesis in anaerobic reactors," *Bioresour. Technol.*, vol. 65, no. 3, pp. 227–242, 1998, doi: 10.1016/S0960-8524(98)00019-4.

[8] A. Kostrytsia *et al.*, "Elemental sulfur-based autotrophic denitrification and denitritation: microbially catalyzed sulfur hydrolysis and nitrogen conversions," *J. Environ. Manage.*, vol. 211, pp. 313–322, Apr. 2018, doi: 10.1016/j.jenvman.2018.01.064.

[9] Y. Liu *et al.*, "Evaluation of nitrous oxide emission from sulfide- and sulfur-based autotrophic denitrification processes," *Environ. Sci. Technol.*, vol. 50, no. 17, pp. 9407–9415, 2016, doi: 10.1021/acs.est.6b02202.

[10] G. Sin *et al.*, “Modelling nitrite in wastewater treatment systems: A discussion of different modelling concepts,” *Water Sci. Technol.*, vol. 58, no. 6, pp. 1155–1171, 2008, doi: 10.2166/wst.2008.485.

[11] W. Gujer, M. Henze, T. Mino, and M. Van Loosdrecht, “Activated Sludge Model No. 3,” in *Water Science and Technology*, Jan. 1999, vol. 39, no. 1, pp. 183–193. doi: 10.1016/S0273-1223(98)00785-9.

[12] B. J. Ni, F. Fang, B. E. Rittmann, and H. Q. Yu, “Modeling microbial products in activated sludge under feast#famine conditions,” *Environ. Sci. Technol.*, vol. 43, no. 7, pp. 2489–2497, 2009, doi: 10.1021/es8026693.

[13] V. Fedorovich, P. Lens, and S. Kalyuzhnyi, “Extension of Anaerobic Digestion Model No. 1 with Processes of Sulfate Reduction,” 2003.

[14] D. J. Batstone *et al.*, “The IWA Anaerobic Digestion Model No 1 (ADM1),” *Water Sci. Technol.*, vol. 45, no. 10, pp. 65–73, May 2002, doi: 10.2166/wst.2002.0292.

Chapter 4

MODELLING OF MICROBIAL DYNAMICS AND EFFICIENCY OF AN ELEMENTAL S-DRIVEN AUTOTROPHIC DENITRIFICATION SBR IN THE PRESENCE OF SOLUBLE MICROBIAL PRODUCTS

This Chapter will be submitted as:

Guerriero G, Mattei MR, Papirio S, Esposito G, Huilinir C, Frunzo L "*Modelling of microbial dynamics and efficiency of an elemental S-driven autotrophic denitrification SBR in the presence of soluble microbial products*".

4.1 INTRODUCTION

Due to its high solubility and frequent use in both industry and agriculture, nitrate is one of the most common pollutants in groundwater and wastewater, leading to serious health problems such as methemoglobinemia, heart diseases and other more if present at high concentrations [1]. In aquatic environments, nitrate is responsible for the growth of undesirable bacteria and algae, which promotes eutrophication and anoxia. As well known, the conventional biological process used for nitrate removal from waters is heterotrophic denitrification (HD), which often requires the support of external organic compounds when treating organic-deficient water streams [2]. However, the addition of external carbon source increases the overall costs of the process [3] besides a higher sludge production, which is a typical drawback of heterotrophic processes [4].

The most promising alternative to HD in terms of economic convenience is sulfur-driven autotrophic denitrification (SdAD). Autotrophic denitrifying bacteria use sulfur as electron donor, not requiring any external source of carbon. Furthermore, autotrophic bacterial families have a lower growth yield compared to heterotrophic families, thus the occurrence of residual organic pollution and the risk of high sludge production are reduced [5], [6]. Among all sulfur compounds to be used for SdAD, elemental sulfur leads to many operational advantages such as high cost effectiveness, low toxicity, easy transport and availability due to its widely use in other applications [3], [7], [8]. During SdAD, sulfur particles could be also used as support for the growth of a denitrifying biofilm, which allows the retention of high biomass concentrations in the reactors [5], [9], [10]. Different reactor configurations capable for maintaining SdAD have been proposed in literature, in the presence or absence of limestone, using both pure and mixed cultures [11].

From the earliest studies, it is made clear that, given the solid nature of elemental sulfur, it is necessary to account for the hydrolysis of sulfur to be effectively utilized by autotrophic denitrifiers (AUT) [10], [12]. The first mathematical model taking into account the biological solubilization of elemental sulfur was proposed by Kostrytsia et al. (2018) [10], and subsequently validated by Huiliñir et al. (2020) [13]. Both studies reported that the hydrolysis step is strongly affected by the sulfur particle size. Notwithstanding, although it has been shown that the preliminary solubilization step is the rate limiting of the whole process, this is not the single disadvantage of SdAD, which can entail a high effluent sulfate production. Indeed,

sulfate in high concentrations is considered a secondary pollutant and requires a further treatment step.

A solution to prevent high effluent sulfate concentrations is to couple autotrophic denitrification with HD by adding organic carbon prior to or during the occurrence of the biological reactions. Previous studies showed that the addition of different forms of soluble chemical oxygen demand (COD), such as acetate and methanol, to the influent of a SdAD reactor mainly colonized by an autotrophic biomass is not detrimental the process [14]–[16]. Moreover, the addition of small amounts of external carbon also allows to maintain a stable alkalinity (usually guaranteed by the addition of limestone) and prevents the accumulation of nitrite and sulfate, which could slow or inhibit SdAD [10], [17]. Nonetheless, experimental evidences show that, even if COD is not added to the reactor, a small part of the sulfate produced during SdAD can be biologically removed [9], [17]. Indeed, sulfate-reducing bacteria (SRB) are heterotrophic microorganisms capable to survive also picking up the necessary carbon from the products of the natural microbial activities [9]. These are known as soluble microbial products (SMP) and are mainly composed by utilization associated products (UAP) and biomass associated products (BAP) [18].

Recently, Guerriero et al. (2022) [19] proposed a mathematical model accounting for the production and consumption of SMP during SdAD, HD and sulfate reduction in a sequencing batch reactor (SBR). The model also took into account the support that these compounds could give to the three processes in the presence of an external carbon source. In the present study, the authors propose to test the aforementioned model and evaluate its applicability under more realistic conditions. The large number of simulations performed was aimed to find the operating conditions in terms of SBR cycle duration, amount of COD injected, and time of COD injection maximizing the removal performances. The production and consumption of SMP were also evaluated to assess their contribution in maintaining the heterotrophic processes and to finetune the supplementation of external organics.

4.2 METHODOLOGY

4.2.1 BIOLOGICAL MODEL

The biological model reported here for convenience could be divided in four different main pathways:

1. Hydrolysis of the elemental sulfur into bioavailable sulfur.
2. Two-step autotrophic denitrification, in which the bioavailable sulfur obtained by hydrolysis of the chemically synthesized elemental sulfur is used as electron donor to transform nitrate into nitrite (step 1) and then nitrite into nitrogen gas (step 2).
3. Heterotrophic denitrification, in which COD, UAP, BAP (both measured as COD) are used to remove both nitrate and nitrite.
4. Sulfate reduction, in which COD, UAP, BAP are used to reduce sulfate into bioavailable sulfur.

The latter is a strong assumption because sulfate reduction generally leads to sulfide production. Nevertheless, when sulfide is used by AUT, this results in a faster denitrification kinetics than with bioavailable sulfur, making the assumption acceptable and conservative.

Simultaneously to the main biological pathways, the production and consumption of all products deriving from biomass activities were taken into account for the model development, as also reported by Guerriero *et al.*, 2022 [19]. The hydrolytic biomass (HID) was not included in the growth balance due to the lack of information on the production of UAP and EPS associated with HID growth.

4.2.2 MATHEMATICAL MODEL

The mathematical model used to describe the process here, use the same equation of the previous work by Guerriero *et al.*, 2022 [19]. Indeed, to model an SBR, which is system that undergoes to instantaneous changing while operating in continuous time, impulsive differential equations was used [20]. Due to the necessary changes performed in the equation to adapt the equation to real performance case, the model equations here are recalled for convenience.

The model considers seven different biomasses X_i: Hydrolytic biomass (HID), autotrophic biomass (AUT), biological organic carbon stocked (STOB), extra polymeric substances (EPS), heterotrophic denitrifiers (HD), sulfate reducing bacteria (SRB), inert (INE); and nine different substrates S_j: elemental sulfur (S_0), bioavailable sulfur (S_b), Nitrate (NO_3^-), nitrite (NO_2^-), nitrogen (N_2), sulfate (SO_4^{2-}), utilization associated products UAP, biomass associated products BAP, COD.

The system of first order Impulsive differential equation (IDEs) is used to model the biological processes occurring in a SBR configuration, for each cycle the following phases are repeated after the first initial filling:

1. First Reaction period (continuous)
2. Injection of COD (instantaneous)
3. Second Reaction period (continuous)
4. Settling (instantaneous)
5. Emptying (instantaneous)
6. Filling (instantaneous)

The impulsive differential equations for both substrates and microbial species:

$$\dot{S}_j(t) = r_{S,j}(t, \boldsymbol{S}, \boldsymbol{X}),\ t \in J = [0,T],\ \ t \neq t_k,\ S_j(0) = S_{j0}, \quad (4.1)$$

$$\dot{X}_i(t) = r_{X,i}(t, \boldsymbol{S}, \boldsymbol{X}),\ t \in J = [0,T],\ \ t \neq t_k,\ X_i(0) = X_{i0}, \quad (4.2)$$

$$\Delta S_j(t_k) = -\alpha_j S_j(t_k^-) + \alpha_j S_{in,j},\ k = 1, \ldots, m, \quad (4.3)$$

$$\Delta X_i(t_k) = -\gamma_i X_i(t_k^-),\ k = 1, \ldots, m, \quad (4.4)$$

Where:

$S_j(t),\ X_i(t)$ are the j[th] substrate and the i[th] biomass concentrations at time t respectively;

$r_{S,j}$ and $r_{X,i}$ are the reaction terms for the j[th] substrate and the i[th] biomass;

S_{j0} and X_{i0} are the initial concentration within the reactor for the j[th] substrate and the i[th] biomass;

$S_{in,j}$ is the concentration of the j[th] substrate in the fresh influent;

$0 = t_0 < t_1 < \ldots < t_m < t_{m+1} = T,\ t_{k+1} - t_k = \tau$, where τ denotes the duration of each cycle,

$$\Delta S_j(t_k) = S_j(t_k^+) - S_j(t_k^-),\ \Delta X_i(t_k) = X_i(t_k^+) + X_i(t_k^-)\ t = t_k;$$

α_j represents the emptying/refilling ratio γ_i takes into account the fraction of biomass removed from the system during the emptying phase and it is function of the settling efficiency performance of the model.

The $r_{S,j}$ and $r_{X,i}$ are expressed as a combination of the kinetic terms and stoichiometric parameters.

The first and second reaction periods are discriminated by the time of soluble COD injection in the system. Such operation is considered to occur instantaneously and does not affect the concentration of the other compounds.

$$\begin{cases} (k-1)\cdot\tau < t \leq (k-1)\tau + \tau_d \quad k = 1,\ldots,n, \quad FIRST\ REACTION\ PERIOD \\ (k-1)\cdot\tau + \tau_d < t \leq k\cdot\tau \quad k = 1,\ldots,n, \quad SECOND\ REACTION\ PERIOD \end{cases} \quad (4.5)$$

The equation that defines the jump function for COD between the two reaction periods is:

$$\Delta S_{\mathrm{COD}}\big((k-1)\tau + \tau_d\big) = S_{in,COD},\ k = 1,\ldots,n \quad (4.6)$$

The equations have been implemented by developing original code in in MatLab platform and the ODEs have been integrated using the MatLab routine ode113.

4.2.3 SIMULATIONS SET

The present work aims to remove the hypothesis of perfect settling efficiency used by Guerriero et al. (2022) [19] and evaluate the variation of the cycle duration (and, thus, the hydraulic retention time - HRT) and the volume of water to be treated. This was performed by increasing the emptying refilling ratio and reducing the settling efficiency. Indeed, in previous work, the system was assumed to have 100% sedimentation efficiency that mathematically means $\gamma = 0$ in equation 4.4.

In the model, the settling efficiency (regulated by the parameter γ) was set to be different for the microbial families considered. The value of γ for the attached biomass, made up of AUT, was 3%, while γ was set at 5% for the other settleable compounds. Elemental sulfur and HID

growing on it were, instead, assumed to remain in the SBR and not washed out with the effluent due to the higher weight.

Table 4. 1 Resume of the simulations performed.

	τ (d)Duration of Cycle			
τ_d *(d) Injection day*	8 HRT =10	10 HRT =12,5	15 HRT =18,75	20 HRT =25
0	X	X	X	X
2.5	X	X	X	X
5	X	X	X	X
7.5	X	X	X	X
10			X	X
12.5			X	X
15				X
17.5				X

The HRT was evaluated as:

$$HRT = \frac{\tau}{\alpha} \quad (4.7)$$

where α was set for all simulations equal to 80%. The day of COD injection τ_d was also varied considering steps of 2.5 days, differently to what carried out by Guerriero *et al.* (2022) [19]. Regarding the choice of different τ values, this is associated with the need of having cycles long enough to make autotrophic denitrification possible and evaluate the competition of AUT with the two microbial families. Likewise, shorter cycle durations were considered to accentuate the benefits given by the addition of external carbon and reduce HRT. Two different amounts of COD injected were considered: 300 and 500 mg/l. The lower amount represents approximately the necessary quantity to remove the sulfate produced during the autotrophic denitrification. The higher amount of the 500 mg/l was chosen to test the support given by the heterotrophic denitrifiers in terms of nitrogen removal, support which could also be used to speed up the process.

For all the simulations, a feed [NO_3^-] concentration of 150 mg N/l was considered, which is lower than that used by Guerriero *et al.*, (2022) [19]. 300 days was used as duration of the entire SBR operation period.

The amount of solid elemental sulfur was supposed to be added at the beginning of each simulation equal quantity of 21 g, which is more than the stoichiometric amount of sulfur required for nitrate removal.

The initial concentrations of microbial families and products were as reported in Table 4.2:

Table 4. 2. Initial condition for all the simulation performed.

X_{HYD} (mg COD/l)	X_{AUT} (mg COD/l)	X_{STOB} (mg COD/l)	X_{EPS} (mg COD/l)	X_{HD} (mg COD/l)	X_{SRB} (mg COD/l)	X_I (mg/l)
500	1100	0	0	10	10	0

S_{S_0} (mg/l)	S_{S_b} (mgS/l)	$S_{NO_3^-}$ (mg N/l)	$S_{NO_2^-}$ (mg N/l)	S_{N_2} (mg/l)	$S_{SO_4^{2-}}$ (mg S/l)	S_{UAP} (mg COD/l)	S_{BAP} (mg/l)	S_{COD} (mg COD/l)
21'000	0	150	0	0	0	0	0	0

The initial concentration of both the heterotrophic families was higher than that used by Guerriero *et al.*, (2022) [19], i.e. increased from 1 to 10 mg/l , but maintained low to keep the hypothesis of the natural growth of both heterotrophic families in a previous acclimatized autotrophic system.

4.2.4 CALCULATIONS

Due to the high number of simulations and for better understanding and summarizing the results, we decided to use four indicators: nitrogen removal percentage, effluent sulfate concentration, percentage of SRB over the heterotrophic species and total effluent SMP.

The main interest of the present model is the ability of the process to remove nitrogen compounds, both nitrate and nitrite. The nitrogen removal percentage was calculated as the average percentage obtained from all simulations as reported in equation 4.8:

$$\overline{N - percentage\ removal(\%)} = \frac{\sum_{i=0}^{n} \frac{\left(NO_{3_{IN}} + NO_{2_{IN}}\right) - \left(NO_{3_{OUT}} + NO_{2_{OUT}}\right)}{\left(NO_{3_{IN}} + NO_{2_{IN}}\right)} * 100}{n} \quad (4.8)$$

$$where\ n = number\ of\ the\ cycles$$

The effluent sulfate concentration is an important parameter to take into account because the presence of sulfate is the main disadvantage of S-based autotrophic denitrification. Indeed, sulfate is produced during the autotrophic denitrification and simultaneously is consumed by SRB. The effluent sulfate concentration was evaluated as the average sulfate concentration at the end of each cycle, as reported in equation 4.9:

$$\overline{SO_{4,OUT}^{2-}} = \frac{\sum_{i=0}^{n} SO_{4,OUT}^{2-}}{n} \quad where\ n = number\ of\ the\ cycles \quad (4.9)$$

To better understand which process is prevalent in the uptake of COD and to observe the main role played by AUT or HD in nitrogen removal, the percentage of SRB over the entirety of heterotrophic families can be a valid parameter. The calculation of the percentage of SRB at the end of each simulation period is reported in equation 4.10:

$$\%SRB = \frac{SRB_{fin}}{SRB_{fin}+HD_{fin}} * 100 \quad (4.10)$$

The effluent SMP concentration represents both an advantage and a disadvantage of the processes here investigated. The presence of SMP is beneficial as a carbon source for HD, while a too high SMP concentration might result in clogging, especially in case filtration is required as further separation step for the biomasses [21]–[23]. An average of the sum of UAP and BAP at the end of each cycle over all cycles was considered (equation 4.11).

$$\overline{SMP} = \frac{\sum_{i=0}^{n} UAP_{OUT} + BAP_{OUT}}{n} \quad where\ n = number\ of\ the\ cycles \quad (4.11)$$

4.3 RESULTS AND DISCUSSION

4.3.1 EFFECT OF COD ADDITION ON AUTOTROPHIC DENITRIFICATION PROCESS, EFFLUENT SULFATE CONCENTRATION AND EVOLUTION OF HETEROTROPHIC FAMILIES

The results in terms of nitrogen removal percentage, effluent sulfate concentration and percentage of SBR over the heterotrophic families are shown in Fig. 4.1. Each point of the line represents a different simulation.

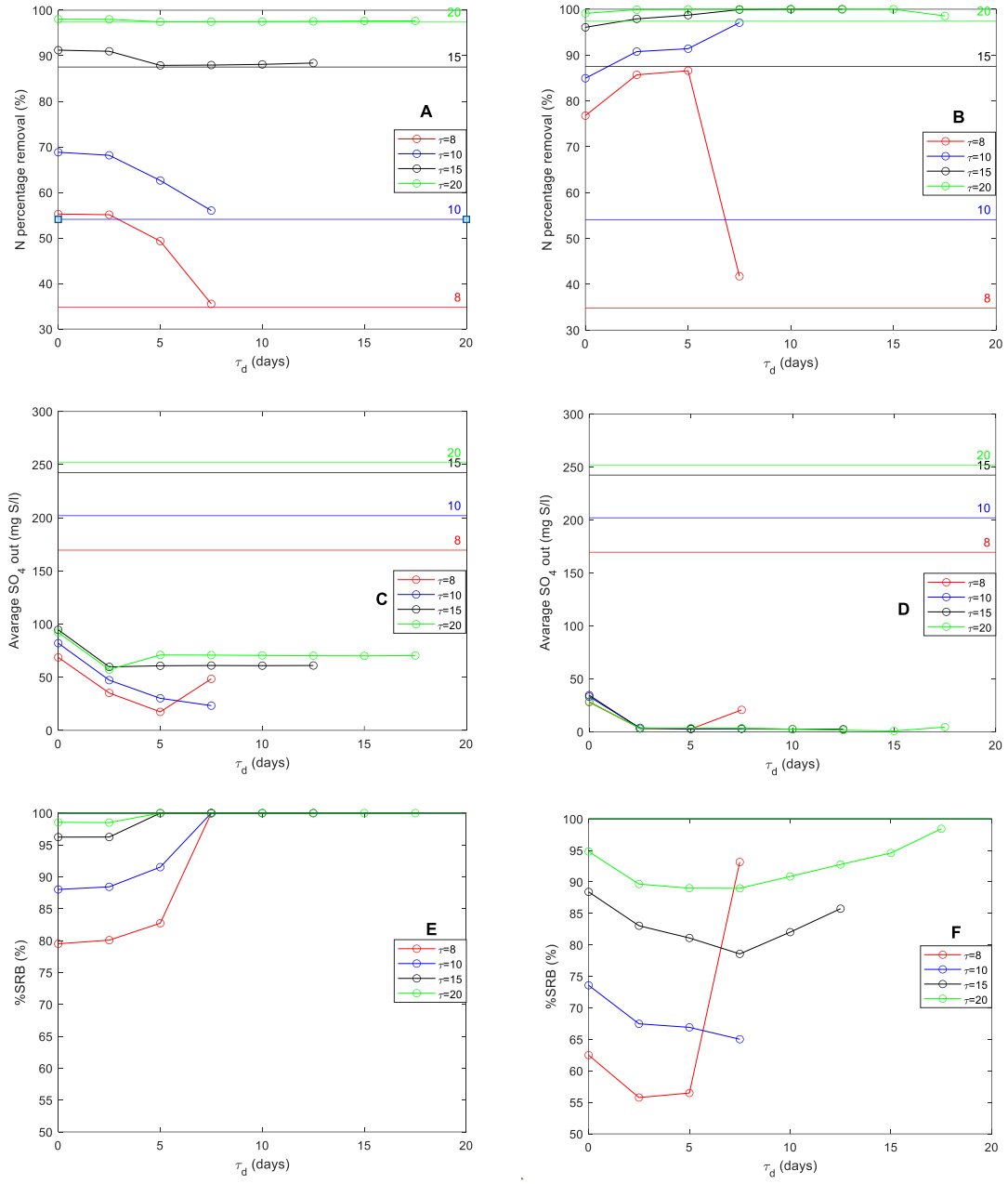

Fig. 4. 1 Nitrogen removal percentage (A, B), effluent sulfate concentration (C, D), and SRB percentage over total heterotrophs (E, F) in the absence of COD (straight horizontal lines) and in the presence of 300 (left panels) and 500 mg/L (right panels) of COD at different SBR cycle durations (τ). Each point represents the result of a simulation obtained at different COD injection times (τ_d).

The contribution given by the COD addition on nitrogen removal can be observed in Fig. 4.1 (A,B) by the difference between the straight lines, representing the simulations performed with no COD addition, and the lines with empty circles obtained in the presence of COD. The nitrogen removal percentage is strongly affected by the amount of COD injected. Comparing the two different COD concentrations, it is evident that the ability of SBR to remove nitrogenous compounds increases when a higher COD amount is added. With 500 mg/L of

COD added, an exception is observed when τ_d=7,5 days and τ=8 days, with the N removal performance markedly decreasing due to the delay of COD injection if compared to the duration of the SBR cycle. When a lower COD amount is added to the reactor, the nitrogen removal percentage decreases at increasing τ_d due to the prevalence of SRB over HD, as reported in Fig. 4.1.E. Conversely, a higher amount of COD allows the increase of nitrogen removal also at increasing τ_d (apart the exception above mentioned), as a higher COD promotes the activity of HD also when COD is injected towards the end of the SBR cycle. Regarding the applicability of the process, the addition of COD during autotrophic denitrification gives the possibility to obtain similar nitrogen removal performances in shorter times, allowing the treatment of higher volumes of influent without excessively sizing the SBR.

The effluent sulfate concentration is strongly affected by the injection of COD as well. In the absence of COD, the highest effluent sulfate concentrations are observed in Fig. 4.1.C, D. Sulfate concentrations in the outlet increase with the SBR cycle duration as a longer time allows AUT to produce more sulfate through biogenic sulfur oxidation (Fig 4.1.C, D). When an excess of COD is injected (i.e. 500 mg/l), at τ_d higher than 2.5 days the effluent sulfate concentration approaches to zero except for τ_d= 7,5 days and τ = 8 days (Fig 4.1 D). As seen for nitrogen removal, this condition does not allow a proper sulfate reduction and the COD injected would likely remain in the effluent without being properly used by heterotrophs. When 300 mg/L of COD is used, the highest effluent sulfate concentrations are observed when the injection of COD is at time 0. Indeed, the growth of HD is enhanced for earlier COD injections and heterotrophic denitrification prevails over autotrophic denitrification due to its higher velocity. Under these conditions, heterotrophic denitrification also prevails over sulfate reduction as sulfate is not produced and SRB have no substrate for their growth. In contrast, sulfate is produced via AUT when a later COD injection occurs, and the growth of SRB will be favored.

These considerations are remarkable observing the percentage of SRB over both the heterotrophic families. Indeed, lower SRB percentages are reported to occur for earlier COD injections at short cycle durations, as reported in Fig. 4.1 (E,F).

Regarding the effluent sulfate concentration, this is low due to sulfate reduction occurring in the presence of 300 mg/l of COD added for all cycle durations. Consequently, nitrogen compounds are removed via autotrophic denitrification at shorter cycle durations and with the lowest amount of COD injected.

The low output sulfate concentrations for τ= 8 and τ= 10 values are associated both with sulfate reduction by SRB and nitrate removal by heterotrophic denitrifiers that results in no sulfate production Fig. 4.1 (A,C,E).

The growth of SRB is also related to the amount of COD injected. At 300 mg/L of COD added, higher values of τ_d result in an increase of the SRB percentage due to the higher sulfate concentration. A COD concentration of 500 mg/l is in excess to the stoichiometric amount needed for complete sulfate reduction and affects the SRB fraction, as part of the COD is used by the heterotrophic denitrifiers.

The lower SRB percentage has a minimum which vary for the different cycle duration and in particular the lowest value (i.e. 55%) is observed when 500 mg/l of COD was added, τ_d= 2.5 days and τ = 8 days, indicating an almost perfect coexistence between SRB and HD. Previous studies confirmed that providing more carbon source leads to an increase of HD concentration [9], [14], [15], [24] This confirms what we observed, as in the absence of external COD the main heterotrophic family detected is represented by SRB. In literature, the effect of external COD injection at different times than t=0 has never been investigated on mixotrophic denitrification, making difficult the comparison with previous experimental studies.

4.3.2 FOCUS ON KEY SIMULATIONS ON AUTOTROPHIC DENITRIFICATION

The explicit performance of the simulations of greatest interest was developed in order to analyze the results shown in Fig. 4.1.

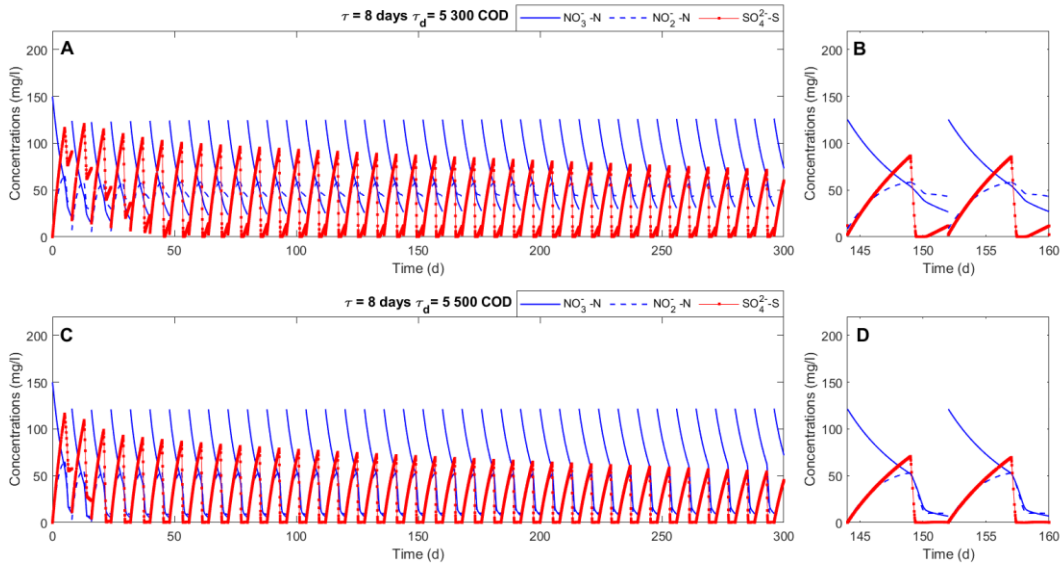

Fig. 4. 2 Autotrophic denitrification performances in terms of nitrate removal (solid blue), nitrite evolution (dashed blue) and sulfate production (solid red) over time at 300 (upper panel) and 500 mg/l (lower panel) of COD added for the same value of τ =8 days and τ_d=5 days.

From Fig. 4.2 where are reported the simulation for the two different values of COD added representing the shortest cycle duration (τ =8 days). Among those simulated, nitrate removal is achieved by heterotrophic denitrifiers and autotrophic denitrifiers. The main consequence of increased heterotrophic growth is the reduction in sulfate output at the end of each cycle. This can be observed in both cases shown in Fig. 4.2, from which a gradual decrease in the peak of sulfate concentration can be observed for both amounts of COD added. Indeed, the peak of sulfate reduced but the same nitrogen removal is achieved is related to an increased work of heterotrophic denitrifiers. Furthermore, Fig. 4.1 shows that if the COD injection occurs in the middle of the cycle, as in the case depicted Fig. 4.2, a complete sulfate reduction occurs only when 500 mg/l of COD are added as in Fig 4.2,C,D, also promoting the removal of nitrogen compounds by HD. In addition, it should be noted that the sulfate concentration in the effluent is the lowest in the case of low COD addition, as also shown in Fig. 4.1.E. This result is not mainly due to the work of SRB as much as due to the lack of time needed by AUT to remove nitrate, which is still present in the effluent as shown in Fig. 4.2.

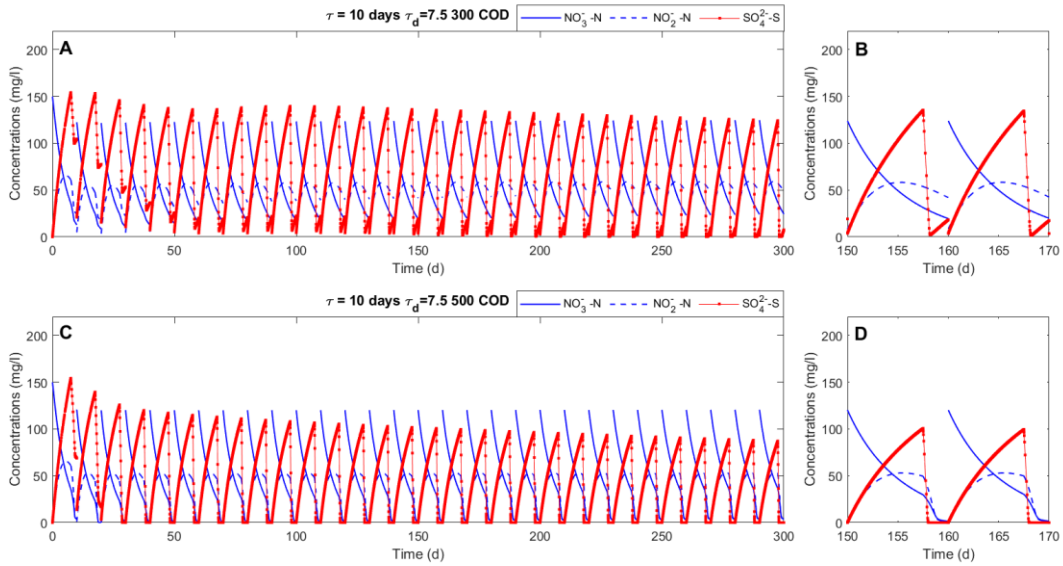

Fig. 4. 3 Autotrophic denitrification performances in terms of nitrate removal (solid blue), nitrite evolution (dashed blue) and sulfate production (solid red) overtime with two different quantities external source of COD injected on top 300 mg/l above 500 mg/l for the same value of τ *=10 days and* τ_d *= 7.5 days.*

Recalling Fig. 4.1 for the shorter cycle durations τ= 8 and τ= 10 days, the addition of more COD is necessary for the removal of nitrogen compounds to enhance heterotrophic denitrification. This happens because autotrophic denitrification has longer reaction times than heterotrophic denitrification. Also, in contrast to the case of Guerriero *et al.*, 2022 [19], it should be noted that the system is assumed not to undergo a complete sedimentation, which results in a lower increase in AUT concentration and, consequently, longer time for removal of autotrophic denitrification.

Comparing Fig 4.2 and 4.3 it possible to observe that longer cycle duration give an increase in the sulfate production which correspond to an increase in nitrate removal. Comparing Fig 4.2.B and 4.3.B with 4.2.D and 4.3.D representing a zoom of two cycles at the pseudo-stationary stage, when higher amount of COD is added, there is a notable changing in the trend of the nitrogen compounds due to the higher support in terms of COD given to the work of heterotrophic denitrifiers. Those observation are also in line with the decreasing of the peak of sulfate produced which could also be related to an increase in the concentration of heterotrophic denitrifiers.

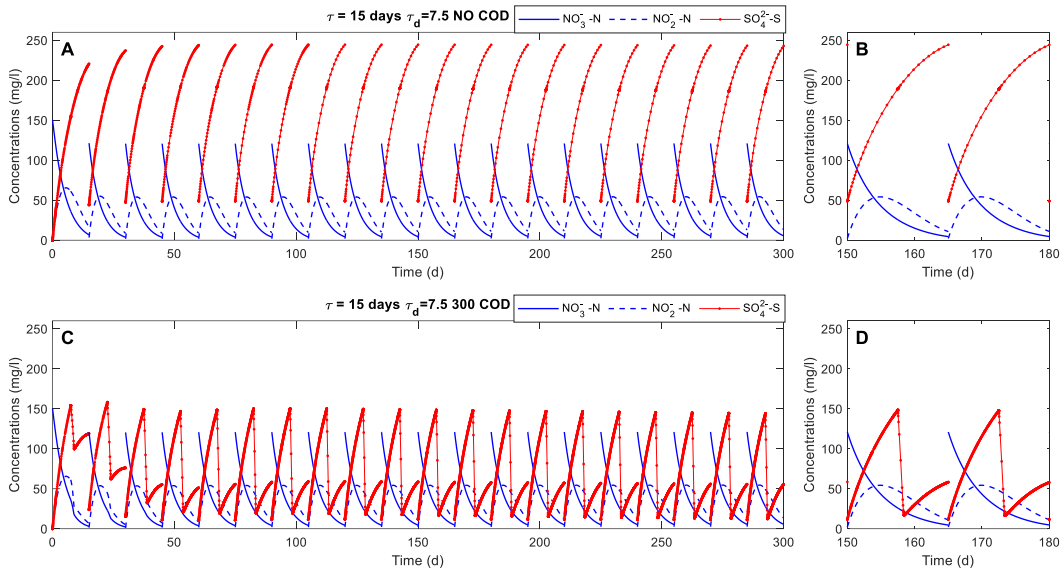

Fig. 4. 4 Autotrophic denitrification performances in terms of nitrate removal (solid blue), nitrite evolution (dashed blue) and sulfate production (solid red) overtime with two different quantities external source of COD injected on top no COD is added above 300 mg/l for the same value of τ *= 15 days and* τ_d *= 7.5 days.*

When no external COD is added, longer cycle durations increase the nitrogen removal percentage via autotrophic denitrification, which translates in an increase of the effluent sulfate concentrations Fig. 4.1.C. Indeed as reported in Fig 4.4.A where the highest nitrogen percentage removal is reached without COD addition it translates in the higher amount of sulfate in the effluent. Instead, even when a low amount of COD is added, the concentration of sulfate in the effluent is greatly reduced Fig. 4.1.C,D. This positive effect is particularly accentuated when the addition is made at instants other than the initial one, which promotes, as shown in Fig 4.1.A, C,E the growth of SRB.

The simulation performed at τ = 15 days, τ_d= 7.5 days and a COD addition of 300 mg/l di COD reported in Fig 4.4 represents one the cases leading to the highest performance in terms of nitrogen removal and effluent sulfate concentration as could be observed also by Fig 4.1.A,B,C,D. The addition of COD occurs while the autotrophic denitrification is still ongoing supporting mainly the sulfate reducing bacteria, removing the already produced sulfate, also because the late injection favor the growth of the SRB.

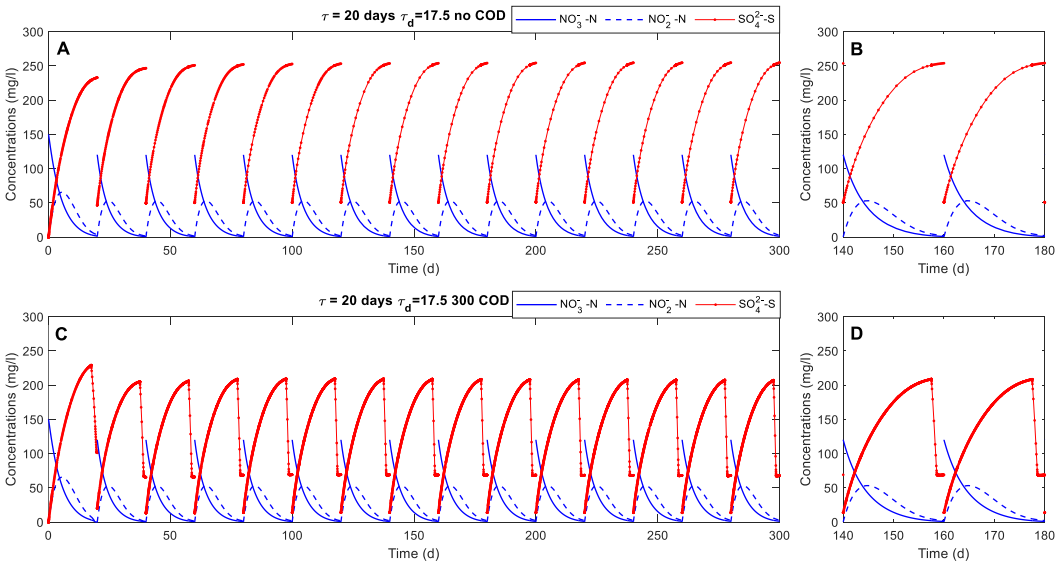

Fig. 4. 5 Autotrophic denitrification performances in terms of nitrate removal (solid blue), nitrite evolution (dashed blue) and sulfate production (solid red) overtime with two different quantities external source of COD injected on top no COD is added above 300 mg/l for the same value of τ *= 20 days and* τ_d *= 17.5 days.*

Further increasing the cycle duration to τ =20 days (Fig. 4.5), HD growth is strongly hindered compared to that of SRB (Fig 4.1.E) because of the high concentration of sulfate produced by autotrophic denitrification. When COD injection occurs towards the end of the cycle duration, sulfate reduction is favored until the COD added to the reactor is consumed. However, in this case the high sulfate production by autotrophic denitrification makes the COD added not enough to achieve a complete sulfate reduction with respect to the case reported in Fig 4.3.D where the excess amount of COD lead to complete sulfate reduction. It should be mentioned that the sulfate concentration does not necessarily need to be zero in the effluent, as it depends on the desired water quality.

4.3.3 EFFECTS ON THE SMP

The relationship between the higher amount of COD injected and the increased nitrogen removal percentage removal associated with HD is evident also observing the increase of the SMP production (Fig. 4.6). This trend is coupled with the lower effluent sulfate concentration and fraction of SRB over total heterotrophs (Fig. 4.1).

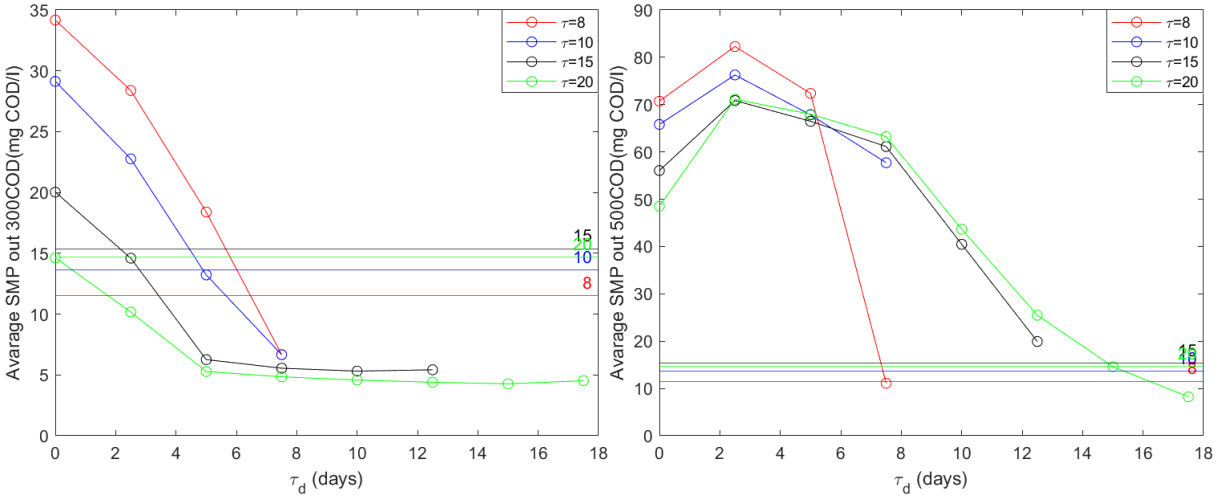

Fig. 4. 6 Average effluent SMP concentration as the sum of UAP and BAP at the end of each SBR cycle at the different SBR cycle durations investigated. The straight lines represent the average of the SMP concentration when no external COD is injected.

The average of the effluent SMP concentration is here evaluated as the sum of BAP and UAP, which are strongly influenced by the activities of the microbial families. Indeed, SMP production is higher when HD significantly intervene to support nitrate removal, mainly at 500 mg/l of COD added (Fig. 4.1.F). In contrast, when 300 mg/l COD is added, the SMP concentration only reaches half of the value obtained with a higher COD concentration. In addition, the day of COD injection also affects the amount of SMP produced. The lowest SMP concentrations are obtained when the COD injection occurs towards the end of the cycle(τ_d>7.5). In particular, the longer cycle duration where autotrophic denitrifiers prevails produces low amounts of SMP. Indeed, one of the main advantages of autotrophic denitrification is the lower amount of subproducts produced with respect to the heterotrophic families [23].

Looking overall at all the simulations carried out and examined, it could be seen that the most significant change in system performance, as the day of COD injection changes, occurs for cycles of duration τ = 10 days and τ_d go from 5 to 7.5 days when 500 mg/l COD is added. This late injection results in higher SMP production and lower SRB fraction. In addition, sulfate concentrations in the effluent are close to 0, and there is also an increase in percent nitrogen removal efficiency. It should be noted that in cases where COD is injected early in the cycle the result reported here may not be in line with experimental evidence where, usually, the presence of SRB is not included in the initial biomass composition.[14], [25]. This observation should be noted because in cases where no external carbon sources are present, SRB turn out to be the major heterotroph family in percentage, a situation well captured by the model

presented. In addition ,previous experiments have found the presence of SMP and organic matter resulting from cell lysis on which SRB are assumed to grow in the absence of external carbon sources. [26], [27].

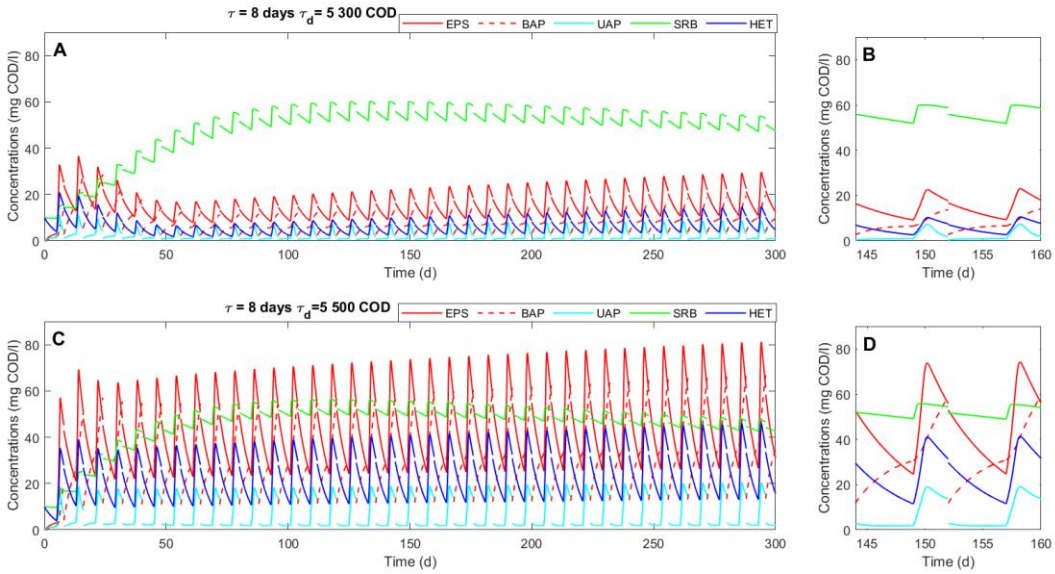

Fig. 4. 7 SMP production and concentration of heterotrophic families (i.e. HD and SRB) over time at 300 (upper panel) and 500 mg/l (lower panel) of COD added for the same value of τ =8 days and τ_d=5 days. The solid dark blue line represents the heterotrophic denitrifiers (HD), while the solid green line indicates the sulfate-reducing bacteria (SRB). The solid red line indicates the EPS, which leads to the production of BAP (red dashed line) after hydrolysis. The solid light blue line represents the UAP.

Fig. 4.7 shows the effect of different amounts of COD injected on SMP production and the evolution of the two heterotrophic families involved in the process, EPS accumulate in the SBR over 300 days of operation. In particular, Fig. 4.7.C, D shows a zoom of two cycles during the pseudo-steady state SBR operation (days 144-160). This zoom confirms that higher COD concentrations result in an enhanced HD growth. Consequently, a higher EPS amount is obtained and, thus, BAP concentrations increase because of EPS hydrolysis. The UAP production also increases due to the increased biological activity.

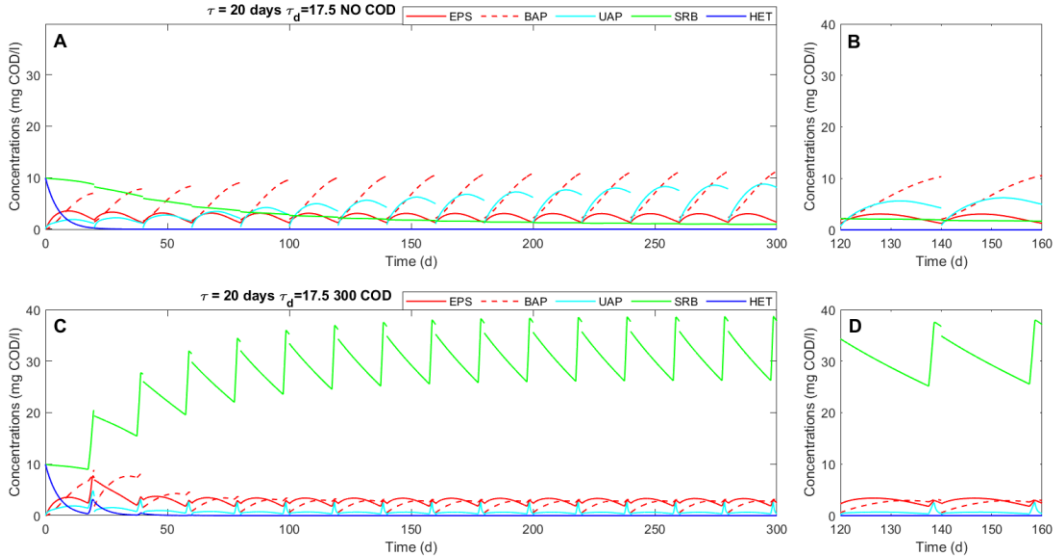

Fig. 4. 8 SMP production and concentration of heterotrophic families (i.e. HD and SRB) over time at 300 (upper panel) and 500 mg/l (lower panel) of COD added for the same of τ *= 20 days and* τ_d *= 17.5 days. The solid dark blue line represents the heterotrophic denitrifiers (HD), while the solid green line indicates the sulfate-reducing bacteria (SRB). The solid red line indicates the EPS, which leads to the production of BAP (red dashed line) after hydrolysis. The solid light blue line represents the UAP.*

Of all the simulations performed, the case reported here for τ = 20 days and τ_d = 17.5 days, when COD injection occurs, results in lower SMP concentration in the effluent. COD injection promotes the growth of SRB that not only produce but also consume SMP; this balance results in lower SMP concentration. Furthermore, longer cycle durations i.e., for τ = 15 days and τ = 20 days confirm the experimental validation of the prevalence of SRB when COD is not added [3], [17]. This trend is observable from Fig.4.3 where the sulfate already produced is quickly removed by the SRB, while the autotrophic denitrification is still ongoing so the final concentration of sulfate in the effluent still results lower if compared to the case, here not reported where no COD injection occurs. The concentrations of SMP and EPS in the case of COD addition for long duration cycles (τ =20 days) Fig 4.8 as already seen in Fig. 4.1 and 4.6 turn out to be always lower than the cases in which no or a large amount of organic matter is supplied. This is due to increased concentrations of heterotrophic biomass, particularly in this case of SRB that consume these substances increasing al effluent quality.

Furthermore, if there is the possibility to have longer reaction time the condition will favor the SRB and lead to better performance of the whole process. Indeed, as reported by Yang *et al.*, 2022 [28] control of the different families considered in the process, when a mixotrophic consortium is present result more useful than pure autotrophic or pure heterotrophic

denitrification process. The different simulations show the possibility of the model to keep the control of the subproducts of the process, which represent a valuable tool to improve and maintain the performance of the whole process.

4.4 CONCLUSION

Concluding the results obtained from the simulations carried out, in the case where there is heavy tank emptying and the reactor is not subject to complete sedimentation only slightly affects the result in terms of sulfate concentration in the effluent and percent nitrogen removal.

As for the competition between heterotrophic biomasses, this is strongly influenced by both the amount and the timing of COD addition. In fact, when large amounts of COD are added in the first half of the cycle duration the denitrifying heterotrophic biomass competes with that of sulfate reducers. In contrast, past the half of the cycle duration, sulfate reducers, due to the high presence of sulfates, tend to strongly outcompete denitrifying heterotrophs.

4.5 REFERENCES

[1] Y. X. Cui *et al.*, “Biological nitrogen removal from wastewater using sulphur-driven autotrophic denitrification,” *Appl. Microbiol. Biotechnol.*, vol. 103, no. 15, pp. 6023–6039, 2019, doi: 10.1007/s00253-019-09935-4.

[2] S. S. Y. S. S. S. Li *et al.*, “The IWA Anaerobic Digestion Model No 1 (ADM1),” *Water Res.*, vol. 99, no. 3, pp. 1–8, Dec. 2020, doi: 10.1016/j.biortech.2007.02.007.

[3] G. Guo *et al.*, “Advances in elemental sulfur-driven bioprocesses for wastewater treatment: From metabolic study to application,” *Water Res.*, vol. 213, no. January, p. 118143, 2022, doi: 10.1016/j.watres.2022.118143.

[4] F. Di Capua, S. Papirio, P. N. L. Lens, and G. Esposito, “Chemolithotrophic denitrification in biofilm reactors,” *Chemical Engineering Journal*, vol. 280. Elsevier, pp. 643–657, Nov. 05, 2015. doi: 10.1016/j.cej.2015.05.131.

[5] R. Sierra-Alvarez, R. Beristain-Cardoso, M. Salazar, J. Gómez, E. Razo-Flores, and J. A. Field, “Chemolithotrophic denitrification with elemental sulfur for groundwater treatment,” *Water Res.*, vol. 41, no. 6, pp. 1253–1262, 2007, doi: 10.1016/j.watres.2006.12.039.

[6] K. Kiskira, S. Papirio, E. D. van Hullebusch, and G. Esposito, “Influence of pH, EDTA/Fe(II) ratio, and microbial culture on Fe(II)-mediated autotrophic denitrification,” *Environ. Sci. Pollut. Res.*, vol. 24, no. 26, pp. 21323–21333, 2017, doi: 10.1007/s11356-017-9736-4.

[7] F. Di Capua, F. Pirozzi, P. N. L. Lens, and G. Esposito, “Electron donors for autotrophic denitrification,” *Chem. Eng. J.*, vol. 362, no. 3, pp. 922–937, 2019, doi: 10.1016/j.cej.2019.01.069.

[8] L. Zhang, Y. Y. Qiu, Y. Zhou, G. H. Chen, M. C. M. van Loosdrecht, and F. Jiang, “Elemental sulfur as electron donor and/or acceptor: Mechanisms, applications and perspectives for biological water and wastewater treatment,” *Water Res.*, vol. 202, no. June, p. 117373, 2021, doi: 10.1016/j.watres.2021.117373.

[9] Y. Wang, C. Bott, and R. Nerenberg, “Sulfur-based denitrification: Effect of biofilm development on denitrification fluxes,” *Water Res.*, vol. 100, pp. 184–193, Sep. 2016, doi: 10.1016/j.watres.2016.05.020.

[10] A. Kostrytsia *et al.*, “Elemental sulfur-based autotrophic denitrification and denitritation: microbially catalyzed sulfur hydrolysis and nitrogen conversions,” *J. Environ. Manage.*, vol. 211, pp. 313–322, Apr. 2018, doi: 10.1016/j.jenvman.2018.01.064.

[11] T. K. Q. Vo, S. Kang, S. A. An, and H. S. Kim, “Exploring critical factors influencing on autotrophic denitrification by elemental sulfur-based carriers in upflow packed-bed bioreactors,” *J. Water Process Eng.*, vol. 40, no. September 2020, p. 101866, 2021, doi: 10.1016/j.jwpe.2020.101866.

[12] B. Batchelor and A. W. Lawrence, “Autotrophic Denitrification Using Elemental Sulfur,” 1978.

[13] C. Huiliñir *et al.*, “Elemental sulfur-based autotrophic denitrification in stoichiometric S0/N ratio: Calibration and validation of a kinetic model,” *Bioresour. Technol.*, vol. 307, Jul. 2020, doi: 10.1016/j.biortech.2020.123229.

[14] Y. Y. Qiu *et al.*, “Overlooked pathways of denitrification in a sulfur-based denitrification system with organic supplementation,” *Water Res.*, vol. 169, 2020, doi: 10.1016/j.watres.2019.115084.

[15] S. E. Oh, Y. B. Yoo, J. C. Young, and I. S. Kim, “Effect of organics on sulfur-utilizing autotrophic denitrification under mixotrophic conditions,” *J. Biotechnol.*, vol. 92, no. 1, pp. 1–8, 2001, doi: 10.1016/S0168-1656(01)00344-3.

[16] C. Peirano *et al.*, “Assessment of simultaneous autotrophic–heterotrophic denitrification with high removal of nitrogen, sulfur and carbon: optimization through response surface methodology,” *J. Chem. Technol. Biotechnol.*, vol. 95, no. 3, pp. 631–638, 2020, doi: 10.1002/jctb.6244.

[17] M. F. Carboni, A. P. Florentino, R. B. Costa, X. Zhan, and P. N. L. Lens, “Enrichment of Autotrophic Denitrifiers From Anaerobic Sludge Using Sulfurous Electron Donors,” *Front. Microbiol.*, vol. 12, no. June, 2021, doi: 10.3389/fmicb.2021.678323.

[18] C. S. Laspidou and B. E. Rittmann, “Non-steady state modeling of extracellular polymeric substances, soluble microbial products, and active and inert biomass,” *Water Res.*, vol. 36, no. 8, pp. 1983–1992, 2002, doi: 10.1016/S0043-1354(01)00414-6.

[19] G. Guerriero, M. R. Mattei, S. Papirio, G. Esposito, and L. Frunzo, “Modelling the effect of SMP production and external carbon addition on S-driven autotrophic denitrification,” *Sci. Rep.*, vol. 12, no. 1, Dec. 2022, doi: 10.1038/S41598-022-10944-Z.

[20] R. Ferrentino, A. Ferraro, M. R. Mattei, G. Esposito, and G. Andreottola, “Process performance optimization and mathematical modelling of a SBR-MBBR treatment at low oxygen concentration,” *Process Biochem.*, vol. 75, no. August, pp. 230–239, 2018, doi: 10.1016/j.procbio.2018.08.023.

[21] B. J. Ni *et al.*, “Evaluation on factors influencing the heterotrophic growth on the soluble microbial products of autotrophs,” *Biotechnol. Bioeng.*, vol. 108, no. 4, pp. 804–812, 2011, doi: 10.1002/bit.23012.

[22] B. J. Ni, F. Fang, B. E. Rittmann, and H. Q. Yu, “Modeling microbial products in activated sludge under feast#famine conditions,” *Environ. Sci. Technol.*, vol. 43, no. 7, pp. 2489–2497, 2009, doi: 10.1021/es8026693.

[23] G. Asik, T. Yilmaz, F. Di Capua, D. Ucar, G. Esposito, and E. Sahinkaya, “Sequential sulfur-based denitrification/denitritation and nanofiltration processes for drinking water treatment,” *J. Environ. Manage.*, vol. 295, no. June, p. 113083, 2021, doi: 10.1016/j.jenvman.2021.113083.

[24] D. U. Lee, I. S. Lee, Y. D. Choi, and J. H. Bae, “Effects of external carbon source and empty bed contact time on simultaneous heterotrophic and sulfur-utilizing autotrophic denitrification,” *Process Biochem.*, vol. 36, no. 12, pp. 1215–1224, 2001, doi: 10.1016/S0032-9592(01)00163-7.

[25] G. Xu *et al.*, “Evaluation of simultaneous autotrophic and heterotrophic denitrification processes and bacterial community structure analysis,” *Appl. Microbiol. Biotechnol.*, vol. 99, no. 15, pp. 6527–6536, Aug. 2015, doi: 10.1007/s00253-015-6532-2.

[26] N. Fernández, R. Sierra-Alvarez, J. A. Field, R. Amils, and J. L. Sanz, “Microbial community dynamics in a chemolithotrophic denitrification reactor inoculated with

methanogenic granular sludge," *Chemosphere*, vol. 70, no. 3, pp. 462–474, 2008, doi: 10.1016/j.chemosphere.2007.06.062.

[27] A. Koenig, T. Zhang, L. H. Liu, and H. H. P. Fang, "Microbial community and biochemistry process in autosulfurotrophic denitrifying biofilm," *Chemosphere*, vol. 58, no. 8, pp. 1041–1047, 2005, doi: 10.1016/j.chemosphere.2004.09.040.

[28] J. Yang *et al.*, "Effect of Glucose on Nitrogen Removal Performance and Microbial Community of Sulfur Autotrophic Denitrification System," *SSRN Electron. J.*, vol. 10, no. 3, p. 107915, 2022, doi: 10.2139/ssrn.4051099.

Chapter 5

GLOBAL SENSITIVITY ANALYSIS OF A S-BASED DENITRIFICATION MODEL

This Chapter will be submitted as:

Guerriero G, Trucchia A, Mattei MR, Frunzo L. "*Global Sensitivity Analysis of a S-based denitrification Model*"

5.1 INTRODUCTION

Nitrate is still considered one of the most common and widespread water pollutants in both natural reservoirs and industrial wastewater. The removal of nitrogen compounds is required since they cause, in high concentrations, severe disease and eutrophication problems in confined water basins. The most widely used biological nitrate removal method in water treatment is heterotrophic denitrification. This process now considered conventional has as main disadvantages the costs associated with the COD adding and the high production of sludge produced from the heterotrophic biomass involved.

Sulfur-based autotrophic denitrification is one of the most promising alternatives to the conventional heterotrophic denitrification process, especially in cases where the contaminated water is deficient in COD. In fact, the costs for the same amount of nitrate removed are lower than the ones associated to heterotrophic denitrification (HD) [1], [2]. The main reasons why elemental sulfur driven autotrophic denitrification (SdAD) is more cost-effective are the lower cost of sulfur as material compared to an external carbon source and the lower sludge production [1], [3]. The main downside of using sulfur as an electron donor in autotrophic denitrification is sulfate production, which is considered also a pollutant [1], [4]. To reduce the negative effects associated with autotrophic denitrification by elemental sulfur, one of the most promising alternatives is to add an external carbon source that promotes the growth of heterotrophic families [5], [6]. In this context, mathematical modeling appears to be a valuable tool to assess and mitigate the effects caused by the simultaneous occurrence of different microbial families.

The most recent work is this framework is represented by the biological model of Guerriero et al., 2022 [7] which present as main objectives nitrogen removal and the minimization of sulfate concentration in the effluent. Those goals are reached by promoting, through the addition of COD, the simultaneous growth of sulfate reducing bacteria (SRB) and HD. These two families are naturally present in sulfur-based autotrophic denitrification systems as evidenced by microbiological analyses, and the addition of different amounts of COD is necessary to support their growth. [5], [8]–[13].

The possible support of soluble microbial products (SMP) was also considered, as these organic compounds can be used as substrates for the growth of both heterotrophic families. In fact, SMP

are naturally produced by microbial activities, and their production and consumption were also included in the model [7]. Briefly, the model was developed considering the simultaneous co-occurrence of the three processes: autotrophic denitrification, heterotrophic denitrification, and sulfate reduction. To support the growth of both heterotrophic families involved in the model, the day of COD injection and the amount of COD added were considered as operational parameters. In addition, a sequential batch reactor (SBR) configuration was chosen to improve the growth and utilization of SMP. Although the processes could occur in pairs simultaneously, no experimental validation of the entire model was performed.

In this context a Global sensitivity analysis on the kinetic and new operational parameters considered, represents a valid opportunity to investigate the most influent parameters of the process and support the experimental calibration and validation. Indeed, as defined by Pianosi et al., 2016 [14], the main aims of the Global SA are represented by the verification of and support to the model calibration, that could lead also to a model simplification. In addition, the autotrophic denitrification process turns out to be close to the possibility of applications at larger scales than laboratory scales, so identifying the parameters that affect the process the most may help for future full-scale realizations [3], [15].

The outputs considered to control the process are represented by the main shortcomings related to the process and are identified as the nitrate removal rate, the concentrations of SMP and sulfate in the output, and the prevailing fraction between HD and SRB.

5.2 MATHEMATICAL MODEL

The mathematical model accounts for the reactor configuration chosen, i.e. an SBR reactor. This system undergoes to instantaneous changes after continuous reaction period and is mathematically modelled by using a system of first order impulsive ordinary differential equations (IDEs). The model is based on mass balance equation on all the substrates and biomasses considered. The model considers nine different compounds $S_j, j = [S_0,\ S_b,\ NO_3^-, NO_2^-,\ N_2,\ SO_4^{2-},\ UAP,\ BAP,\ COD]$and seven different biomasses $X_I,\ i = [HYD,\ AUT,\ STO,\ EPS, HD, SRB,\ I]$. The equations governing the dynamics of such variables are the following:

$$\dot{S}_j(t) = \rho_{S,j}(t, \boldsymbol{S}, \boldsymbol{X}), \qquad t \in J = [0,T]\,, \;\; t \neq t_k, \qquad S_j(0) = S_{j0} \;\; (5.1)$$

$$\dot{X}_i(t) = \rho_{X,i}(t, \boldsymbol{S}, \boldsymbol{X}), \qquad t \in J = [0,T]\,, \;\; t \neq t_k, \qquad X_i(0) = X_{i0}, \qquad (5.2)$$

$$\Delta S_j(t_k) = -\alpha_j S_j(t_k^-) + \alpha_j S_{in,j}\,, \qquad k = 1, \dots, m, \qquad (5.3)$$

$$\Delta X_i(t_k) = -\gamma_i X_i(t_k^-)\,, \qquad k = 1, \dots, m, \;\; (5.4)$$

where:

$S_j(t)$, $X_i(t)$ are the j[th] substrate and the i[th] biomass concentrations at time t respectively,

$\rho_{S,j}$ and $\rho_{X,i}$ are the reaction terms for the j[th] substrate and the i[th] biomass,

S_{j0} and X_{i0} are the initial concentration within the reactor for the j[th] substrate and the i[th] biomass,

$S_{in,j}$ is the concentration of the j[th] substrate in the fresh influent.

$0=t_0 < t_1 < \cdots < t_m < t_{m+1} = T$, $t_{k+1} - t_k = \tau$, where τ denotes the duration of each cycle, $\Delta S_j(t_k) = S_j(t_k^+) - S_j(t_k^-)$, $\Delta X_i(t_k) = X_i(t_k^+) + X_i(t_k^-)$, with $S_j(t_k^+)$, $X_i(t_k^+)$, $S_j(t_k^-)$, $X_i(t_k^-)$, being the right and left limits of $S_j(t)$ and $X_i(t)$ at time $t = t_k$; α_j represents the emptying/refilling ratio and γ_i takes into account the fraction of biomass removed from the system during the emptying phase.

The equations that define the jump function for COD between the two reaction periods is:

$$\begin{cases} (k-1)\cdot\tau < t \leq (k-1)\tau + \tau_d \;\; k = 1, \dots, n, \;\; FIRST\ REACTION\ PERIOD \\ (k-1)\cdot\tau + \tau_d < t \leq k\cdot\tau \;\; k = 1, \dots, n, \;\; SECOND\ REACTION\ PERIOD \end{cases} \qquad (5.5)$$

$$\Delta S_{\mathrm{COD}}\big((k-1)\tau + \tau_d\big) = S_{in,COD}, k = 1, \dots, n \quad (5.6)$$

From the second cycle onwards, the initial conditions are recalculated considering that 50% of the reactor is emptied, which correspond to α=0.5. Furthermore, this term also considers that the dilution of the influent is applied only to the substrates considered in the dissolved form, which are: SO_4^{2-}, UAP , BAP, COD, NO_3, NO_2. The other compounds evaluated in the model are supposed to undergoes to a complete sedimentation, which implies $\gamma = 0$ for all the suspended compounds.

The differential equations representing the continuous period in an SBR cycle are the following for the Substrates $\dot{S}_j$ and the Biomasses $\dot{X}_i$

$$\dot{S}_1 = -\rho_1 \quad (5.7)$$

$$\dot{S}_2 = \rho_1 - \frac{r_1}{y_{2-3}} \cdot \rho_2 - \frac{r_2}{y_{2-4}} \cdot \rho_3 + \frac{1}{2}\left(\frac{1 - Y_{SRB,AC}}{Y_{SRB,AC}}\right) \cdot (\rho_{15} + \rho_{16} + \rho_{17}) \quad (5.8)$$

$$\dot{S}_3 = -\frac{1}{y_{2-3}} \cdot \rho_2 - \frac{(1 - y_{H,S})(1 - k_{UAP} - K_{EPS})}{2{,}86 y_{H,S}} \cdot \rho_9 - \frac{(1 - y_{H,UAP})}{2{,}86 y_{H,UAP}} \cdot \rho_{11} - \frac{(1 - y_{H,BAP})}{2{,}86 y_{H,BAP}} \cdot \rho_{13} \quad (5.9)$$

$$\dot{S}_4 = \frac{1}{y_{2-3}} \cdot \rho_2 - \frac{1}{y_{2-4}} \cdot \rho_3 - \frac{(1 - y_{H,S})(1 - k_{UAP} - K_{EPS})}{1{,}71 y_{H,S}} \cdot \rho_8 - \frac{(1 - y_{H,UAP})}{1{,}71 y_{H,UAP}} \cdot \rho_{10} - \frac{(1 - y_{H,BAP})}{1{,}71 y_{H,BAP}} \cdot \rho_{12} \quad (5.10)$$

$$\dot{S}_5 = \frac{1}{y_{2-4}} \cdot \rho_3 + \frac{(1 - y_{H,S})(1 - k_{UAP} - K_{EPS})}{1{,}71 y_{H,S}} \cdot \rho_8 + \frac{(1 - y_{H,S})(1 - k_{UAP} - K_{EPS})}{2{,}86 y_{H,S}} \cdot \rho_9 + \frac{(1 - y_{H,UAP})}{1{,}71 y_{H,UAP}} \cdot \rho_{10} + \frac{(1 - y_{H,UAP})}{2{,}86 y_{H,UAP}} \cdot \rho_{11} + \frac{(1 - y_{H,BAP})}{1{,}71 y_{H,BAP}} \cdot \rho_{12} + \frac{(1 - y_{H,BAP})}{2{,}86 y_{H,BAP}} \cdot \rho_{13} \quad (5.11)$$

$$\dot{S}_6 = \frac{r_1}{y_{2-3}} \cdot \rho_2 + \frac{r_2}{y_{2-4}} \cdot \rho_3 - \frac{1}{2}\left(\frac{1 - Y_{SRB,AC}}{Y_{SRB,AC}}\right) \cdot (\rho_{15} + \rho_{16} + \rho_{17}) \quad (5.12)$$

$$\dot{S}_7 = f_{UAP} \cdot (\rho_2 + \rho_3 + \rho_{15}) + \frac{k_{UAP}}{y_{H,S}} \cdot (\rho_8 + \rho_9) - \frac{1}{y_{H,UAP}} \cdot (\rho_{10} + \rho_{11}) - \frac{1}{Y_{SRB,AC}} \cdot \rho_{16} \quad (5.13)$$

$$\dot{S}_8 = f_{BAP} \cdot (\rho_4 + \rho_5) + \rho_7 - \frac{1}{y_{H-BAP}} \cdot (\rho_{12} + \rho_{13}) + f_{BAP} \cdot (\rho_{14} + \rho_{18}) \quad (5.14)$$

$$\dot{S}_9 = \rho_6 - \frac{1}{y_{H-S}} \cdot (\rho_8 + \rho_9) - \frac{1}{Y_{SRB,AC}} \cdot \rho_{15} \quad (5.15)$$

$$\dot{X}_1 = \rho_1 - \rho_4 \quad (5.16)$$

$$\dot{X}_2 = (1 - \mathrm{f_{EPS}} - \mathrm{f_{UAP}}) \cdot \rho_2 + (1 - \mathrm{f_{EPS}} - \mathrm{f_{UAP}}) \cdot \rho_3 - \rho_5 \quad (5.17)$$

$$\dot{X}_3 = (1 - f_I - f_{BAP}) \cdot \rho_4 + (1 - f_I - f_{BAP}) \cdot \rho_5 - \rho_6 + (1 - f_i - f_{BAP}) \cdot \rho_{14} + (1 - f_i - f_{BAP}) \cdot \rho_{16} \quad (5.18)$$

$$\dot{X}_4 = f_{EPS} \cdot (\rho_2 + \rho_3 + \rho_{15}) - \rho_7 + \frac{k_{EPS}}{y_{H-S}} \cdot \rho_8 + \frac{k_{EPS}}{y_{H-S}} \cdot \rho_9 \quad (5.19)$$

$$\dot{X}_5 = \left(1 - \frac{k_{UAP}}{y_{H-S}} - \frac{k_{EPS}}{y_{H-S}}\right) \cdot \rho_8 + \left(1 - \frac{k_{UAP}}{y_{H-S}} - \frac{k_{EPS}}{y_{H-S}}\right) \cdot \ \rho_9 + \rho_{10} + \ \rho_{11} + \rho_{12} + \rho_{13} - \rho_{14} \quad (5.20)$$

$$\dot{X}_6 = (1 - \mathrm{f_{EPS}} - \mathrm{f_{UAP}}) \cdot \rho_{15} - \rho_{16} + \rho_{17} + \ \rho_{18} \ (5.21)$$

$$\dot{X}_7 = (\rho_4 + \rho_5 \ + \ \rho_{14} + \ \rho_{16}) \cdot f_I \quad (5.22)$$

Table 5. 1 Values of the stoichiometric parameters involved in the model.

	Description	Value	Unit	Source
$f_{EPS,AUT}$	Fraction of X_{EPS} for X_{AUT}biomass growth	0.09	mg COD/mg N	[16]
$f_{UAP,AUT}$	Fraction of S_{UAP} forX_{AUT} biomass growth	0.14	mg COD/mg N	[16]
f_{BAP}	Fraction of S_{BAP} for biomass growth	0.0215	mg COD/mg COD	[17]
f_I	Fraction of X_I in biomass decay	0.08	mg COD/mg COD	[18]
k_{EPS}	Yield coefficient for X_{EPS} for X_{HD}	0.14	mg COD/mg COD	[19]
k_{UAP}	Yield coefficient for S_{UAP} for X_{HD}	0.09	mg COD/mg COD	[19]
b_1	S_{S_b} to $S_{NO_3^-}$ stoichiometric ratio	1.2	mg S/ mg N	[20]
b_2	S_{S_b} to $S_{NO_2^-}$ stoichiometric ratio	0.55	mg S/ mg N	[20]
y_{AUT,NO_3^-}	Yield coefficient for X_{AUT} on $S_{NO_3^-}$	0.37	mg COD/mg N	[21]
y_{AUT,NO_2^-}	Yield coefficient for X_{AUT} on $S_{NO_2^-}$	0.414	mg COD/mg N	[21]
$f_{EPS,SRB}$	Fraction of X_{EPS} for X_{SRB} biomass growth	0.9	mg COD/mg COD	assumed
$f_{UAP,SRB}$	Fraction of S_{UAP} for X_{SRB} biomass growth	0.14	mg COD/mg COD	assumed
$y_{H,COD}$	Yield coefficient for X_{HD} on S_{COD}	0.34	mg COD/mg COD	[19]
$y_{H,UAP}$	Yield coefficient for X_{HD} on S_{UAP}	0.45	mg COD/mg COD	[19]
$y_{H,BAP}$	Yield coefficient for X_{HD} on S_{BAP}	0.45	mg COD/mg COD	[19]
y_{SRB}	Yield coefficient for X_{SRB}	0.0568	mg COD/mg COD	[22]

5.2.1 REACTION TERMS

The kinetic model considers a first hydrolysis step conducted by the hydrolytic biomass, where elemental sulfur is biologically hydrolyzed to be further utilized by autotrophic denitrifiers. Then the biological sulfur produced by hydrolysis is used by autotrophic denitrifiers for autotrophic denitrification, which is the main process in the model (Table 5.2, 5.3). This process occurs in two steps, an initial one converting nitrate to nitrite and then from nitrite to nitrogen gas. Simultaneously, heterotrophic denitrification and sulfate reduction take place using the same organic compounds consisting of: COD, UAP, BAP (Table 5.6, 5.7, 5.8, 5.9). Additionally, a

fraction term is added to classical Monod kinetic terms to consider that the two heterotrophic families compete for the same substrates and cannot take up all of them at the same time.

The following sub-processes have been also considered in association to the main ones previously described:

- the hydrolyzation of the biological carbon stocked (STOB) which derives from the dead microorganisms and leaded by the heterotrophic denitrifiers (Table 5.4, 5.5),
- the hydrolysis of the EPS produced by the microbial activities into BAP (Table 5.4 5.5),
- the production of UAP which derives from microbial activities.

Another assumption of the model is related to the sulfate reduction product, which is experimentally reported as S^{2-} but, in the present model, is assumed to become bioavailable sulfur again. However, experimental results report that when sulfide is used as an electron donor in autotrophic denitrification it has faster kinetics than elemental sulfur, so this assumption does not negatively affect the model results.

5.2.1.1 The autotrophic denitrification

Reaction terms

Table 5. 2 Process rates related autotrophic denitrification.

j- process		Process rate (ρ_j)
1	**Hydrolysis of elemental sulfur** $\mathbf{S_0 \rightarrow S_{bio}}$	$K_0 \cdot k_1 \frac{S_1}{\frac{k_1}{a^*} + S_1} X_1$
2	**Autotrophic denitrification** $\mathbf{NO_3 \rightarrow NO_2}$	$\mu_{2,3}^{max} \frac{S_2}{k_{2,2} + S_2} \cdot \frac{S_3}{k_{2,3} + S_3} \cdot \frac{S_3}{S_3 + S_4} \cdot X_2$
3	**Autotrophic denitrification** $\mathbf{NO_2 \rightarrow N_2}$	$\mu_{2,4}^{max} \frac{S_2}{k_{2,2} + S_2} \cdot \frac{S_4}{k_{2,4} + S_4} \cdot \frac{S_4}{S_3 + S_4} \cdot X_2$
4	**Decay of HID**	$k_{d,1} \cdot X_1$
5	**Decay of AUT**	$k_{d,2} \cdot X_2$

Kinetics Terms

Table 5. 3 Kinetic terms related to the autotrophic denitrification.

	Description	*Value*	*Unit*	*Ref.*
K_0	Efficiency growth coefficient for X_1	0.1	mg COD/ mg S	[23]
$\mu_{2,3}^{max}$	Maximum growth rate for X_2 on S_3	0.0067	d^{-1}	[23]
$\mu_{2,4}^{max}$	Maximum growth rate for X_2 on S_4	0.0058	d^{-1}	[23]
$k_{2,2}$	Half-saturation constant for S_2	0.215	mg S/l	[24]
$k_{2,3}$	Half-saturation constant for S_3	36	mg N/l	[23]
$k_{2,4}$	Half-saturation constant for S_4	40	mg N/l	[21]
k_1	Hydrolysis kinetic constant	0.081	mg S/ mg COD ·d	[23]
κ_1	Volume specific half-saturation constant for S_1	5.1	1/dm	[23]
a^*	Mass specific area	0.0008164	dm2/mg	[23]
$k_{d,1}$	Decay rate coefficient for X_1	0.0006	d^{-1}	[25]
$k_{d,2}$	Decay rate coefficient for X_2	0.0006	d^{-1}	[25]

5.2.1.2 Formation & utilization of SMP

Table 5. 4 Process rate relatives to formation and utilization of SMP.

	j- process	*Process rate (ρ_j)*
6	**Hydrolysis of organic carbon STOB → COD**	$k_H \cdot \frac{X_3 / X_5}{k_x + X_3 / X_5} X_5$
7	**Release of EPS EPS → BAP**	$K_{HID} X_4$

Table 5. 5 Kinetic terms related to formation and utilization of SMP.

	Description	*Value*	*Unit*	*Ref.*
k_H	Hydrolysis rate constant	3	d^{-1}	[26]
k_x	Hydrolysis saturation constant	1	g COD / g COD	[26]
K_{HID}	EPS hydrolysis rate coefficient	0.1704	d^{-1}	[19]

5.2.1.3 Heterotrophic denitrification

Reaction terms

Table 5. 6 Process rates related to the heterotrophic denitrification.

	j- process	*Process rate (ρ_j)*
8	**Growth of X_{HET} on S_{COD} and S_{NO2}**	$\mu_{H,S} \cdot \eta_{ox} \cdot \frac{S_9}{k_s + S_9} \cdot \frac{S_4}{k_{NO_2}^{HET} + S_4} \cdot \frac{S_4}{S_4 + S_3} \cdot \frac{S_9}{S_7 + S_8 + S_9} \cdot X_5$

9	**Growth of X_{HET} on S_{COD} and S_{NO3}**	$\mu_{H,S} \cdot \eta_{ox} \cdot \frac{S_9}{k_s + S_9} \cdot \frac{S_3}{k_{NO_3}^{HET} + S_3} \cdot \frac{S_3}{S_4 + S_3} \cdot \frac{S_9}{S_7 + S_8 + S_9} \cdot X_5$
10	**Growth of X_{HET} on S_{UAP} and S_{NO2}**	$\mu_{H,UAP} \cdot \eta_{OX} \cdot \frac{S_7}{k_{UAP} + S_7} \cdot \frac{S_4}{k_{NO_2}^{HET} + S_4} \cdot \frac{S_4}{S_4 + S_3} \cdot \frac{S_7}{S_7 + S_8 + S_9} \cdot X_5$
11	**Growth of X_{HET} on S_{UAP} and S_{NO3}**	$\mu_{H,UAP} \cdot \eta_{OX} \cdot \frac{S_7}{k_{UAP} + S_7} \cdot \frac{S_4}{k_{NO_3}^{HET} + S_4} \cdot \frac{S_4}{S_4 + S_3} \cdot \frac{S_7}{S_7 + S_8 + S_9} \cdot X_5$
12	**Growth of X_{HET} on S_{BAP} and S_{NO2}**	$\mu_{H,BAP} \cdot \eta_{OX} \cdot \frac{S_8}{k_{BAP} + S_8} \cdot \frac{S_4}{k_{NO_2}^{HET} + S_4} \cdot \frac{S_4}{S_4 + S_3} \cdot \frac{S_8}{S_7 + S_8 + S_9} \cdot X_5$
13	**Growth of X_{HET} on S_{BAP} and S_{NO3}**	$\mu_{H,BAP} \cdot \eta_{OX} \cdot \frac{S_8}{k_{BAP} + S_8} \cdot \frac{S_4}{k_{NO_3}^{HET} + S_4} \cdot \frac{S_4}{S_4 + S_3} \cdot \frac{S_8}{S_7 + S_8 + S_9} \cdot X_5$
14	**Decay of X_{HET}**	$b_H \cdot X_5$

Kinetics Terms

Table 5. 7 Kinetic terms related to the heterotrophic denitrification.

	Description	Value	Unit	Ref.
η_{OX}	Anoxic reduction factor	0.6		[26]
$\mu_{H,S}$	Maximum growth rate of X_{HET} on S_{COD}	5.76	d^{-1}	[27]
$\mu_{H,UAP}$	Maximum growth rate of X_{HET} on S_{UAP}	1.272	d^{-1}	[19]
$\mu_{H,BAP}$	Maximum growth rate of X_{HET} on S_{BAP}	0.0696	d^{-1}	[19]
b_H	Death rate coefficient of X_{HET}	0.1992	d^{-1}	[18]
$k_{NO_2}^{HET}$	S_{NO2} affinity constant for X_{HET}	0.5	mg/l	[18]
$k_{NO_3}^{HET}$	S_{NO3} affinity constant for X_{HET}	0.5	mg/l	[18]
k_s	Biomass affinity constant for S_{COD}	2	mg/l	[18]
k_{UAP}	Biomass affinity constant for S_{UAP}	100	mg/l	[19]
k_{BAP}	Biomass affinity constant for S_{BAP}	85	mg/l	[19]

5.2.1.4 Sulfate reduction

Reaction terms

Table 5. 8 Process rates related to sulfate reduction.

	j- process	*Process rate (ρ_j)*
15	**Growth of X_{SRB} on S_{COD}**	$\mu_{H,SRB} \cdot \frac{S_9}{k_{s,SRB} + S_S} \cdot \frac{S_6}{k_{H,SO_4} + S_6} \cdot \frac{S_9}{S_7 + S_8 + S_9} \cdot X_6$
16	**Growth of X_{SRB} onS_{UAP}**	$\mu_{H,SRB} \cdot \frac{\mu_{H,UAP}}{\mu_{H,S}} \cdot \frac{S_7}{k_{s,SRB} + S_7} \cdot \frac{S_6}{k_{H,SO_4} + S_6} \cdot \frac{S_7}{S_7 + S_8 + S_9} \cdot X_6$
17	**Growth of X_{SRB} on BAP**	$\mu_{H,SRB} \cdot \frac{\mu_{H,BAP}}{\mu_{H,S}} \cdot \frac{S_8}{k_{s,SRB} + S_8} \cdot \frac{S_6}{k_{H,SO_4} + S_6} \cdot \frac{S_8}{S_7 + S_8 + S_9} \cdot X_6$
18	**Decay of X_{SRB}**	$b_{SRB} \cdot X_6$

Kinetics Terms

Table 5. 9 Kinetic terms related to sulfate reduction.

	Description	*Value*	*Unit*	*Ref.*
$\mu_{H,SRB}$	Maximum growth rate of X_{SRB}	0.55	d^{-1}	[22]
$k_{s,SRB}$	Half saturation value of $X_{SRB}$for COD	6	mg/l	[22]
k_{H,SO_4}	Half saturation value of X_{SRB} for SO_4^{2-}	3.2	mg/l	[28]
b_{SRB}	Death rate coefficient of X_{SRB}	0.02	d^{-1}	[29]

5.3 SOURCE OF UNCERTANY, QUANTITY OF INTEREST, EXPERIMENTAL DESIGN

5.3.1 SOURCE OF UNCERTANY

The parameter which has been in investigated in the Global SA are reported in Table 5.10 and mainly consists in kinetic parameters and operational parameters. The latter analyzed in the overall SA are represented by τ_d and the amount of injected COD. These parameters influence the whole process, specifically they affect the competition between the two heterotrophic families for COD. In the previous work by Guerriero et al., 2022 [7], it was shown that an introduction in the first half of the cycle of even small amounts of COD promoted the growth of heterotrophic denitrifiers. Moreover, the amounts of COD injected also have a strong influence on the rate of nitrogen removal, since heterotrophic denitrification is faster than autotrophic denitrification.

Table 5. 10 Range of values used to perform the sensitivity analysis.

		MIN	MAX
Kinetic parameter			
K0	$\boldsymbol{K_0}$	0,01	1
mu_aut_no3	$\boldsymbol{\mu^{max}_{S_b,NO_3^-}}$	0,0015	0,02
mu_aut_no2	$\boldsymbol{\mu^{max}_{S_b,NO_2^-}}$	0,0015	0,02
K2_2	$\boldsymbol{k_{AUT,S_b}}$	0,001	500
K2_3	$\boldsymbol{k_{AUT,NO_3^-}}$	0,01	50
K2_4	$\boldsymbol{k_{AUT,NO_2^-}}$	0,05	100
k1	$\boldsymbol{k_1}$	0,01	1
K1	$\boldsymbol{\kappa_1}$	0,1	10
A	$\boldsymbol{a^*}$	0,00001	0,0001
kd_hid	$\boldsymbol{k_{d,HID}}$	0,00001	0,001
kd_aut	$\boldsymbol{k_{d,AUT}}$	0,0001	0,001
k_H	$\boldsymbol{k_{HID,STOB}}$	0,1	10

K_X	$k_{STOB,COD}$	0,01	10
K_hyd	$K_{HID,EPS}$	0,01	5
eta_NOx	η_{OX}	0,1	0,8
mu_h_s	$\mu_{HET,COD}$	1	7
mu_h_UAP	$\mu_{HET,UAP}$	0,5	5
mu_h_BAP	$\mu_{HET,BAP}$	0,05	1
b_H	$k_{d,HET}$	0,01	0,5
K_Het_NO2	$k_{NO_2}^{HET}$	0,01	10
K_Het_NO3	$k_{NO_3}^{HET}$	0,01	10
K_s	$k_{COD,HET}$	0,1	50
K_UAP	k_{UAP}	10	1000
K_BAP	k_{BAP}	10	1000
mu_srb	μ_{SRB}	0,1	1
K_cod	$k_{COD,SRB}$	1	100
K_SO4	k_{SRB,SO_4}	0,1	100
b_srb	$k_{d,SRB}$	0,01	0,1
f_EPS	$f_{EPS,AUT}$	0,01	0,1
f_UAP	$f_{UAP,AUT}$	0,01	0,2
f_BAP	f_{BAP}	0,01	0,1
f_i	f_I	0,01	0,1
k_EPS	k_{EPS}	0,05	0,5
k_uap	k_{UAP}	0,01	0,1
Y2_3	y_{AUT,NO_3^-}	0,1	0,9
Y2_4	y_{AUT,NO_2^-}	0,1	0,9
Y_H_S	$y_{H,COD}$	0,1	0,9
Y_H_UAP	$y_{H,UAP}$	0,1	0,9
Y_H_BAP	$y_{H,BAP}$	0,1	0,9
Y_SRB	y_{SRB}	0,01	0,9
	Operational parameter		
τ_d		0,1	0,99
COD IN 2		0	500

5.3.2 QUANTITY OF INTEREST

5.3.2.1 N-removal

The total nitrogen percentage removal represents a key parameter of the model, since the main aim of the process is the nitrogen removal via autotrophic denitrification. This quantity was evaluated as an average of the percentage of N-removal at the end of each cycle.

$$\%\ \text{Nremoval} = \frac{(NO_{3_{IN}} + NO_{2_{IN}}) - (NO_{3_{OUT}} + NO_{2_{OUT}})}{(NO_{3_{IN}} + NO_{2_{IN}})} * 100, \qquad (5.23)$$

where $NO_{3,IN}$ and $NO_{2,IN}$ are the concentrations in the SBR at begging of each cycle, $NO_{3,OUT}$ out and $NO_{2,OUT}$ out are the concentrations in the SBR at the end of each cycle.

The removal of nitrogen-based compounds occurs in two ways: the first is via autotrophic denitrification, that is influence by the parameter connected to the reaction terms ρ_2 and ρ_3, the second is via heterotrophic denitrifiers supported by COD (ρ_8, ρ_9), UAP (ρ_{10}, ρ_{11}) and BAP (ρ_{12}, ρ_{13}).

5.3.2.2 SO_4 OUT

Sulfate concentration in the effluent represents the main shortcoming of sulfur based autotrophic denitrification. This output is strongly affected by the percentage of nitrogen compounds removed via SdAD or HD, indeed if the last is favored less sulfate will be produced. This concentration is evaluated as an average of the sulfate concentration at the end of each cycle for every simulation performed.

The production of sulfate depends on the reaction terms ρ_2 and ρ_3, that is the two-step autotrophic denitrification. Those terms are affected by the concentration of bioavailable sulfur, which is supposed to be in excess, but need firstly to be hydrolyzed by the hydrolytic biomass. The sulfate reduction depends on the terms $\rho_{15}, \rho_{16}, \rho_{17}$, which are related to the activity of the sulfate reducing bacteria. The reaction terms related to the sulfate reducing bacteria are strongly influenced by the quantity of COD added to the system and the sulfate produced by the autotrophic denitrifiers. Indeed, if the COD is used also by the heterotrophic denitrifiers the sulfate reducing bacteria will be in competition for the COD uptake.

5.3.2.3 SMP OUT

SMP could be considered either as a favorable presence since they can support the growth of the heterotrophic families involved in the model, or an undesirable compound since they could compromise effluent quality. SMP concentrations are evaluated as the average of the sum of BAP and UAP at the end of each cycle. SMP production is related to the main microbial activities in particular: biomass growth mainly influences UAP while decay mainly influences BAP production.

SMP consumers are both heterotrophic families involved in the model, the SRB (ρ_{16}, ρ_{17}) and the HD ($\rho_{10}, \rho_{11}, \rho_{12}, \rho_{13}$).

5.3.2.4 Ratio of HD and SRB

Due to the novelty of the simultaneous work of SRB and HD, a relevant quantity of interest is represented by the evaluation of the prevalence of a heterotrophic family against an another. This percentage is mainly influenced by the operational parameter τ_d and $COD_{INJ.}$ To analyze the ratio when a pseudo-steady state is reached, so the ratio is evaluated using the concentration at the end of each simulation.

$$\%SRB = \frac{X_{SRB,FIN}}{X_{SRB,FIN} + X_{HET,FIN}} * 100 \quad (5.24)$$

$$\%HET = \frac{X_{HET,FIN}}{X_{SRB,FIN} + X_{HET,FIN}} * 100 \quad (5.25)$$

5.3.3 EXPERIMENTAL DESIGN

Due to the lack of experimental validation of the whole process, the same initial conditions of Guerriero et al., 2022 [7] are used to perform the simulation, reported here for convenience.

Table 5. 11 Initial condition for the simulations performed.

X_{HYD} (mg/l)	X_{AUT} (mg/l)	X_{STOB} (mg/l)	X_{EPS} (mg/l)	X_{HD} (mg/l)	X_{SRB} (mg/l)	X_I (mg/l)
500	1100	0	0	1	1	0

S_{S_0} (mg/l)	S_{S_b} (mg/l)	$S_{NO_3^-}$ (mg/l)	$S_{NO_2^-}$ (mg/l)	S_{N_2} (mg/l)	$S_{SO_4^{2-}}$ (mg/l)	S_{UAP} (mg/l)	S_{BAP} (mg/l)	S_{COD} (mg/l)
21’000	0	210	0	0	0	0	0	0

The results are evaluated for three different durations of the cycle τ=10, 15, 20 days, and the duration of each simulation is fixed to 300 days, indeed for each cycle duration different number of cycles are performed.

5.4 METHODOLOGY

5.4.1 MORRIS METHOD

The first methodology applied is the Morris method which is relatively inexpensive from a computational point of view, giving the opportunity to reduce the number of parameters analyzed in the further step. The Morris parameters have been evaluated using a set of simulations composed by 430 different variables combination, whose values are supposed to be uniformly distributed. The data analysis of each random sample, is carried out hypnotizing that all the observations are independent, and is summarized using two parameters: the sample mean μ reported in equation 5.26 and the sample standard deviation σ reported in equation 5.27 according to Campolongo and Saltelli, 1997 [30].

$$\mu(\boldsymbol{z}) = \frac{\sum_{i=1}^{r} z_i}{\boldsymbol{r}} \quad (5.26)$$

$$\sigma(\boldsymbol{z}) = \left(\frac{\sum_{i=1}^{r} (z_i - \mu(\boldsymbol{z}))^2}{(\boldsymbol{r} - \mathbf{1})} \right)^{1/2} \quad (5.27)$$

The quantities obtained in absolute values represent the two sensitive parameters because the mean represent the entire the influence on the output while the standard deviation represents the interaction between the factors giving important information about the linearity of the parameter [30].

5.4.2 MACHINE LEARNING-BASED METHOD

For the surrogate-based study, two databases of size N =2^{14} by using different quasi-Monte Carlo sampling methods were realized. A first database was generated using Sobol type sampling and is used as a training set. Then a second database is realized using a Halton method in order to validate the results obtained with the first set. The choice of making a second set is necessary to estimate the accuracy of the results obtained by the algorithm which learns with the first set. Those sets are used to train two different machine learning algorithms: Random Forest and XGBoost. The algorithms are trained using the Sobol set and the are validated using the Halton set.

The quality of the machine learning methodologies was estimated using quantitative errors by evaluating the empirical error and Q2 error, the equations for which are given in the next section for more clarity on the results obtained. In addition, a qualitative graphical representation of the

error is given by the adequacy plots made with the XGBoost algorithm, comparing the learning results with the Sobol set, first with the same Sobol set and then tested using the Halton set.

Then SHAP method was used to perform analysis and develop the SHAP feature importance plot in which are reported the mean absolute Shapley values and the SHAP summary plot where are condensed the importance of each feature.

Lastly a partial dependence plots are also carried out to evaluate the simultaneous variation of the two operational conditions presented in the model: the day of the COD injection and the quantity of COD injected.

5.5 RESULTS AND DISCUSSION

5.5.1 INITIAL SCREENING VIA MORRIS METHOD

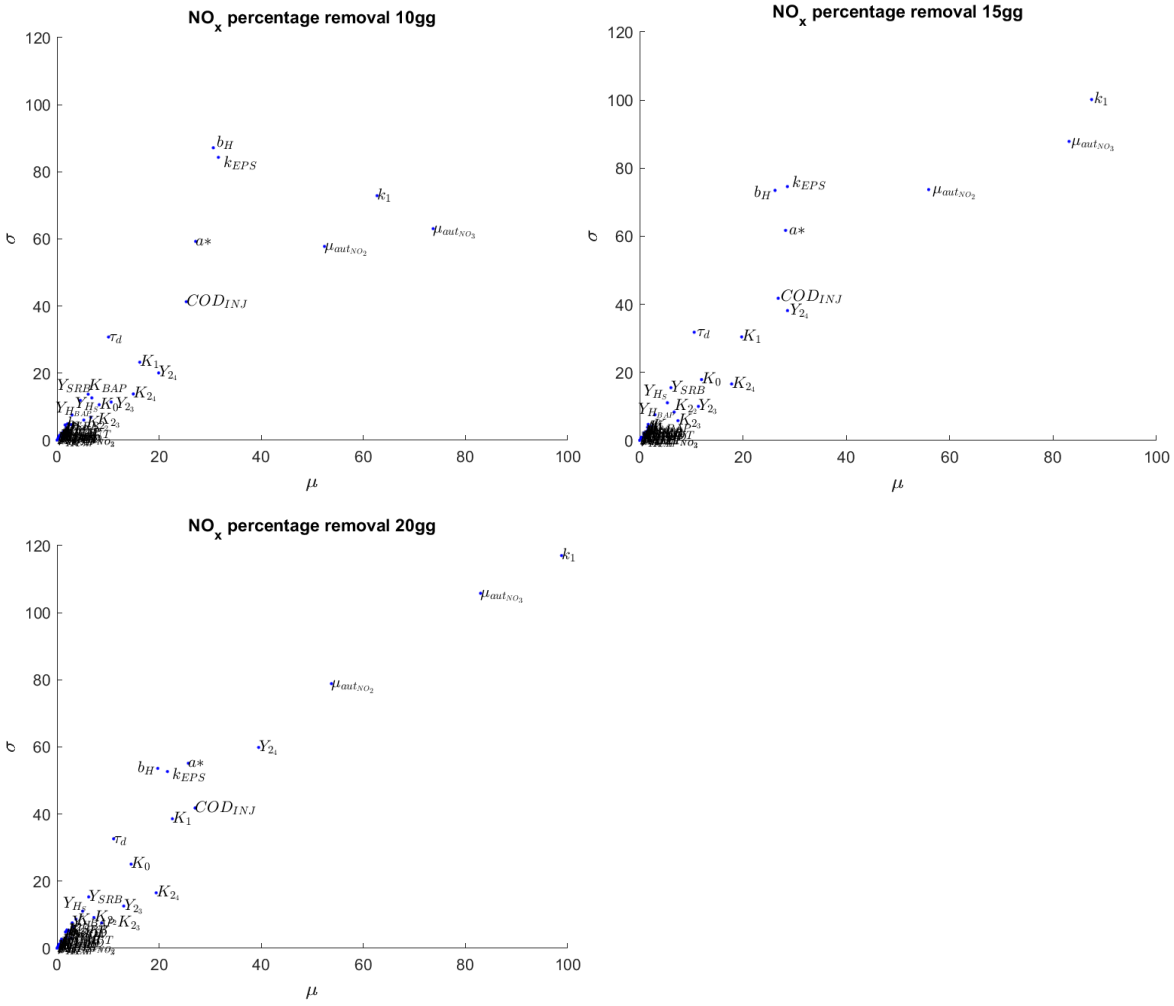

Fig. 5. 1 Morris results regarding the nitrogen percentage removal for three different cycle durations (τ=10,15,20 days).

The initial screening suggests that the most influent parameters of the model are related to the sulfur-based denitrification process and in particular to the first step related to this process, represented by the hydrolysis of the elemental sulfur into the bioavailable sulfur. Indeed, the hydrolysis constant k_1 which governs the transformation from elemental sulfur into bioavailable sulfur, represents the most influential parameter in the denitrification process also because is the starting point of the whole process. In particular, this parameter assumes an enhanced importance for longer cycle durations where autotrophic denitrification represents the main denitrification

process. Furthermore, other two constants K_0 and κ_1 related to the hydrolysis step, strongly affect the process, representing respectively the efficiency growth coefficient for the hydrolytic biomass and volume specific half-saturation constant for elemental sulfur. Moreover, it should be noticed that as k_1 also the effect of these parameters increase with the cycle duration.

Another parameter related to the hydrolysis step is a^*, a geometric factor that influences the process and represents the specific area of the mass; unlike the previous ones, this is not affected by the cycle duration.

The parameters related to the hydrolytic phase have also been identified as some of the most sensitive parameters in previous local sensitivity analyses performed for sulfur-based autotrophic denitrification system that also considered the hydrolysis phase [31], [32].

As reported by Guerriero et al., 2022 [7], longer cycle duration makes the autotrophic denitrification prevails within the whole process, explaining the increasing sensitivity of the nitrogen percentage removal to the maximum growth rate of both the denitrification steps $\mu_{aut,NO3}$, $\mu_{aut,NO2}$ and the Yield coefficient for autotrophic denitrifiers growing on nitrite. In addition, the half- saturation constants of the process $K_{2,2}$, $K_{2,3}$, $K_{2,4}$ are also sensitive parameters but conversely to the previous ones those are not affected by the cycle duration.

Regarding the parameters connected with the two heterotrophic species involved in the model, the most sensitive are found as b_H, the death rate coefficient of the heterotrophic denitrifiers and Y_{SRB} yield coefficient for the sulfate reducing bacteria. While b_H is strongly sensitive also to τ because shortest cycle favors the heterotrophic denitrification, the y_{SRB} remains almost constant as the cycle length changes because of the increased sulfate production due to autotrophic denitrification.

With respect to the parameters involved in the production and consumption of the SMP, the most sensitive parameter is represented by the k_{EPS} which is the Yield coefficient for EPS for heterotrophic denitrifiers which as the death rate coefficient of the heterotrophic denitrifiers decreases with the cycle duration.

As expected, the operational parameters COD_{inj} and τ_d result sensitive for the nitrogen percentage removal due to their influence on the heterotrophic families involved, but their impact is not subjected to the cycle duration.

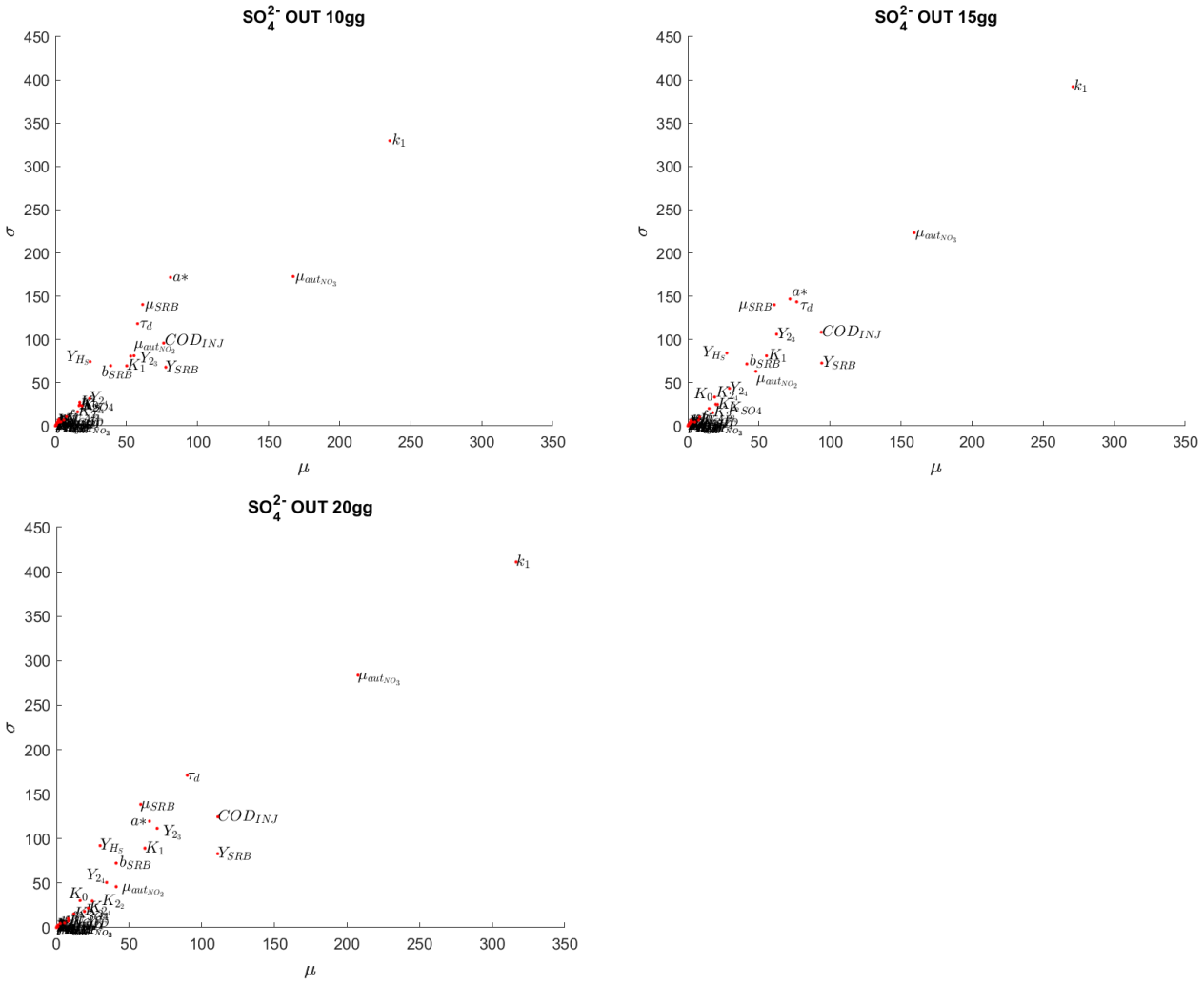

Fig. 5. 2 Morris results regarding the avarage of sulfate concentration in the effluent for three different cycle durations(τ=10,15,20 days).

The second quantity of interest investigated is the sulfate concentration in the effluent, which is strongly connected to the percentage of N-based compounds removed. As for the percentage of nitrogen removal also for the sulfate concentration, the parameters related to the autotrophic denitrification, and consequently to the sulfur hydrolyzation, represent the most sensitive from this analysis.

As previously observed, the maximum growth rate for autotrophic denitrifiers with respect to the first stage of denitrification $\mu_{aut,NO3}$ and the hydrolysis constant kinetics k_1 are more sensitive than the other parameters. Moreover, the relative sensitivity to these parameters as for nitrogen removal

rate increases for longer cycles because of their strong connection. Sulfate production is also sensitive to the maximum growth rate of the second stage of denitrification $\mu_{aut,NO2}$.

Other kinetic parameters related to the autotrophic denitrification which increase with the cycle duration are represent by the yield coefficients of the autotrophic denitrifiers in both the denitrification steps. However, comparing those results with the ones observed for the nitrogen percentage removal, the sulfate concentration is not sensitive to any the semi-saturation constants of the autotrophic denitrification. Furthermore, the physical parameter a^* is less influent when increasing the cycle duration maybe because if less sulfur is transformed into bioavailable sulfur, less sulfate could be result by the autotrophic denitrification. However, sulfate is also sensitive to κ_1 the volume specific half-saturation constant which have also, as a^* a strong influence on the hydrolyzation of sulfur.

The sulfate concentration is also sensitive to the sulfate reduction related parameters: μ_{SRB} the maximum growth rate of the sulfate reducing bacteria, b_{SRB} the death rate of the sulfate reducing bacteria, and the yield coefficient of the sulfate reducing bacteria Y_{SRB} . Those parameters are not affected by the duration of the cycle. Regarding the operational parameters, the sulfate concentration is more sensitive to the day of COD injection than to the quantity injected in that day. In addition, due to the competition between the two heterotrophic families for COD, the sulfate concentration is also affected by the relative efficiency coefficient of the heterotrophic denitrifiers, taking into account that HD is associated with lower sulfate concentration in the effluents.

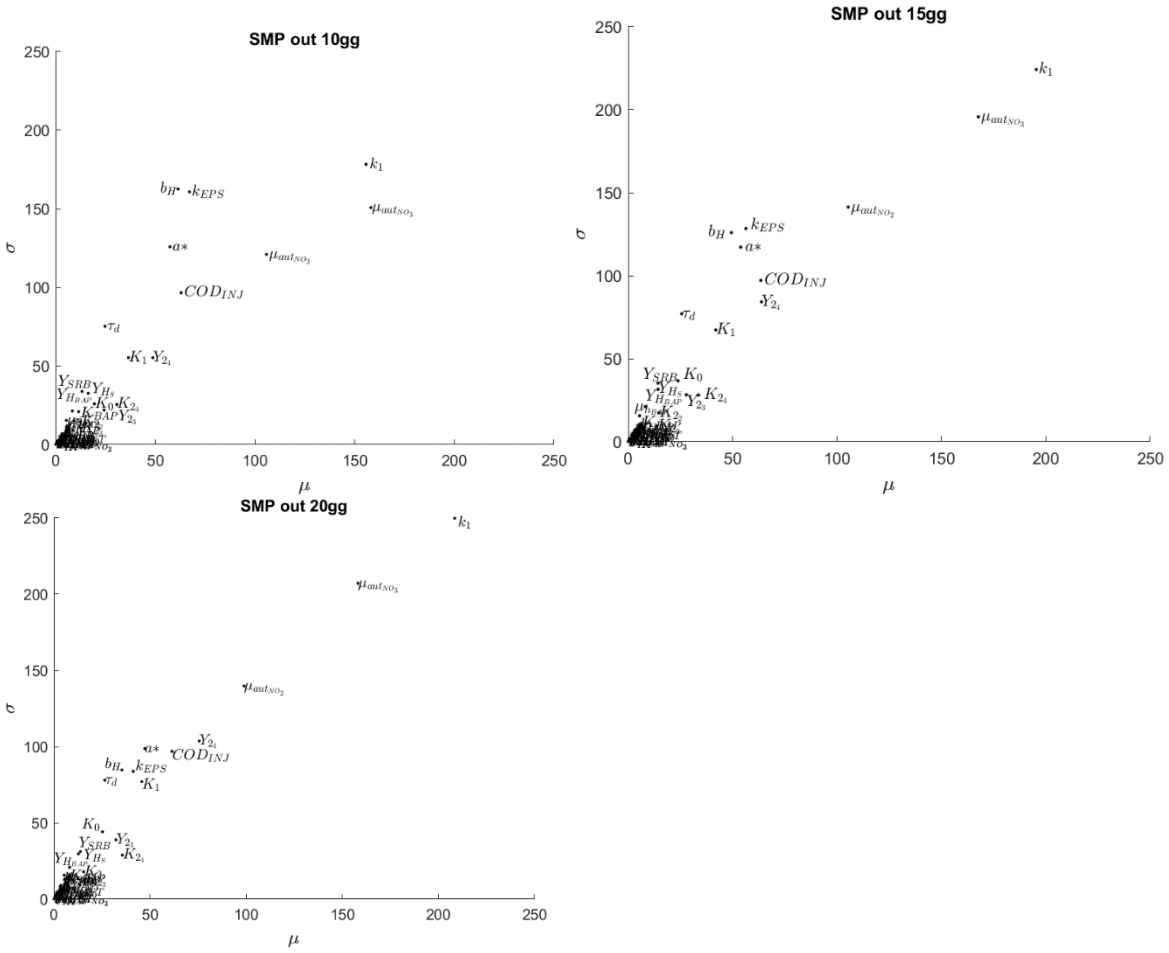

Fig. 5. 3 Morris results regarding the average of the concentration of the SMP in the effluent for three different cycle durations (τ=10,15,20 days).

Being strongly correlated with biomass activities, the SMP productions influenced by the biomasses that produce them in greater amounts represented by autotrophic denitrifiers also due to their higher initial abundance as could be observable from Fig 5.3. Also, for this quantity the aforementioned parameters related to the hydrolysis step (a^*,k_1, κ_1,K_0) and autotrophic denitrification ($\mu_{aut,NO3}$, $\mu_{aut,NO2}$, $Y_{2,3}$, $Y_{2,4}$) represent sensitive parameters, since both can be considered the bottleneck of the process and are related to the most abundant biomass of the system.

As expected, the yield of heterotrophic denitrifiers and sulfate reducing bacteria affects SMP production, being a parameter that links substrate to biomass growth. Heterotrophic denitrifiers are linked to SMP production and consumption, and their decay term is found to be strongly influenced by cycle duration. Also k_{EPS} , the EPS yield coefficient for heterotrophic denitrifiers, turns out to be a sensitive parameter contrary to what is observed for the other quantities of interest. Regarding

the operational parameters considered, COD_{inj} and τ_d are not affected by cycle duration and their importance always remains in the same region.

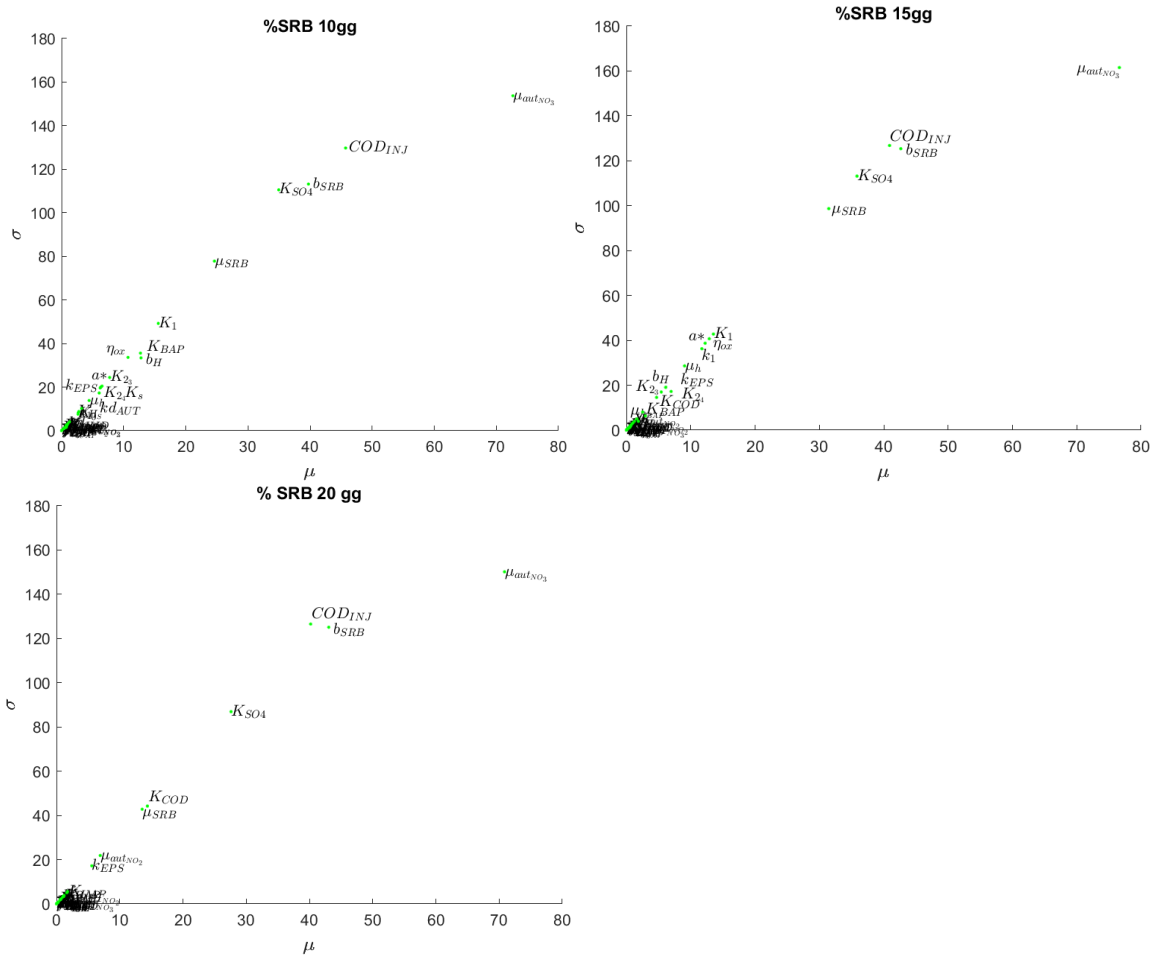

Fig. 5. 4 Morris results regarding the percentage of the SRB and HET overe the heterotrophic consortium, for three different cycle durations (τ=10,15,20 days).

In case of shortest cycle duration τ =10 days, the prevalence of a heterotrophic family against another is influenced by the maximum growth rate and the decay coefficient of both heterotrophic families. Furthermore, in this case it is present also a parameter only related to the heterotrophic denitrifiers represented by η_{ox} i.e., the anoxic coefficient which accounts for the reduced heterotrophic denitrifiers growth rate under anoxic conditions.

Since it is a reduction coefficient it could quickly bring down the concentration of heterotrophic denitrifiers. Moreover, the semi-saturation constant of the heterotrophic denitrifiers with respect to

the BAP also result also an influent parameter, probably because BAP represents the second source in terms of abundance of organic matter, so it could affect the growth of both heterotrophic families.

For cycle duration τ =15 days, the prevalence of a species is influenced by the anoxic coefficient, but in this case the parameters related to COD consumption by denitrifying heterotrophs $\mu_{H,S}$ and b_H also become more relevant. By increasing the cycle duration from τ =15 days to τ =20 days, the most influential parameter is the semi saturation constant of sulfate-reducing bacteria with respect to COD. Linked to this parameter, for the relation between autotroph denitrification and sulfate concentration, during τ =20 days the maximum growth rate of autotrophs related to the second denitrification phase also becomes relevant. For a longer cycle duration, the sensitivity with respect to μ_{SRB}also increases due to the prevalence of autotrophic denitrification, and consequently a higher sulfate concentration leads to an increase in sulfate-reducing growth. The main biological pathway involved in the process represented by autotrophic denitrification is also found to influence the prevalence of the heterotrophic family over another. It may also be noted from the observation that both the maximum growth relative to the first step of autotrophic denitrification that converts nitrate to nitrite $\mu_{aut,NO3}$ and the half-saturation coefficient of sulfate during autotrophic denitrification represent sensitive parameters.

Because of the prevalence of autotrophic denitrification by enlarging the cycle duration, the influence of these parameters decreases for longer cycles. Namely, the higher the sulfate production, the higher the growth of sulfate-reducing bacteria. In addition, reducing the cycle duration results in the prevalence of one family over another being influenced by more parameters, as expected because this quantity is evaluated only on the heterotrophic biomasses involved in the model.

5.5.1.1 Overall analysis on Morris

All the quantities investigated are more sensitive to the parameter connected with the sulfur hydrolyzation k_1 which represents the bottleneck step of the whole process. Associate to k_1 also, regarding the hydrolysis step the importance of the physical parameter a^*, which is already known to be an important parameter in the elemental sulfur based autotrophic denitrification.

What must be noticed with respect to all the previous experimental studies is that the influence of the dimension of the particles become less relevant when increasing the duration of the cycle. This investigation has never been carried out before, but from an engineering perspective, whose main objective is the reduction of the time reaction, this result provides valuable information. Conversely κ_1 assume an opposite trend with respect to a^*. Furthermore, the prevalence of one heterotrophic family against another represents the quantity of interest which results more affected by the amount of COD injected. Also, it should be noted that the initial concentration of both the heterotrophic species involved in the model are considered very low with respect to the autotrophic denitrifiers to simulate the natural growth of both heterotrophic families. This assumption was made assuming that the biomass was already acclimatized for autotrophic denitrification, and it may explain why the kinetic parameters related to the heterotrophic species do not strongly affect the quantity of interest investigated.

5.5.2 MACHINE LEARNING RESULT

After the first analysis performed using the Morris technique which could lead to an overall look at the parameters involved in the model, two other random sets of simulations have been carried out using the SOBOL indices and a HALTON sequence both derived from Montecarlo method. Those sets have been used in two different machine learning algorithm: Random Forest and XGBoost. Based on the preliminary results of the Morris method, some parameters have been excluded due to their low sensitivity, so the number of the parameter investigated is passed from 42 to 30. The sample set to perform for each method consists of 16’384 simulations, so more accuracy will be present in the next results. Furthermore, the same quantities of interest have been investigated for the three different cycle durations. Here for convenience are reported just the result for a cycle duration of 20 days due to the very close results obtained for the other cycle durations, which are reported in the appendix.

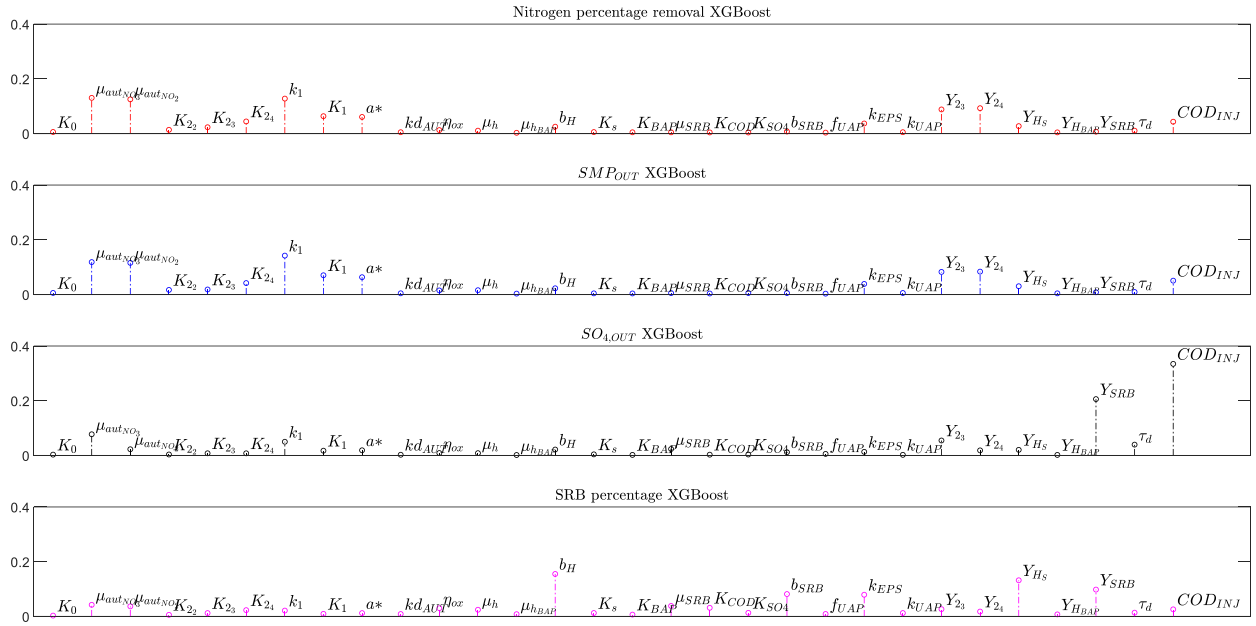

Fig. 5. 5 Importance of the parameter exanimated using XGBoost algorithm.

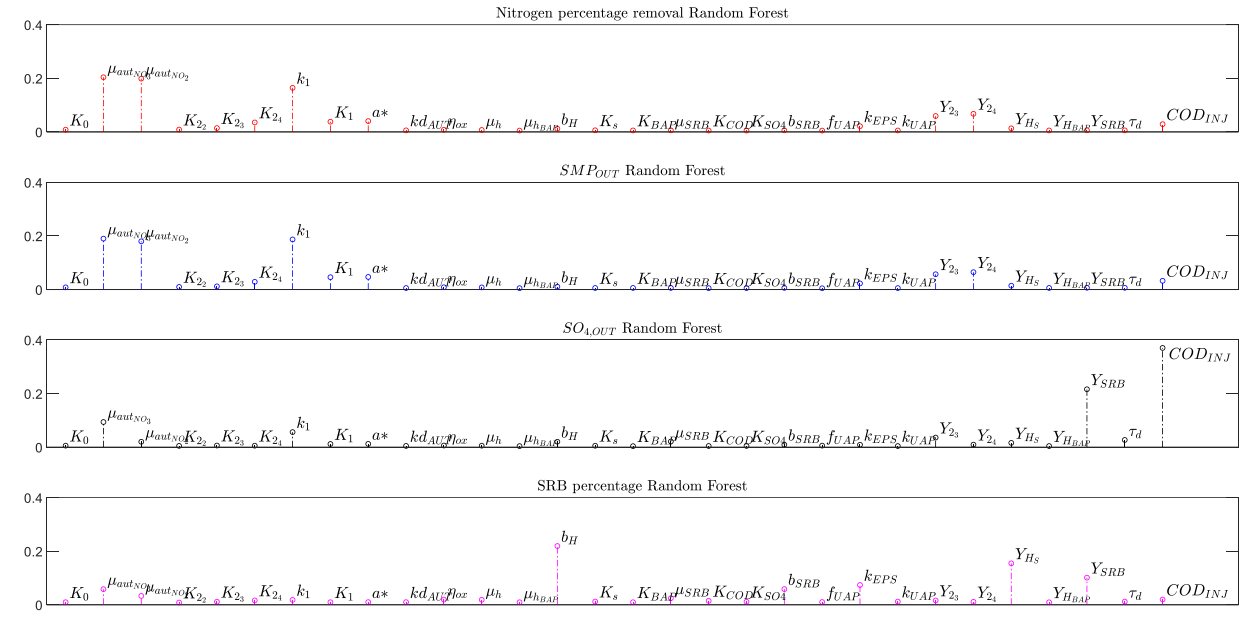

Fig. 5.6 Importance of the parameter exanimated using Random Forest algorithm.

From the analysis of the importance with the XGBoost (Fig. 5.5) and Random Forest (Fig. 5.6) machine learning algorithms, it appears clear that for different quantities of interest, there are different sensitive parameters. Nitrate removal rate appears to be strongly correlated with the output SMP concentration, since SMP concentration is related to biological activities. The main parameters affecting nitrogen removal rate have the same order of importance in the process order. The parameter with the greatest importance is the hydrolysis constant k_1, in line with previous observations since the hydrolysis of elemental sulfur is the bottleneck of SdAD. Also experimentally, the low solubility of elemental sulfur represents the main bottleneck of the process [3].

Then the other relevant parameters are represented by the biological constants related to the two steps of the autotrophic denitrification which are $\mu_{S_b,NO_3^-}^{max}$, $\mu_{S_b,NO_2^-}^{max}$, y_{AUT,NO_3^-}, y_{AUT,NO_2^-}.

For the sulfate concentration, the most important parameter is represented by the COD injection amount which is strongly related to the possibility of the sulfate production or consumption. Indeed, if the denitrification process is mainly performed by the heterotrophic denitrifiers less sulfate will be produced. Similarly, when COD_{inj} occurs after τ /2, a lower sulfate concentration is observed but, in this case, the reduced sulfate concentration is due to the activity of sulfate reducing bacteria.

Furthermore, also the maximum growth rate related to the first step of the autotrophic denitrification is important for sulfate concentration. Moreover, apart from the quantity of COD_{inj}, the other biological parameters related to the sulfate concentration in the effluent is the yield of the SRB which are not stimulated to growth if sulfate is not present.

Regarding the SRB percentage, if higher amount of COD is not added the SRB percentage on the heterotrophic consortium is always favored. This is in line with the importance of the constant b_h which represents the decay of the heterotrophic denitrifiers. Indeed, if the heterotrophic denitrifiers die the sulfate reducing bacteria are the only COD consumers. The decay of sulfate reducing bacteria assumes the same importance for the same reason.

5.5.2.1 A posteriori error estimation of surrogate error

The construction of a surrogated model could lead to two different types of error that could be computed to understand the differences and the straightness between the metamodel and the model. The empirical error can be evaluated using the following equation

$$\varepsilon_{emp} = \frac{\sum_{i=1}^{N_{sobol}} (y^{(l)} - \widehat{y^{(l)}})}{N_{sobol} Var\boldsymbol{Y}} \quad (5.28)$$

where: $y^{(l)}$is the lth element of the training set and $\widehat{y^{(l)}}$ is the corresponding prediction by the surrogate model; $N_{sobol} = 2^{14}$ is the number of simulations in the set of the Sobol training set. The estimation of the empirical error is carried out to prevent the overfitting problem. The empirical error is evaluated for the different quantity of interest firstly observing the difference between the random forest surrogate model and secondly using as surrogate model the XGBoost algorithm.

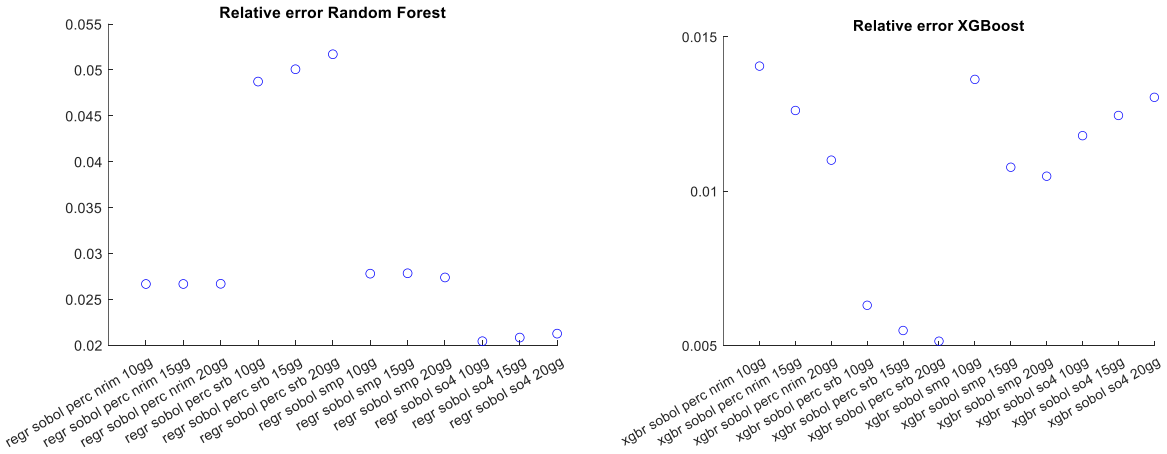

Fig. 5. 7 Relative error evaluated using the different machine learning methods used: on the left side the Random Forest relative error and on the right side the relative error on XGBoost algorithm.

As reported in Fig. 5.7, in both cases the percentage of SRB is the most variable error when varying the cycle duration, but with different trends. The error on the percentage of the SRB increases on the left side while decrease on the right side also presenting lower values for XGBoost algorithm. In addition, another quantity that exhibits the same trends but with different values is the output sulfate concentration, whose error increases as the cycle duration increases. The relative error using Random Forest method for the nitrogen percentage removal and the SMP production, are not affected by the variation of the cycle duration. Conversely when XGBoost algorithm is used, the relative error on the nitrogen percentage removal decreases with the increasing of τ, probably

because longer cycle implies more nitrogen compounds removed via autotrophic denitrification. The relative error on SMP in the effluent also vary, decreasing faster with respect to the nitrogen percentage removal.

Another index that could be used to evaluate the error and validate the surrogate model is represented by the predictive coefficient Q2 that is a cross-validation error metric. For the estimation of Q2, it has been used another independent set that in this case is represented by the Halton set to validate the data.

$$Q_2 = \frac{\sum_{l=1}^{N_{Halton}} (y^{(l)} - \widehat{y^{(l)}})^2}{\sum_{l=1}^{N_{Halton}} (y^{(l)} - \bar{y})^2} \quad (5.29)$$

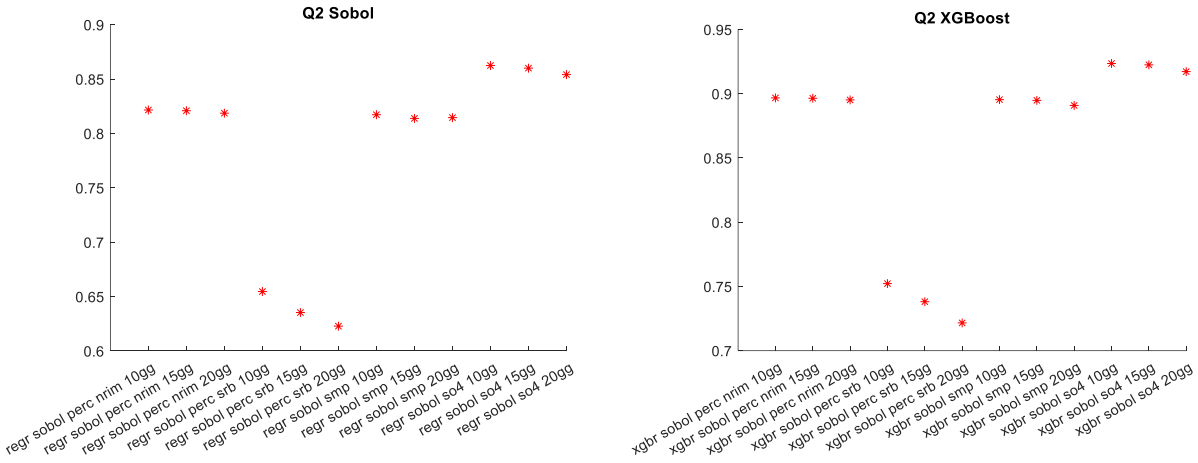

Fig. 5. 8 Relative error Q2. On the right the error evaluated using Random Forest on the left the error using XGBoost.

In contrast to the relative error, the Q2 error has the same trend for all quantities of interest, the only exception being the variability on the sulfate reducing bacteria percentage. Notably, this error decreases with increasing cycle length as in the case of the relative error calculation.

5.5.2.2 Adequacy plot

To test what the machine learning system have learned on the Sobol set using the XGBoost algorithm, qualitative graphical representation has been also carried out using the adequacy plot. Those are the representation of the simulation tests performed for analyzing graphically the error that is carried out by the different machine learning methods. Such representations are carried out

comparing the results obtained using the same set on which the algorithm has been trained (Sobol set), and another validating set (Halton set).

Table 5. 12 Resume of the adequacy plot of the machine learning system XGBoost trained on Sobol set and validated using Sobol set the first column report the results obtained for cycle duration of 10 days and the second column for cycle duration of 20 days.

Test of XGBoost which learn on Sobol set and respond to Sobol set		
	10 days	20 days
Sulfate	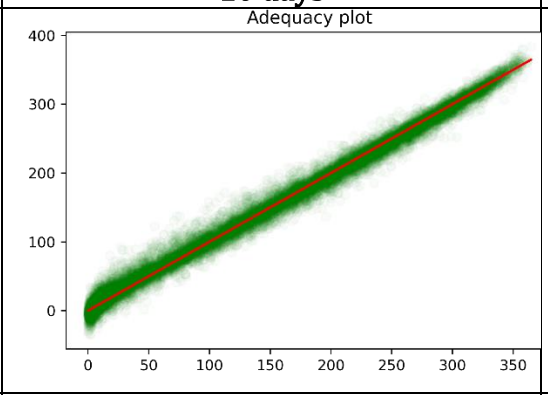	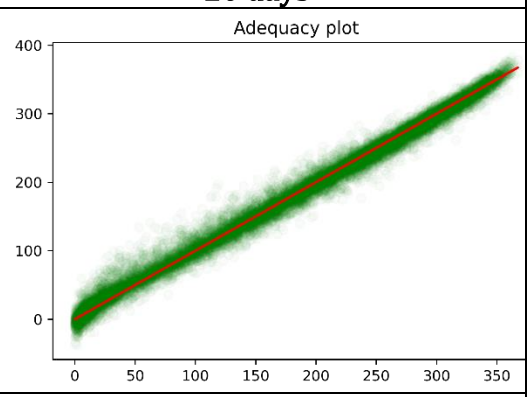
Perc_SRB	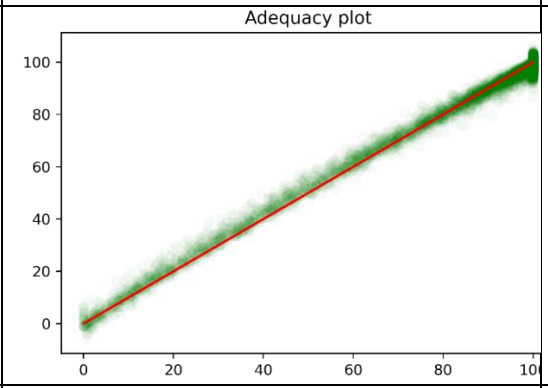	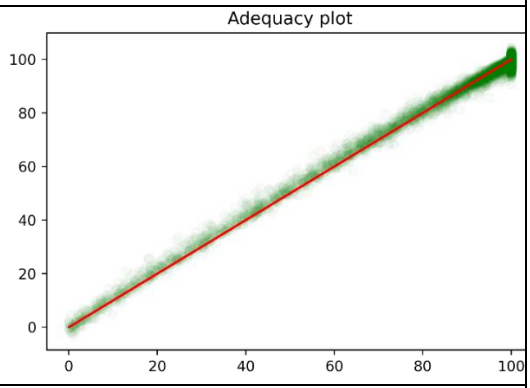
Perc_N_Rim	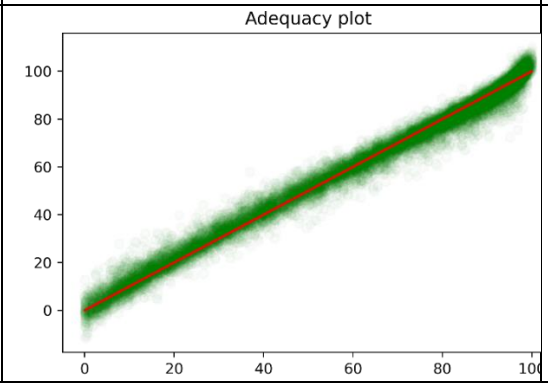	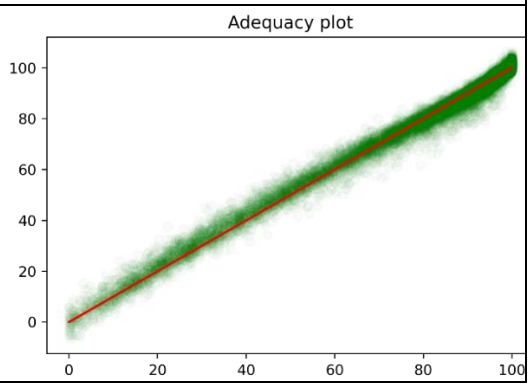

SMP	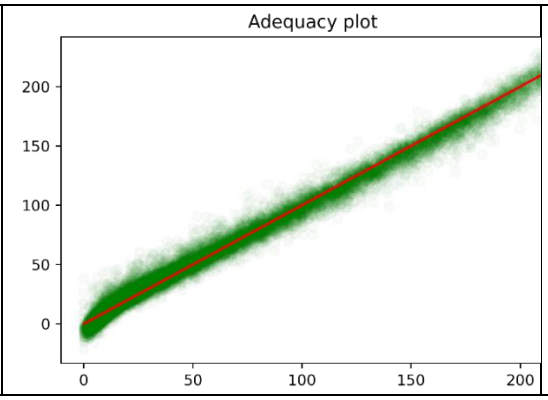	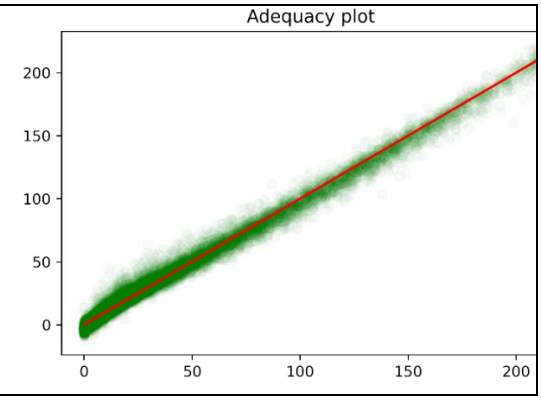

The results reported in Table 5.12 have been obtained by testing the XGBoost machine learning algorithm on the Sobol set, that is the same set on which the algorithm was trained. The results obtained show that the system responds uniformly for all quantities of interest examined. In the case where the duration is longer i.e. a duration of 20 days the dispersion of the evaluated results represented by the green point cloud is tightest and close to the red line that represent the optimum result.

Table 5. 13 Resume of the adequacy plot of the machine learning system XGBoost trained on Sobol set and validated using Sobol set the first column report the results obtained for cycle duration of 10 days and the second column for cycle duration of 20 days.

Test of XGBoost which learn on Sobol set and respond to Halton set		
	10 days	**20 days**
Sulfate	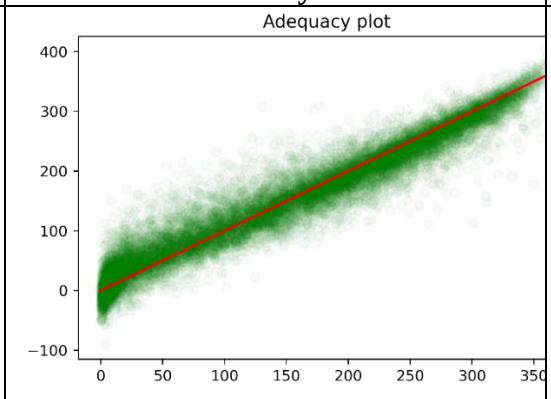	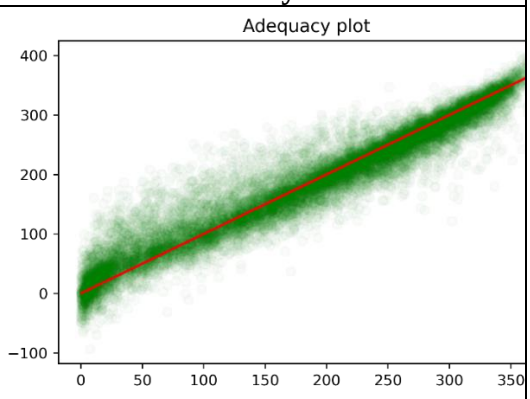
Perc_SRB	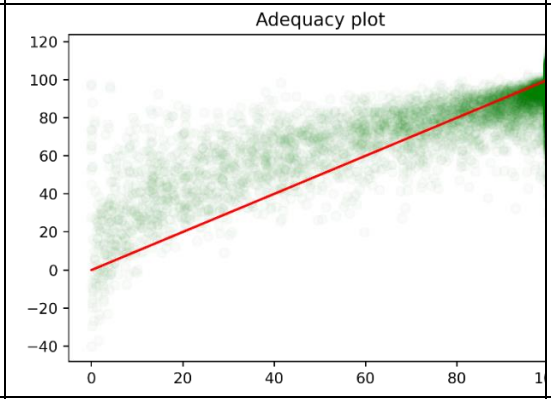	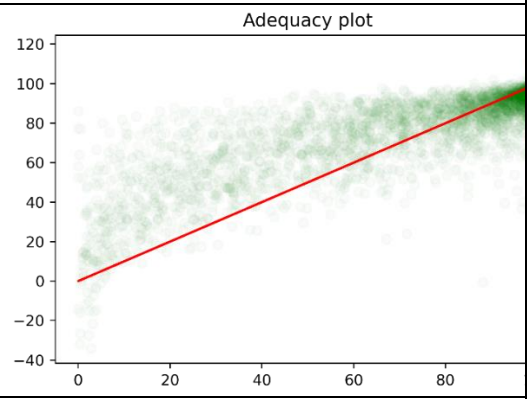
Perc_N_Rim	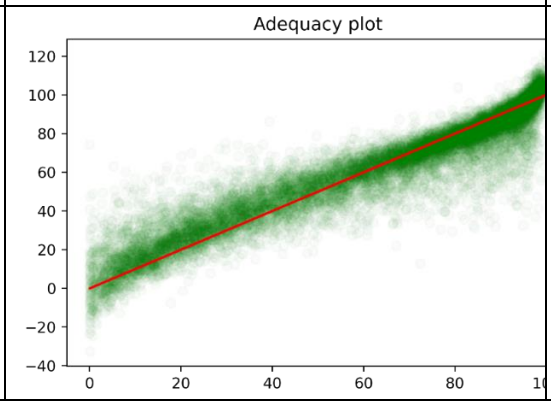	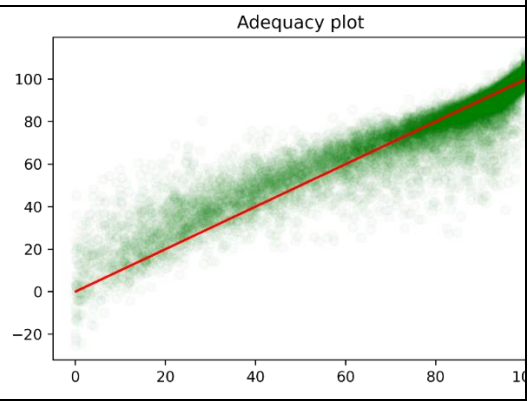
SMP	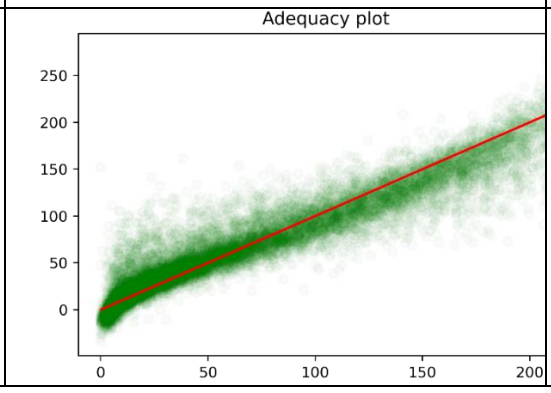	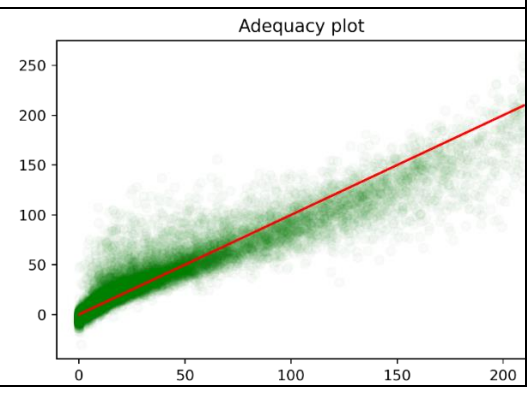

Validation of the algorithm with a second set other than the learning set shows greater dispersion of the results obtained, the green dots representing the individual results being much further away from the red line of the primary result. In particular, the results for the percentage of reducing sulfate versus heterotrophic consortium show the greatest dispersion. The outcomes are scattered in both cases, resulting in a very different output from that in Table 5.12 in which the reducing sulfate percentage was the best investigated quantity. In contrast to the results shown in Table 5.12, in Table 5.13 a greater dispersion of results is observed in cases where the cycle duration is longer i.e., 20 days.

5.5.3 SHAP METHOD

5.5.3.1 Shap feature importance

Shapley characteristics are evaluated to understand the overall importance. Important values are those with a large absolute value of Shapley number, so the results obtained are represented ordered from most to least important. The values shown are an average of the absolute Shapley values for each feature in the data:

$$I_j = \frac{1}{n}\sum_{i=1}^{n}\left|\Phi_j^{(i)}\right| \quad (5.30)$$

The score obtained for each parameter represents the effect of this parameter on the quantity of interest of the model. The following Shapley feature data are trained with XGBoost algorithm.

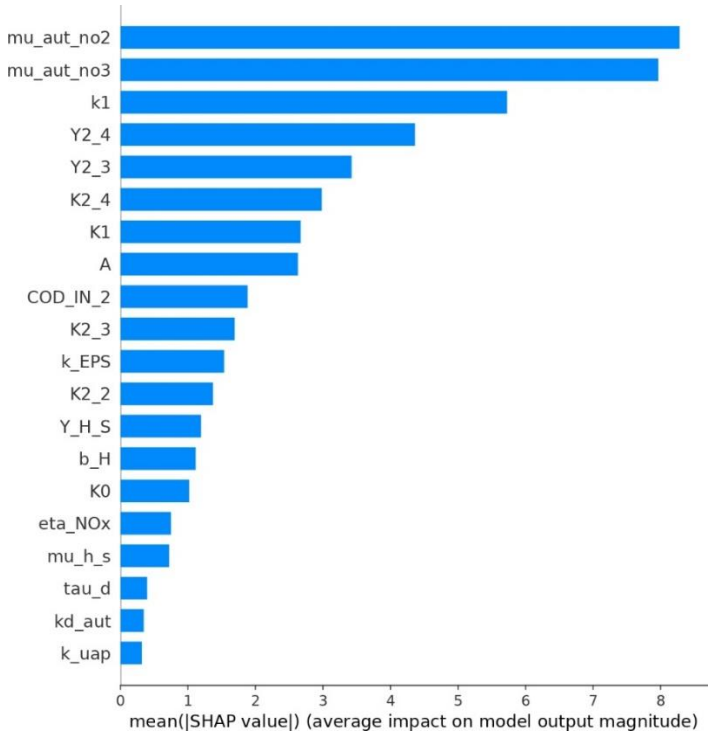

Fig. 5. 9 SHAP feature importance measured as the mean absolute Shapley values. Those values are related to a cycle duration of 20 days trained with XGBoost for predicting the Nitrogen percentage removal.

As expected as it possible to observe from Fig 5.9 for longer cycle duration, the most relevant parameters affecting the Nitrogen percentage removal are the maximum growth rate of the autotrophic denitrifiers over nitrate and nitrate and also the hydrolysis constant for the elemental sulfur. With respect to the Morris analysis which is based on a smaller simulation set, here the biological parameters such the maximum growth rate but also the yield coefficient for the biomasses has more importance than the parameters related to the sulfur hydrolysis. Furthermore, the quantity of COD injected becomes more relevant as well as the maximum growth rate related to the growth of the heterotrophic biomass.

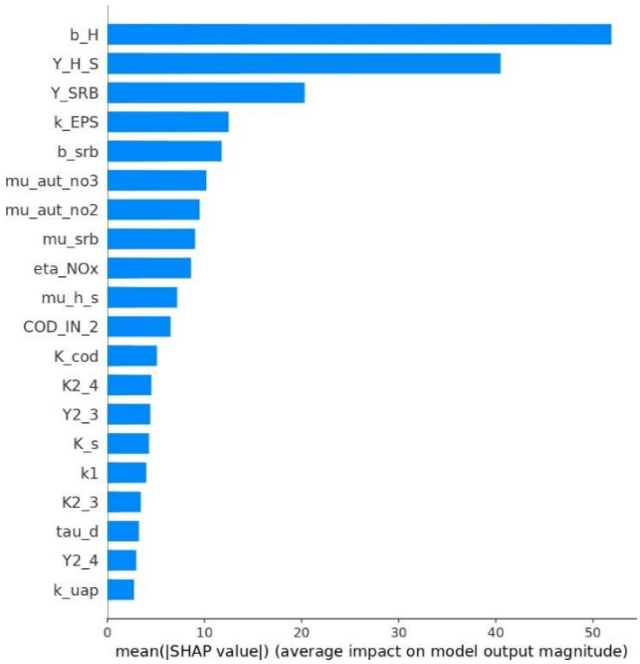

Fig. 5. 10 SHAP feature importance measured as the mean absolute Shapley values. Those values are related to a cycle duration of 20 days trained with XGBoost for predicting the Percentage of prevalence of sulfate reducing bacteria.

The results obtained for the SRB reported in Fig. 5.10 prevalence with respect to the heterotrophic consortium are partially different from the Morris results. Indeed, the decay constant for the heterotrophic denitrifiers was not considered a highly sensitive parameter as in the Morris result. Instead, the growth rate and decay constant related to the SRB maintain the relevance in both methods, since for higher amount of COD added to the system the SRB represent the most abound biomass in the consortium. Furthermore, the growth rate related to the autotrophic denitrifiers still maintain higher relevance since affects both the heterotrophic biomass. This occurs because if the autotrophic biomass is not responsible of the denitrification, then no sulfate is produced and consequently the growth of sulfate reducers is not promoted. For cases where no COD addition occurs, the other organic matter derives from the SMP that could be uptaken by the heterotrophic species; the constant k_EPS related to the BAP production becomes relevant to support the growth of the heterotrophic consortium.

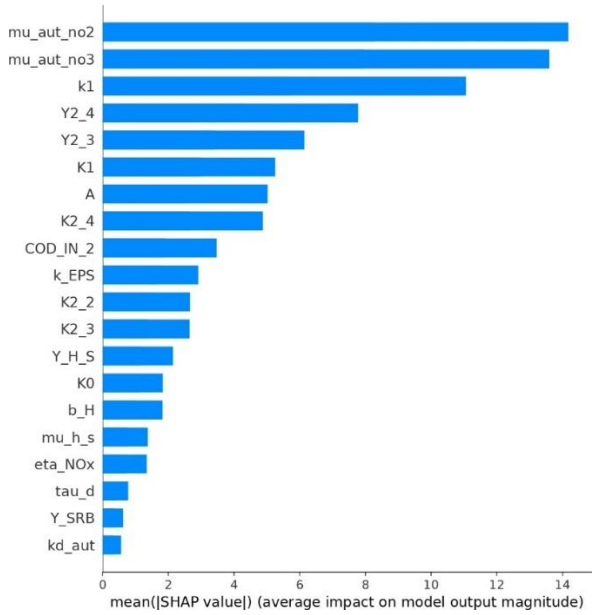

Fig. 5. 11 SHAP feature importance measured as the mean absolute Shapley values. Those values are related to the cycle duration of 20days trained with XGBoost for predicting the SMP concentration in the effluent.

The first eight most important parameters in this classification reported in Fig. 5.11 concerning the SMP are all related to the autotrophic denitrifiers and the sulfur hydrolyzation as expected because the autotrophic denitrifiers are the most abundant family present in the system. SMP production is related to all the microbial activities performed and the autotrophic denitrification always occurs even without COD addition. In fact, after these eight parameters, the injected COD is also relevant because it will increase SMP production due to increased microbial activities of all the biomasses involved in the model. Furthermore, considering the SMP as the sum of UAP and BAP, the hydrolyzation constant of the EPS which leads to the production of BAP is also relevant.

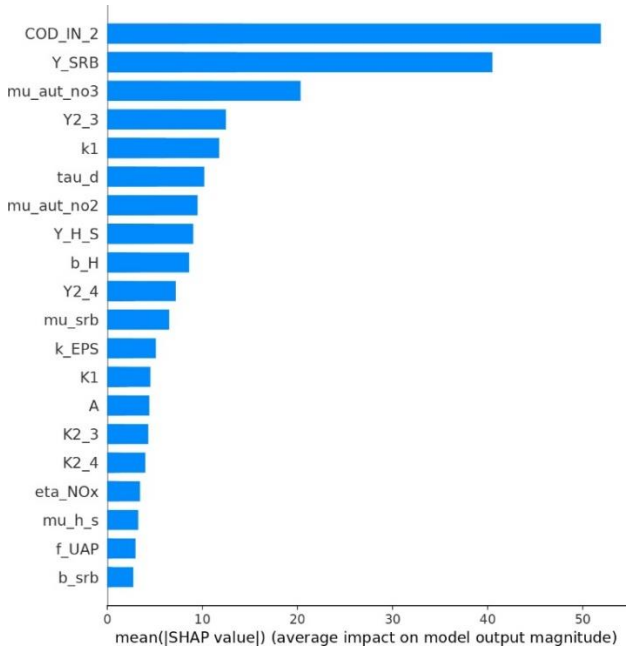

Fig. 5. 12 SHAP feature importance measured as the mean absolute Shapley values. Those values are related to the cycle duration of 20days trained with XGBoost for predicting the Sulfate concentration in the effluent.

According to Fig. 5.12 The concentration of the COD injected in the system represents the most important parameter since it is necessary to have a relevant reduction in the Sulfate concentration in the effluent. Furthermore, the concentration will not increase if the autotrophic denitrification does not take place. Indeed, the maximum growth rate of the autotrophic denitrifiers and the yield coefficient related to the first step of the denitrification process and the hydrolysis constant are also reported as important parameters.

The day of the COD injection in this case is in the highest position compared to the results obtained for the other quantity of interest since a later injection favors the sulfate production and reduction due to the higher nitrogen concentration removed via autotrophic denitrification. Those results are close to the one observed with the Morris analysis in which, however, the sulfur hydrolysis constant retains wider relevance by being the bottleneck of the autotrophic denitrification process.

5.5.3.2 Overall consideration on Shap importance

The operational parameters of the model τ_d and COD_{inj} influence the output sulfate concentration more than any other quantity of interest, a result perfectly in line with what could be observed from the simulations reported within the other chapters.

Regarding the parameters connected to the autotrophic denitrification process, those still remain in the first places of the ranking importance for all the quantities of interest investigated. The other strictly biological parameters are related to the decay of both the heterotrophic families considered in the reactor.

The quantity of interest that is affected by different parameters depending on the sensitivity analysis methodology is represented by the percentage prevalence of sulfate-reducing over heterotrophic consortium. Indeed, comparing the results obtained by the Morris method and SHAP analysis, several parameters are apparently influencing the quantity, most of them related to the decay of heterotrophic species and the growth of autotrophic biomass. Thus, the variability in the percentage of sulfate-reducing bacteria due to the fluctuation of many parameters is probably the cause of the variation in errors in both assessments performed as the cycle duration varies.

5.5.3.3 Shap summary plot

SHAP analysis also leads to the development of a summary graph in which the Shapley values for a feature and an instance are condensed at each point. This graph combines: sorting features by importance and, using color to explain the value of the feature. Each point on this graph represents a Shapley value.

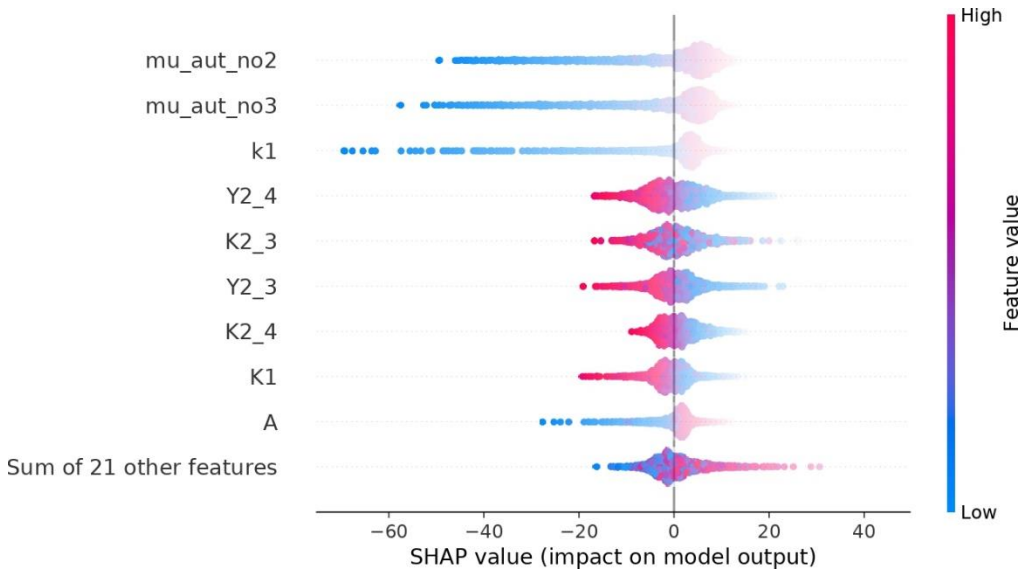

Fig. 5. 13 SHAP summary plot for τ=20 days for the nitrogen percentage removal.

From Fig. 5.13 result that the rate of nitrogen removal over the cycle duration is strongly dependent on the kinetic parameters related to the autotrophic denitrification, such as the maximum growth rate and parameters related to the hydrolysis step. The k1 constant is more evident here than in the previous SHAP analysis as the bottleneck constant of the process. In fact, constant k1 for a lower value reduces the nitrogen removal rate. In addition, it is also shown that low values of the growth rate reduce the efficiency of the nitrogen compound removal process. The particle size a*, reported here as affects the process as does the k1 constant. Furthermore, it must be noticed that since the autotrophic denitrification is the main biological pathways for the N-based compounds removal, the parameter connected to the heterotrophic denitrification are not present in this summary plot.

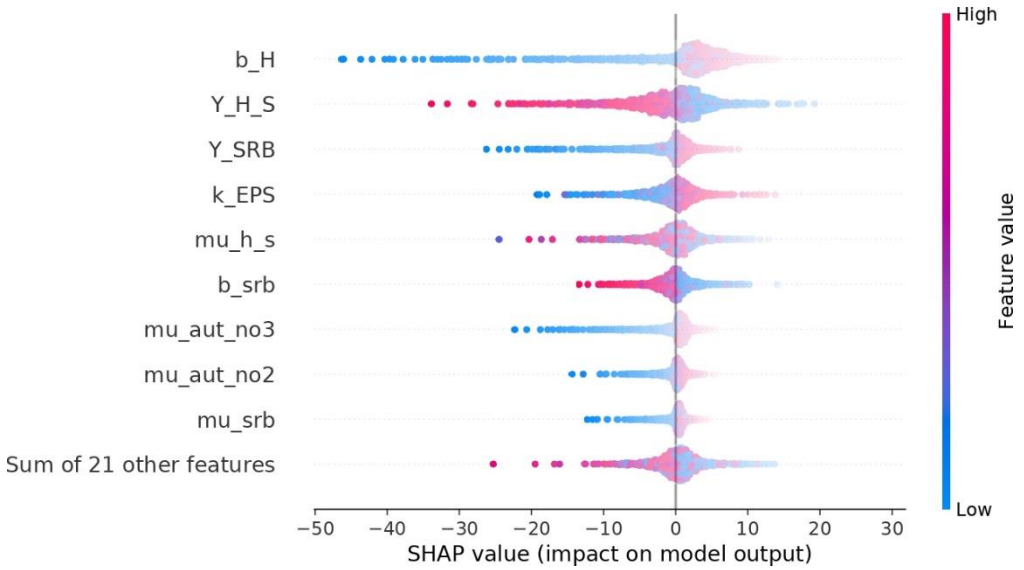

Fig. 5. 14 SHAP summary plot for τ=20 days for the SRB Percentage on the heterotrophic consortium.

According to Fig. 5.14, for the heterotrophic consortium, the most affecting parameter is reported to be for an extent range of values the decay constant of the heterotrophic denitrifiers. Related to this constant there is also the yield constant for both heterotrophic biomasses, heterotrophic denitrifiers and sulfate reducing bacteria. Regarding the variability of these two heterotrophic families all the parameters related to the growth and decay of the biomass are reported to be important and strongly affecting the final percentage of the sulfate reducing bacteria with respect to both the heterotrophic families. Furthermore, it must be noticed that if the heterotrophic denitrifiers disappear the sulfate reducing bacteria will be the only consumers of the COD added during the process. However, the growth rate of the autotrophic denitrifiers maintain their

importance because it must be remembered that, if autotrophic denitrification does not take place sulfate will be not produced and consequently the sulfate reducing bacteria will not have substrate to grow on. In addition, K_EPS is also present in this list since it is the responsible for the BAP production which represents the growth support for both heterotrophic families. It should also be noted that the analysis is conducted referring to sulfate reducing bacteria which explains why heterotrophs related parameter are more important, taking into account as already mentioned that if heterotrophs disappear sulfate reducers remains the only consumers of organic matter.

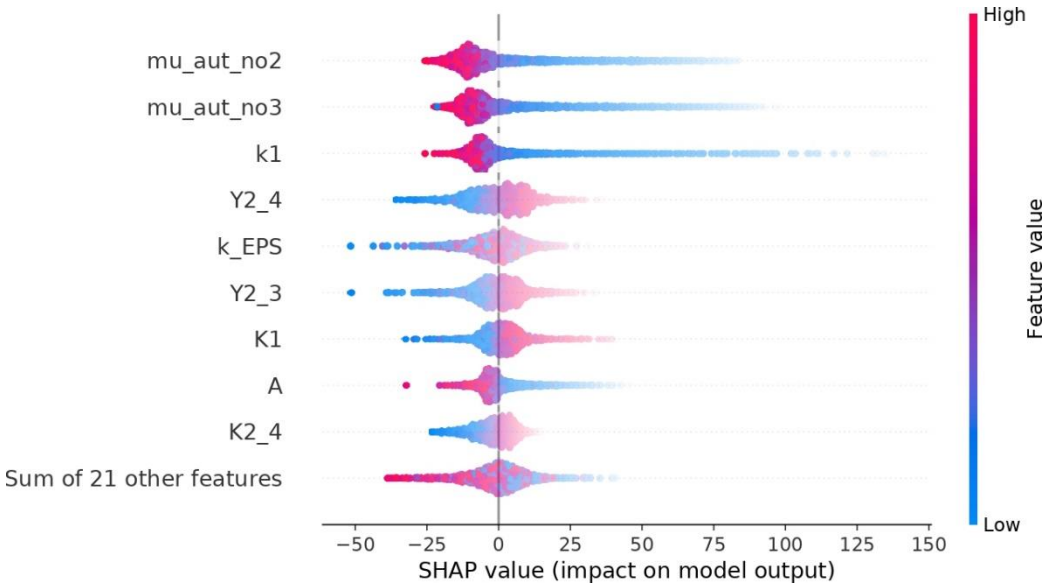

Fig. 5. 15 SHAP summary plot. For τ=20 days of the concentration of the SMP in the effluent.

As the other quantities of interest, from Fig 5. 15 it results that also the SMP concentration is related to autotrophic denitrification parameters, since it is the main biological process and the one which involves more biomass. Furthermore, the hydrolyzation constant of the EPS (k_EPS) is still confirmed as in the previous results the most influential parameter strictly related to the SMP production.

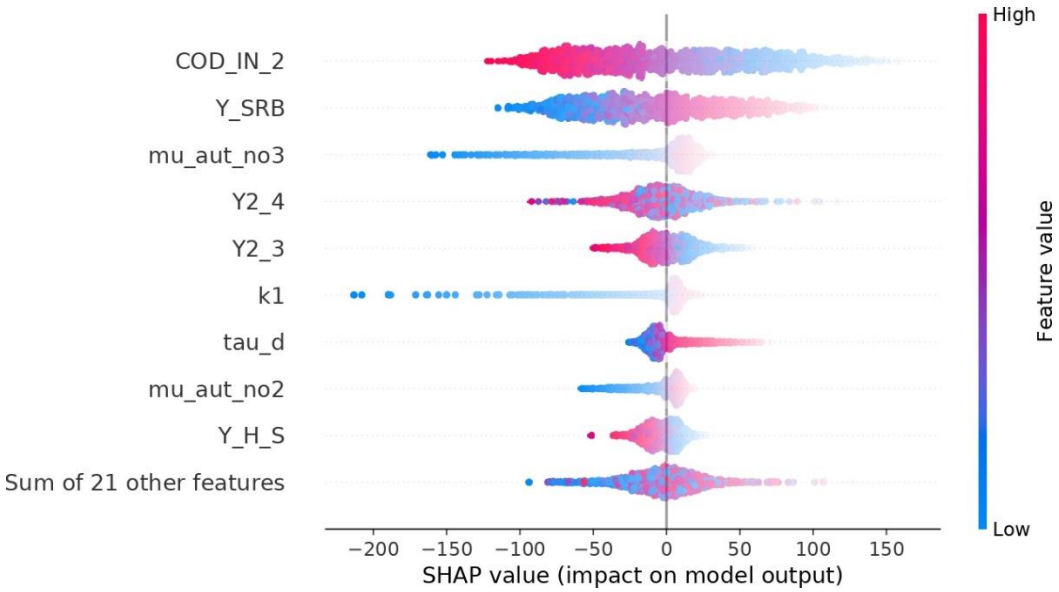

Fig. 5. 16 SHAP summary plot. For τ=20 days of the concentration of the sulfate in the effluent.

As reported in Fig 5.16 Sulfate concentration is confirmed to be the quantity of interest most affected by the addition of COD during the process, since sulfate reduction must be carried out. In contrast to nitrogen compounds, it should be remembered that sulfate is produced in the system by autotrophic denitrifiers consequently the dependence on parameters related to the growth of this biomass is necessary. Concomitantly, the significance of the yield of sulfate-reducing bacteria is explained by the fact that they are the only biomass responsible for the decrease in sulfate concentration. Furthermore, sulfate concentration is the only quantity of interest for which the operational parameter related to the day of injection is also important. This parameter does not have the same importance as the COD amount since it affects mainly the removal of sulfates rather than their production contrary to the parameters related to autotrophic denitrification. Moreover, the yield coefficient of heterotrophic biomass is also present, since if nitrate removal is carried out by this biomass no sulfates are produced.

5.5.4 PARTIAL DEPENDENCE PLOT (PDP)

The last analysis performed will strongly help for the future calibration of the model because it is carried out to understand the variation of τ_d and COD_{inj} on the more engineering quantity of interest analyzed: the nitrogen percentage removal and the sulfate concentration. Indeed, the partial dependence plot is a useful tool to predict the effect that each parameter has on the outcome in machine learning model [33]. The results are obtained by marginalizing the other parameters

involved and varying the ones of interest. The analysis has been carried out varying simultaneously the two variables for τ =10 and 20 days reported in Fig. 5.17-5.20.

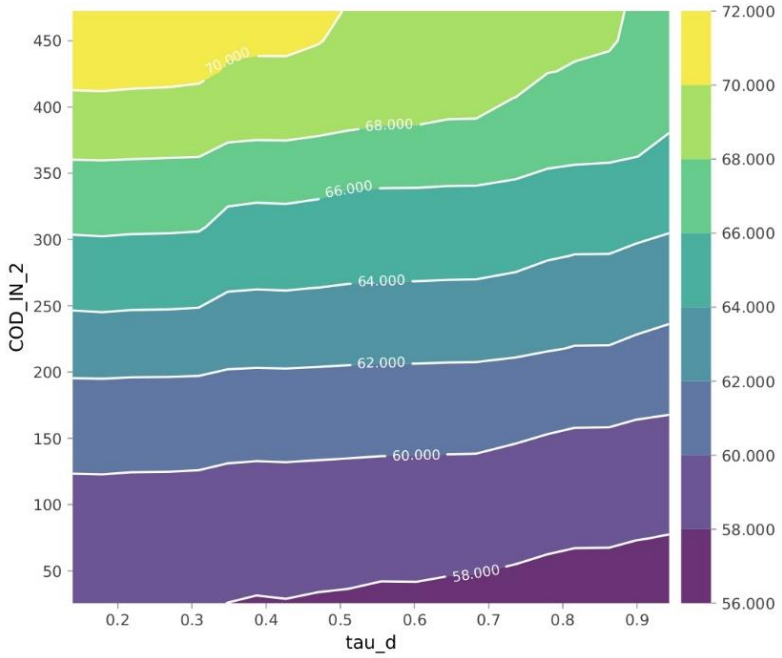

Fig. 5.17 PdP figure representing the effect of the simultaneous variations of τ_d and COD_{inj} on the Nitrogen percentage removal for τ =10 days.

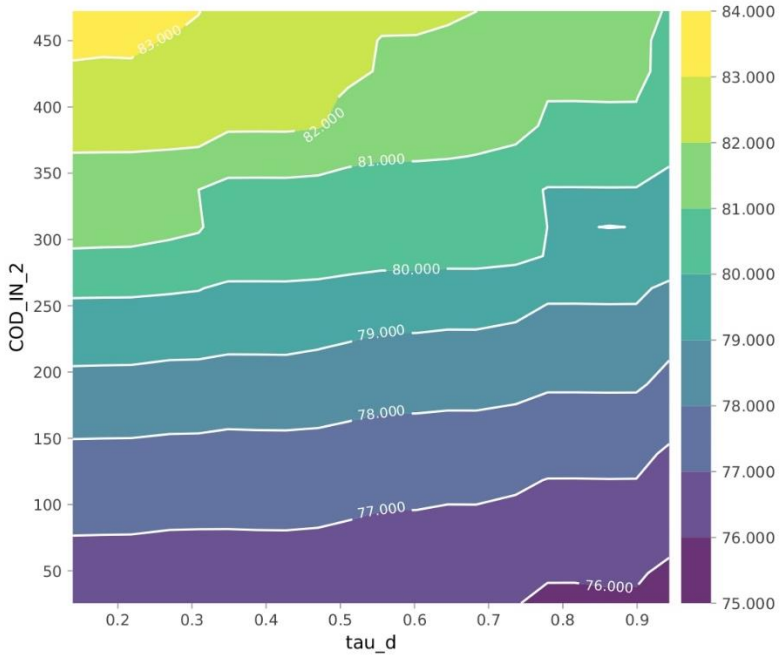

Fig. 5. 18 PdP figure representing the effect of the simultaneous variations of τ_d and COD_{inj} on the Nitrogen percentage removal for τ =20 days.

The nitrogen percentage removal is strongly affected by the operational parameters τ_d and COD_{inj}, giving prove with the two Fig. 5.18-5.19 of the flexibility of the model. Indeed, varying two operational parameters the same result could be obtained. From the analysis it results that nitrogen percentage removal is higher for the longer cycle duration as widely discussed in previous chapters. However, those new representations highlight the strong increased efficiency of the process when the COD addition occurs for τ_d>0.5 τ which is more evident for τ=20 days. Furthermore, it could be also noticed that also for τ =10 days the nitrogen percentage removal is lower even when the maximum quantity of COD is added but increases with the increasing of $\tau_d$in particular when the value of 350 mg/l of COD is added.

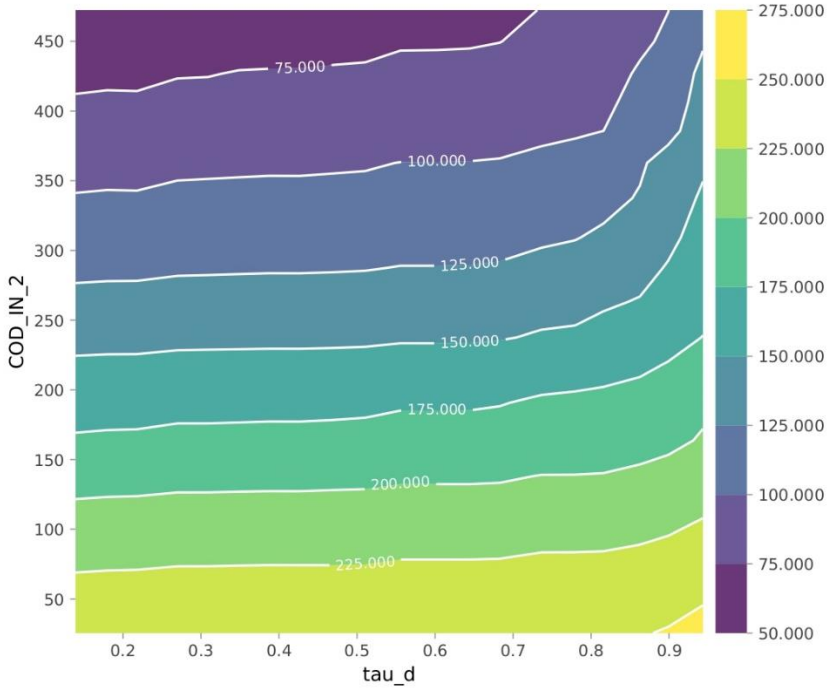

Fig. 5. 19 PdP figure representing the effect of the simultaneous variations of τ_d and COD_{inj} on the Sulfate concentration for τ =10 days.

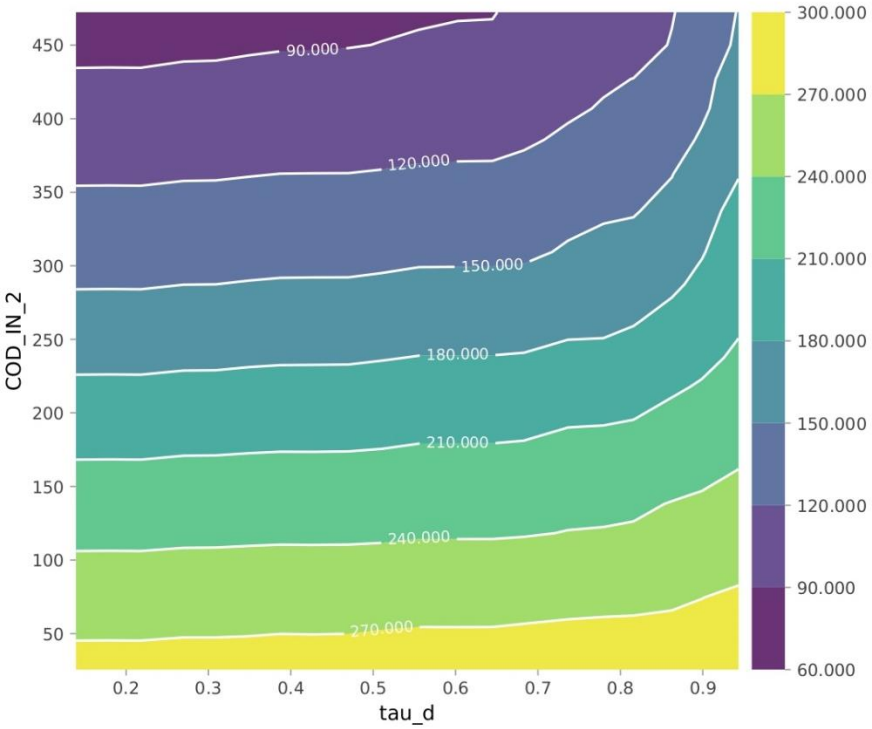

Fig. 5. 20 PdP figure representing the effect of the simultaneous variations of τ_d and COD_{inj} on the Sulfate concentration for $\tau = 20$ days.

The Concentration of sulfate as reported from Fig 5.19,20 is almost constant varying the values of τ_d but it will rapidly increase when the COD addition occurs almost at the end of the cycle. This trend could be explained by two factors: the first is that for earlier COD injection, the latter will be used mostly by the heterotrophic denitrifiers that will reduce the amount of nitrogen removal by autotrophic denitrifiers reducing the quantity of sulfate produced; the second is related to τ_d indeed, later the injection occurs the more the sulfate reducing bacteria could not have the possibility to complete the removal of sulfate produced.

Comparing the results in terms of Nitrogen percentage removal and sulfate concentration it is possible to reach higher performances in terms of such quantities of interest simply varying the operational conditions.

5.6 CONCLUSION

The results obtained through the different methodologies to measure the sensitivity of different parameters revealed that what mainly affects the autotrophic denitrification is process is sulfur hydrolysis. Other parameters, on the contrary, affect the results related to the heterotrophic families i.e., the prevalence of sulfate reducers over heterotrophs and the amount of sulfate output are mainly related to the decay constants of denitrifying heterotrophs and to the growth and death of sulfate reducers. Such results also highlight that one of the parameters that mainly influence the production of SMP is the hydrolysis constant of EPS. Furthermore, the results also demonstrate that for a previous acclimatized biomass the nitrogen percentage removal is affected by the maximum growth rate of the autotrophic denitrifiers. All these considerations will serve as a valuable tool in future experimental calibration and validation of the model and highlight from an application perspective that the system can easily react to possible changes in terms of nitrogen loading or quality of the effluent required, that can always occur within any wastewater treatment plant.

5.7 REFERENCES

[1] Y. X. Cui *et al.*, “Biological nitrogen removal from wastewater using sulphur-driven autotrophic denitrification,” *Appl. Microbiol. Biotechnol.*, vol. 103, no. 15, pp. 6023–6039, 2019, doi: 10.1007/s00253-019-09935-4.

[2] G. Guo *et al.*, “Advances in elemental sulfur-driven bioprocesses for wastewater treatment: From metabolic study to application,” *Water Res.*, vol. 213, no. January, p. 118143, 2022, doi: 10.1016/j.watres.2022.118143.

[3] L. Zhang, Y. Y. Qiu, Y. Zhou, G. H. Chen, M. C. M. van Loosdrecht, and F. Jiang, “Elemental sulfur as electron donor and/or acceptor: Mechanisms, applications and perspectives for biological water and wastewater treatment,” *Water Res.*, vol. 202, no. June, p. 117373, 2021, doi: 10.1016/j.watres.2021.117373.

[4] A. S. Oberoi, H. Huang, S. K. Khanal, L. Sun, and H. Lu, “Electron distribution in sulfur-driven autotrophic denitrification under different electron donor and acceptor feeding schemes,” *Chem. Eng. J.*, vol. 404, Jan. 2021, doi: 10.1016/j.cej.2020.126486.

[5] Y. Y. Qiu *et al.*, “Overlooked pathways of denitrification in a sulfur-based denitrification system with organic supplementation,” *Water Res.*, vol. 169, 2020, doi: 10.1016/j.watres.2019.115084.

[6] Y. Liu *et al.*, “Optimizing sulfur-driven mixotrophic denitrification process: System performance and nitrous oxide emission,” *Chem. Eng. Sci.*, vol. 172, no. 2017, pp. 414–422, 2017, doi: 10.1016/j.ces.2017.07.005.

[7] G. Guerriero, M. R. Mattei, S. Papirio, G. Esposito, and L. Frunzo, “Modelling the effect of SMP production and external carbon addition on S-driven autotrophic denitrification,” *Sci. Rep.*, vol. 12, no. 1, Dec. 2022, doi: 10.1038/S41598-022-10944-Z.

[8] Y. Wang, C. Bott, and R. Nerenberg, “Sulfur-based denitrification: Effect of biofilm development on denitrification fluxes,” *Water Res.*, vol. 100, pp. 184–193, Sep. 2016, doi: 10.1016/j.watres.2016.05.020.

[9] Y. X. Cui, B. K. Biswal, M. C. M. van Loosdrecht, G. H. Chen, and D. Wu, “Long term

performance and dynamics of microbial biofilm communities performing sulfur-oxidizing autotrophic denitrification in a moving-bed biofilm reactor," *Water Res.*, vol. 166, 2019, doi: 10.1016/j.watres.2019.115038.

[10] L. Guerrero *et al.*, "Autotrophic and heterotrophic denitrification for simultaneous removal of nitrogen, sulfur and organic matter," *J. Environ. Sci. Heal. - Part A Toxic/Hazardous Subst. Environ. Eng.*, vol. 51, no. 8, pp. 650–655, 2016, doi: 10.1080/10934529.2016.1159875.

[11] D. Yánez, L. Guerrero, R. Borja, and C. Huiliñir, "Sulfur-based mixotrophic denitrification with the stoichiometric S0/N ratio and methanol supplementation: effect of the C/N ratio on the process," *J. Environ. Sci. Heal. Part A*, vol. 56, no. 13, pp. 1420–1427, Nov. 2021, doi: 10.1080/10934529.2021.2004839.

[12] S. E. Oh, Y. B. Yoo, J. C. Young, and I. S. Kim, "Effect of organics on sulfur-utilizing autotrophic denitrification under mixotrophic conditions," *J. Biotechnol.*, vol. 92, no. 1, pp. 1–8, 2001, doi: 10.1016/S0168-1656(01)00344-3.

[13] C. Peirano *et al.*, "Assessment of simultaneous autotrophic–heterotrophic denitrification with high removal of nitrogen, sulfur and carbon: optimization through response surface methodology," *J. Chem. Technol. Biotechnol.*, vol. 95, no. 3, pp. 631–638, 2020, doi: 10.1002/jctb.6244.

[14] F. Pianosi *et al.*, "Sensitivity analysis of environmental models: A systematic review with practical workflow," *Environ. Model. Softw.*, vol. 79, pp. 214–232, 2016, doi: 10.1016/j.envsoft.2016.02.008.

[15] E. Sahinkaya, A. Kilic, and B. Duygulu, "Pilot and full scale applications of sulfur-based autotrophic denitrification process for nitrate removal from activated sludge process effluent," *Water Res.*, vol. 60, pp. 210–217, 2014, doi: 10.1016/j.watres.2014.04.052.

[16] B. J. Ni, M. Ruscalleda, and B. F. Smets, "Evaluation on the microbial interactions of anaerobic ammonium oxidizers and heterotrophs in Anammox biofilm," *Water Res.*, vol. 46, no. 15, pp. 4645–4652, Oct. 2012, doi: 10.1016/j.watres.2012.06.016.

[17] T. Jiang *et al.*, “Modelling the production and degradation of soluble microbial products (SMP) in membrane bioreactors (MBR),” *Water Res.*, vol. 42, no. 20, pp. 4955–4964, 2008, doi: 10.1016/j.watres.2008.09.037.

[18] M. Henze, W. Gujer, T. Mino, and M. van Loosedrecht, “Activated Sludge Models ASM1, ASM2, ASM2d and ASM3.” IWA Publishing, Oct. 01, 2006. doi: 10.2166/9781780402369.

[19] C. S. Laspidou and B. E. Rittmann, “Non-steady state modeling of extracellular polymeric substances, soluble microbial products, and active and inert biomass,” *Water Res.*, vol. 36, no. 8, pp. 1983–1992, 2002, doi: 10.1016/S0043-1354(01)00414-6.

[20] R. Sierra-Alvarez, R. Beristain-Cardoso, M. Salazar, J. Gómez, E. Razo-Flores, and J. A. Field, “Chemolithotrophic denitrification with elemental sulfur for groundwater treatment,” *Water Res.*, vol. 41, no. 6, pp. 1253–1262, 2007, doi: 10.1016/j.watres.2006.12.039.

[21] G. Xu, F. Yin, S. Chen, Y. Xu, and H. Q. Yu, “Mathematical modeling of autotrophic denitrification (AD) process with sulphide as electron donor,” *Water Res.*, vol. 91, pp. 225–234, 2016, doi: 10.1016/j.watres.2016.01.011.

[22] S. V. Kalyuzhnyi and V. V. Fedorovich, “Mathematical modelling of competition between sulphate reduction and methanogenesis in anaerobic reactors,” *Bioresour. Technol.*, vol. 65, no. 3, pp. 227–242, 1998, doi: 10.1016/S0960-8524(98)00019-4.

[23] A. Kostrytsia *et al.*, “Elemental sulfur-based autotrophic denitrification and denitritation: microbially catalyzed sulfur hydrolysis and nitrogen conversions,” *J. Environ. Manage.*, vol. 211, pp. 313–322, Apr. 2018, doi: 10.1016/j.jenvman.2018.01.064.

[24] Y. Liu *et al.*, “Evaluation of nitrous oxide emission from sulfide- and sulfur-based autotrophic denitrification processes,” *Environ. Sci. Technol.*, vol. 50, no. 17, pp. 9407–9415, 2016, doi: 10.1021/acs.est.6b02202.

[25] G. Sin *et al.*, “Modelling nitrite in wastewater treatment systems: A discussion of different modelling concepts,” *Water Sci. Technol.*, vol. 58, no. 6, pp. 1155–1171, 2008, doi:

10.2166/wst.2008.485.

[26] W. Gujer, M. Henze, T. Mino, and M. Van Loosdrecht, “Activated Sludge Model No. 3,” in *Water Science and Technology*, Jan. 1999, vol. 39, no. 1, pp. 183–193. doi: 10.1016/S0273-1223(98)00785-9.

[27] B. J. Ni, F. Fang, B. E. Rittmann, and H. Q. Yu, “Modeling microbial products in activated sludge under feast#famine conditions,” *Environ. Sci. Technol.*, vol. 43, no. 7, pp. 2489–2497, 2009, doi: 10.1021/es8026693.

[28] V. Fedorovich, P. Lens, and S. Kalyuzhnyi, “Extension of Anaerobic Digestion Model No. 1 with Processes of Sulfate Reduction,” 2003.

[29] D. J. Batstone *et al.*, “The IWA Anaerobic Digestion Model No 1 (ADM1),” *Water Sci. Technol.*, vol. 45, no. 10, pp. 65–73, May 2002, doi: 10.2166/wst.2002.0292.

[30] F. Campolongo and A. Saltelli, “Sensitivity analysis of an environmental model: An application of different analysis methods,” *Reliab. Eng. Syst. Saf.*, vol. 57, no. 1, pp. 49–69, 1997, doi: 10.1016/S0951-8320(97)00021-5.

[31] A. Kostrytsia, S. Papirio, M. R. Mattei, L. Frunzo, P. N. L. Lens, and G. Esposito, “Sensitivity analysis for an elemental sulfur-based two-step denitrification model,” *Water Sci. Technol.*, vol. 78, no. 6, pp. 1296–1303, Nov. 2018, doi: 10.2166/wst.2018.398.

[32] C. Huiliñir *et al.*, “Elemental sulfur-based autotrophic denitrification in stoichiometric S0/N ratio: Calibration and validation of a kinetic model,” *Bioresour. Technol.*, vol. 307, Jul. 2020, doi: 10.1016/j.biortech.2020.123229.

[33] J. H. Friedman, “Greedy function approximation: A gradient boosting machine,” *Ann. Stat.*, vol. 29, no. 5, pp. 1189–1232, 2001, doi: 10.1214/aos/1013203451.

Chapter 6

CONCLUSION
AND
FUTURE PRESPECTIVES

6.1 CONCLUSION

Mathematical modeling represents a useful tool to investigate a new process that has never been experimentally studied before. Indeed, as reported in the first chapter, none of the previous studies have analyzed the simultaneous work of autotrophic denitrifiers using elemental sulfur, sulfate reducing bacteria and heterotrophic denitrifiers. Furthermore, the evaluation of the growth and the consumption of the Soluble Microbial Products (SMP) has never been evaluated for autotrophic denitrifiers using sulfur compounds. In this case, the model developed served also to assess the competition between three microbial families and, consequently, the performances of three different processes occurring simultaneously.

In this work, the operational conditions of a sequential batch reactor (SBR) were widely investigated for the first time, giving a key role in the process to cycle duration, day of injection and the amount of COD added. Such parameters are a novelty if compared to previous models and experimental studies reported in the first chapter, in which COD is usually added at the beginning of the process or is already present in the influent.

The model simulations are presented in chapter 3 and 4 using high nitrogen concentrations, typical of industrial wastewater effluent. However, the process works properly also for lower concentrations of nitrogen compounds in the influent, as experimentally shown in the studies described in chapter 2. Even if it was not possible to evaluate the inhibition caused by nitrite accumulation (it could have been investigated only with experimental validation), the results obtained in terms of nitrogen removal efficiency are over the 60 % almost in every case. Such results make hard to suppose that nitrite accumulation could occur since it is explicitly removed both via heterotrophic denitrification and autotrophic denitrification.

In **chapter three**, the mathematical model is defined and described. To model the biological processes occurring in SBR reactor, impulse differential equations are used. Autotrophic denitrification is supposed to be the main biological process, and the heterotrophic families are stimulated to grow by the addition of two different COD values: one stoichiometric with respect to the amount needed to remove sulfate produced by autotrophic denitrification and another in excess of this amount. Using the model, several simulations were carried out varying the duration of the cycle, the amount of COD input and the day it is added. In cases where COD input occurs past the first half of the cycle duration sulfate reducers prevail on heterotrophic denitrifiers. This study shows the possibility to stimulate sulfate reducers after the autotrophic

denitrification takes place, which takes longer reaction time. Conversely, when the addition of COD occurs before half the cycle duration, heterotrophic denitrifiers are favored, making the process faster, but being deficient in COD can lead to less nitrate removal if the cycle duration is not sufficient for autotrophic denitrifiers to complete the removal of nitrogen compounds. In addition, it should be noted that in cases where no external COD source is fed, the SMP produced by the microbial activities are unable to support a significant sulfate removal.

From the results presented in **chapter four**, the low accumulation and utilization of SMP is even more pronounced as the operating conditions of the reactor are modified, increasing the emptying/refilling ratio of the reactor, and reducing the sedimentation efficiency. Emptying the system of a larger amount of liquid inside leads to the possibility of achieving a higher removal of nitrate in comparison to the simulations performed in the second chapter. The results obtained in this chapter indicate that maintaining optimal sedimentation conditions for the process is necessary, in order to maintain high biomass concentrations within the system even with shorter cycle durations. Given the large number of simulations performed and parameters involved, is hard to achieve the minimum concentration of sulfate in the effluent in the minimum time and simultaneously maintain high the nitrogen removal efficiency as evidenced by the sensitivity analysis in chapter four.

In **chapter five,** the global sensitivity analysis is carried out on all the kinetic parameters involved in the model. Based on the Morris method, the main sensitive parameters are reported to be the ones related to the autotrophic denitrifiers and the hydrolyzation step of the elemental sulfur. Indeed, the maximum growth rate of the autotrophic denitrifiers of both the steps of denitrification process have an important role. The quantity of interest which resulted harder to define due to the extreme variability in the results is reported to be the percentage of the prevalence of the sulfate reducing bacteria on the heterotrophic consortium due to its dependence from many parameters. Given the lack of experimental data on the simultaneous work of these three microbial species, the global sensitivity analysis will give the main support to model calibration and experimental validation. Moreover, assuming the experimental tests that could be carried out to validate the model presented here, this analysis will be a useful tool to intervene on the parameters found to be the most sensitive.

6.2 FUTURE PERSPECTIVES

The presented model represents the ultimate tool for achieving optimal COD addition without losing the advantages associated with the application of autotrophic instead of heterotrophic denitrification. The overall sensitivity analysis shows that, as seen experimentally before, the elemental sulfur hydrolysis step is the bottleneck of this process.

Further studies must be carried out for experimental validation of the model promoting the simultaneous growth of the three microbial families. It was indeed already proved experimentally that such families can growth together by couple, but their growth have never been stimulated all together. The advanced global sensitivity analysis carried out have been evidenced the parameter on which the future experimentation necessary to experimentally calibrate and validate the model.

Sequencing batch reactor was chosen as reactor configuration but the most widely used is represented by the packed bed reactor so probably further experimentation could be carried out using this reactor configuration. However, the proper reactor configuration is also always subjected to the necessity related to the influent characteristic. Furthermore, if different reactor configuration will be chosen for experimental validation and scale up of the process it will result necessary a configuration which enhance the biomass accumulation. In addition, studies on the different forms of elemental sulfur that may be used by autotrophic denitrifiers also need to be implemented given the wide variety of forms found. Another parameter that could be the subject of further interest and investigation is the evaluation of the maximum growth rate of denitrifying autotrophs on nitrite since in some studies a higher growth rate is reported in the transformation from nitrite to nitrate while in others the reverse is reported. According to what revealed by the sensitivity analysis regarding the main quantities of interest represented by nitrate removal and sulfate output concentration, the most influential parameter of the process is the maximum growth rate constant related to the transformation of nitrate to nitrite. Therefore, it might be of strong interest for the calibration purposes to monitor the nitrous oxide production, in order to evaluate also the effects of the addition of the external carbon source on the emissions of this gas.